

THE UNIVERSITY OF CALGARY

The Photophysics and Photochemistry of Fulvic Acid

by

Aldo Gaetano Bruccoleri

A DISSERTATION

**SUBMITTED TO THE FACULTY OF GRADUATE STUDIES
IN PARTIAL FULFILMENT OF THE REQUIREMENTS FOR THE
DEGREE OF DOCTOR OF PHILOSOPHY**

DEPARTMENT OF CHEMISTRY

CALGARY, ALBERTA

JANUARY, 2000

© Aldo Gaetano Bruccoleri 2000



**National Library
of Canada**

**Acquisitions and
Bibliographic Services**

**395 Wellington Street
Ottawa ON K1A 0N4
Canada**

**Bibliothèque nationale
du Canada**

**Acquisitions et
services bibliographiques**

**395, rue Wellington
Ottawa ON K1A 0N4
Canada**

Your file Votre référence

Our file Notre référence

The author has granted a non-exclusive licence allowing the National Library of Canada to reproduce, loan, distribute or sell copies of this thesis in microform, paper or electronic formats.

The author retains ownership of the copyright in this thesis. Neither the thesis nor substantial extracts from it may be printed or otherwise reproduced without the author's permission.

L'auteur a accordé une licence non exclusive permettant à la Bibliothèque nationale du Canada de reproduire, prêter, distribuer ou vendre des copies de cette thèse sous la forme de microfiche/film, de reproduction sur papier ou sur format électronique.

L'auteur conserve la propriété du droit d'auteur qui protège cette thèse. Ni la thèse ni des extraits substantiels de celle-ci ne doivent être imprimés ou autrement reproduits sans son autorisation.

0-612-49484-5

Canada

Abstract

This study concerns the primary photophysics and photochemistry of two well characterized humic substances, the Mossy Point and Laurentian fulvic acid. Quantum yields for solvated electron and cation radical production were determined directly from time resolved absorption spectra recorded at 20 ps (irradiation at 355 nm) for various solutions of Laurentian and Mossy Point fulvic acid. Quantum yields for formation of the solvated and corresponding free radical at 20 ps range from 0.12 for Laurentian fulvic acid solutions prepared at pH 4.0 to 0.18 for solutions prepared at pH 9.0.

Time resolved photoacoustic spectroscopy in conjunction with magnetic circular dichroism (MCD) spectroscopy has been applied to determine energies and quantum yields for the formation of triplet states in aqueous solutions of Mossy Point and Laurentian fulvic acids with irradiation at 337.1 nm. For the Laurentian sample, intersystem crossing quantum yields range from 0.79 to 0.28 for the pH range 2.0-9.5. The average triplet energy is estimated as $1.8 \times 10^2 \text{ kJmol}^{-1}$ from MCD spectra. For the Mossy Point sample, intersystem crossing quantum yields range from 0.82 to 0.35 for the pH range 2.0-9.5. The triplet energy is estimated as $1.7 \times 10^2 \text{ kJmol}^{-1}$. With the primary photoproduct quantum yields, the overall photophysics and primary photochemistry of the fulvic acid may be described.

Photodegradation studies involving Laurentian fulvic acid solutions and a three component chemical model mixture, comprised of a quinone, hydroquinone and phenol indicate that a parallel exists between the near ultra violet (350nm) photochemical behaviour of Laurentian fulvic acid solutions and the quinonoid model mixtures. A quinonoid free-radical photodegradation mechanism is suggested for the Laurentian fulvic acid. The study uses a relatively small non-substituted quinone (1,4 benzoquinone) and a larger substituted ubiquinone (coenzyme Q 10) to explore the effect of substitution in the quinone both experimentally and by computational modeling to further support the quinoid model of fulvic acid photochemistry. The uv-vis spectral behaviour of the model and the fulvic acid is correlated with photoinduced changes in the ^{13}C NMR spectra of the fulvic acid.

Acknowledgements

I wish to thank Dr. C.H. Langford for his supervision, assistance, encouragement and keen interest he has shown throughout this project.

I thank the members of our group, past and present for their support.

I would also like to thank Dr. B. Hollebome and Ms. Pam Wolff of Carlton University for their help recording the MCD spectra and Dr. R.L.Cook and Ms. Qiao Wu for their help with the NMR spectra.

Table of Contents

Approval Page.....	ii
Abstract.....	iii
Acknowledgments.....	iv
Table of Contents.....	v
List of Tables.....	vii
List of Figures.....	viii
CHAPTER 1: INTRODUCTION.....	1
1.2 Organic Matter in Soil.....	1
1.2.1 Soil Humus.....	3
1.3 Photoprocesses.....	7
References.....	11
CHAPTER 2: EXPERIMENTAL.....	14
Materials and Methods of Preparation.....	14
Equipment.....	16
Absorption Spectra.....	16
Fluorescence.....	16
Picosecond Laser Spectroscopy.....	17
Magnetic Circular Dichroism Spectroscopy.....	22
Time Resolved Pulsed Photoacoustic Spectroscopy.....	24
¹³ C Nuclear Magnetic Resonance Spectroscopy.....	28
Photoreactor-Photochemical Studies.....	29
Computational Chemistry.....	29
References.....	29
CHAPTER 3: THEORETICAL ASPECTS OF ORGANIC PHOTOPHYSICS AND PHOTOCHEMISTRY.....	30
3.1 Introduction.....	30
3.2 Photophysics - Introduction to Terms.....	30
3.3 Electronic Excitation of Representative Organic Compounds in the near U.V.....	31
3.4 The n,π* Excited State.....	38
3.5 Difference in Electronic Energy of Singlet and Triplet n,π* Carbonyl States.....	39
3.6 Intersystem Crossing.....	44
3.7 Fluorescence and Phosphorescence.....	45
3.8 Radiative Transitions Involving More Than One Molecule.....	45
3.9 State Mixing.....	47
3.10 Photochemistry.....	50
References.....	56

CHAPTER 4: PRIMARY PHOTOPHYSICAL AND PHOTOCHEMICAL BEHAVIOUR OF FULVIC ACID.....	58
4.1 Introduction.....	58
4.2 Laser Flash Photolytic Studies of Fulvic Acid.....	58
4.3 Formation and Decay of the Solvated Electron.....	61
4.4 Formation Yield for the Solvated Electron.....	64
4.5 Radical Coproducts.....	67
4.6 The Triplet Transient.....	68
References.....	69
CHAPTER 5: PHOTOPHYSICS IN FULVIC ACID SOLUTIONS.....	71
5.1 Introduction.....	71
5.2 Intersystem Crossing and Photophysical Radiationless Transitions of Excited State Carbonyl Compounds.....	70
5.3 Evaluation of Apparent Intersystem Crossing Quantum Yields in Fulvic Acid Solutions.....	73
5.3.1 Magnetic Circular Dichroism Spectroscopy.....	74
5.3.2 Time Resolved Pulsed Photoacoustic Spectroscopy.....	76
References.....	81
CHAPTER 6: THE PHOTOCHEMISTRY OF FULVIC ACID AND RELATED COMPOUNDS.....	83
6.1 Introduction.....	83
6.2 Organic Charge Transfer Complexes and Organic Photochemistry.....	85
6.3 Photodegradation of Laurentian Fulvic Acid and Quinonoid Model Mixtures.....	92
6.3.1 Photodegradation of Quinonoid Model Mixtures..	94
6.3.2 Photodegradation of Laurentian Fulvic Acid.....	105
6.4 Molecular Modeling.....	111
6.5 Conclusion and Future Work.....	114
References.....	118
APPENDIX I	121

List of Tables

Table 1.1: Functional Group Analysis.....	6
Table 3.1: Energetics and Dynamics of Carbonyl Compounds.....	42
Table 3.2: The Singlet and Triplet Energies of some Conjugated and related Carbonyls.....	43
Table 3.3: Self-Quenching Rate Constants of Triplet Ketones.....	54
Table 4.1: Quantum Yields for Formation of the Solvated Electron for Mossy Point and Laurentian Fulvic Acid.....	65
Table 5.1: Singlet – Triplet Splittings.....	72
Table 5.2: Quantum Yields for Intersystem Crossing.....	73
Table 5.3: Apparent Triplet Quantum Yields Calculated for Various Solutions of Mossy Point Fulvic Acid.....	77
Table 5.4: Apparent Triplet Quantum Yields Calculated for Various Solutions of Laurentian Fulvic Acid.....	78
Table 6.1: Absorption Maxima of Selected Semiquinone Radicals.....	91

List of Figures

Figure 1.1: Map description of the two areas where soil samples were obtained.....	5
Figure 1.2: Absorption spectrum of Mossy Point fulvic acid	8
Figure 2.1: Schematic representation of the picosecond flash photolysis experimental setup.....	18
Figure 2.2: Schematic representation of the photoacoustic detection system.....	26
Figure 3.1: Type of excited state energies of electronic states of organic Compounds.....	32
Figure 3.2: Summary of electronic energy levels of unsaturated organic compounds with a heteroatom.....	32
Figure 3.3: The main absorption bands in the electronic spectra of 1,2 benzoquinone, 1,4 benzoquinone, 1,4 naphthoquinone , and anthraquinone	34
Figure 3.4: Absorption spectra of some aromatic aldehydes and ketones.....	35
Figure 3.5: The electronic absorption spectra of a variety of quinone radicals.....	36
Figure 3.6: Electronic absorption spectra of representative quinoid radicals.....	37
Figure 3.7: Overlap of the n and π^* orbitals at a carbonyl.....	41
Figure 3.8: Overlap of a π, π^* configuration.....	41
Figure 3.9: Qualitative comparison of the energetics for hydrogen atom abstraction from different H donors HX by the n, π^* states of ketones and aryl ketones.....	50
Figure 4.1: Schematic summary of lifetime components observed for the photolysis of Mossy Point fulvic acid.....	60
Figure 4.2: Wavelength dependence of quantum yield for solvated electron production from Swanee River fulvic acid (anaerobic) solutions.....	61
Figure 5.1: Representative MCD spectrum of the Mossy Point fulvic acid solution...	75
Figure 5.2: Representative MCD spectrum of the Laurentian fulvic acid solution.....	75
Figure 6.1: Solid state ^{13}C NMR of Laurentian fulvic acid before and after irradiation at 350nm.....	93
Figure 6.2: Color formation (dark) during 'dark' equilibrium of quinoid mixture.....	95
Figure 6.3: UV-Visible absorption spectrum of the quinoid model mixture.....	97
Figure 6.4: Percent change in absorbance vs. wavelength for the quinoid model (1,4benzoquinone-hydroquinone-phenol) after irradiation for 30 min at 350nm.....	98
Figure 6.5: Percent change in absorbance vs. wavelength for fulvic acid (17mg/L) and the quinoid model (1,4 benzoquinone-hydroquinone-phenol) with irradiation for 30 min under a nitrogen atmosphere.....	98
Figure 6.6: Percent change in absorbance vs. wavelength for fulvic acid (17mg/L with 1mg/L added phenol) and quinoid model (with 1mg/L added phenol).....	99
Figure 6.7: UV-Visible absorption spectrum of the quinoid model mixture: Ubiquinone-Hydroquinone-Phenol solution.....	102
Figure 6.8: Relative change in absorbance vs. wavelength for the quinoid model (Ubiquinone-hydroquinone-phenol) after irradiation for 5 min at 350 nm.	103

Figure 6.9: Relative absorbance change vs. wavelength for the quinoid mixture (Ubiquinone-hydroquinone- phenol;) irradiated for 30 min at 350 nm.....	103
Figure 6.10: Percent change in absorbance vs. wavelength for Laurentian fulvic acid (17mg/L) at pH 2 and pH 5 after irradiation for 30 min at 350 nm...	105
Figure 6.11: Ionic strength effect: Percent absorbance change vs. wavelength for fulvic acid (17mg/L) at pH 11 and at pH 11 with 1 M KCl.....	106
Figure 6.12: Percent absorbance change vs. wavelength for Laurentian fulvic acid at a concentration of 17mg/L and 9mg/L.....	106
Figure 6.13: Relative change in absorbance vs. wavelength for high molecular weight fraction solutions of Laurentian fulvic acid.....	107
Figure 6.14: Geometrical optimization semi-empirical PM3 calculations (aqueous) performed on 1,4benzoquinone-hydroquinone (quinhydrone), and a methyl substituted 1,4 benzoquinone-hydroquinone (quinhydrone) in water	111
Figure 6.15: Hypothetical 'monomer' structure of Laurentian fulvic acid.....	113
Figure 6.16: EPR of Mossy Point Fulvic acid and Quinonoid Model	117

1.1 Introduction

Humic substances are major organic light absorbers in natural waters and have been implicated in a number of important photochemical pathways. To begin to unravel the contributing steps in such pathways, we require knowledge of the primary photophysics and photochemistry of well-characterized humic substances.

The first portion of this chapter will introduce the properties of the well-characterized organic fraction of soils (fulvic acid) used in this study. The latter portion will outline the various photophysical and photochemical procedures and experimental methods employed in this work. It's intent is to provide an introductory view of the physical-chemical processes that will be described in order study the underlying mechanisms involved in oxidative photochemistry of natural water systems.

The main focus of this work is the evaluation of primary photoproduct quantum yields of fulvic acid. This required the use of three spectroscopic techniques: picosecond laser spectroscopy, magnetic circular dichroism spectroscopy and time resolved pulsed photoacoustic spectroscopy. Fulvic acid degradation depends upon the subsequent fate of the primary photoproducts. After determination of primary photoproduct quantum yields degradation studies were carried out with the use of solid state NMR and differential ultra-violet/visible spectra.

1.2 Organic Matter in Soil

Though typically comprising less than 5% of a productive soil, organic matter largely determines soil productivity. It serves as a source of food for microorganisms; undergoes

chemical reactions such as ion exchange; and influences the physical properties of the soil. Some organic compounds even contribute to the weathering of mineral matter, the process by which soil is formed. For example oxalate ion produced as a soil fungi metabolite occurs in soil as the calcium salts whewellite and weddelite. Oxalate in soils dissolves minerals, thus speeding the weathering process and increasing the availability of nutrient ion species. Some soil fungi produce citric acid and other chelating organic acids which can react with silicate minerals and release potassium and other metal ions held by these minerals (1.1, 1.6).

Biologically active components of the organic soil fraction include polysaccharides, amino sugars, nucleotides, organic sulfur and phosphorous compounds. Humus, described in detail below, is the most abundant organic component and makes up the bulk of the soil organic matter.

The accumulation of organic matter in soil is strongly influenced by temperature and availability of oxygen. Since the rate of biodegradation decreases with decreasing temperature, organic matter does not degrade rapidly in colder climates and tends to build up in the soil. In water and waterlogged soils, decaying vegetation does not have easy access to oxygen, and therefore organic matter accumulates. The organic content may reach 90% in areas where plants grow and decay in soil saturated with water.

The presence of naturally occurring polycyclic aromatic compounds is another interesting feature of soil organic matter. These compounds are sometimes the result of grass fires or forest fires (benzopyrene). Oxidation products include epoxides, quinones, phenols, aldehydes and carboxylic acids. It must be noted that quinones and lignins are present also as portions of biodegraded plant materials (1.1, 1.3, 1.7).

1.2.1 Soil Humus

Of all the organic components in soil, humus is by far the most significant. Saussure (1804) has been credited with introducing the term 'humus' (Latin equivalent of soil) to describe the dark colored organic matter in soil. Later, Dobereiner (1822) designated this dark colored component of soil organic matter as humus acid. The origin of the term humic acid to identify the alkali-soluble and acid insoluble fraction is somewhat obscure, but it was in common use at the time of Berzelius (1839). Wakesman (1936) pointed out that humus acid and humic acid were often used indiscriminately and seldom was there any differentiation made between the two. When distinguished, however, the former referred to the alkali extracted material whereas the latter referred to the precipitate obtained by subsequent acidification. Use of the term 'humin' then, to describe the alkali insoluble material had a similar development and was often used synonymously with humus coal (1.8).

After years of research, it became apparent that humic substances consisted of heterogeneous mixtures of compounds for which no single structural formula could be given. Humic substances have therefore been traditionally defined according to their solubilities. If a material containing humic substances is extracted with a strong base, and the resulting solution acidified, the products are:

- (1) a nonextractable organic residue called humin;
- (2) a material that precipitates from the acidified extract, called humic acid; and
- (3) organic material that remains in the acidified solution, called fulvic acid.

Because of their acid-base, sorptive, and complexing properties, both the soluble and insoluble humic substances have a strong effect upon natural water systems. In general, fulvic acid dissolves in water and exerts its effects as the soluble species. An understanding of the role

played by soluble fulvic acid is critically important to aquatic chemistry and aquatic photochemistry.

Fulvic acid is a complex heterogeneous mixture of polyelectrolyte macromolecules with a relatively high number of carboxylic acid functional groups. Molecular weights range from a few hundred to a few thousand. Functional groups will vary depending on where the samples were obtained. This present work involves the study of two well characterized fulvic acids (described below). Fulvic acid samples are an organic fraction taken typically from what is called a 'B' horizon podzol. In typical soils distinctive layers with increasing depth can be visible. These layers are called horizons. Horizons form as the result of complex interactions among processes that occur during weathering. Rainwater percolating through soil carries dissolved and colloidal solids to lower horizons where they are deposited. Biological processes, such as bacterial decay of residual plant biomass, produces slightly acidic conditions (due to the production of CO_2), organic acids, and complexing compounds that are carried by rainwater to lower horizons where they interact with clays and other minerals, altering the properties of the minerals. The top layer of soil, typically several centimeters in thickness, is known as the 'A' horizon, or topsoil. This is the layer of maximum biological activity in the soil and contains most of the soil organic matter. Metal ions and clay particles in the 'A' horizon are subject to considerable leaching (1.4).

The next layer is the 'B' horizon, or subsoil. It receives material such as organic matter, salts, and clay particles leached from the top soil. The 'C' horizon is composed of weathered parent rocks from which the soil originated. This study involves work of two well characterized organic fractions (see Appendix I) obtained from 'B' horizon podzols originating from (Mossy Point) P.E.I. and the Laurentians (Quebec), namely the Mossy Point fulvic acid and the

Laurentian fulvic acid, Figure 1.1 (1.11-1.15). With characterization information available relating changes in the observed photophysics to the physicochemical properties of the sample becomes possible.

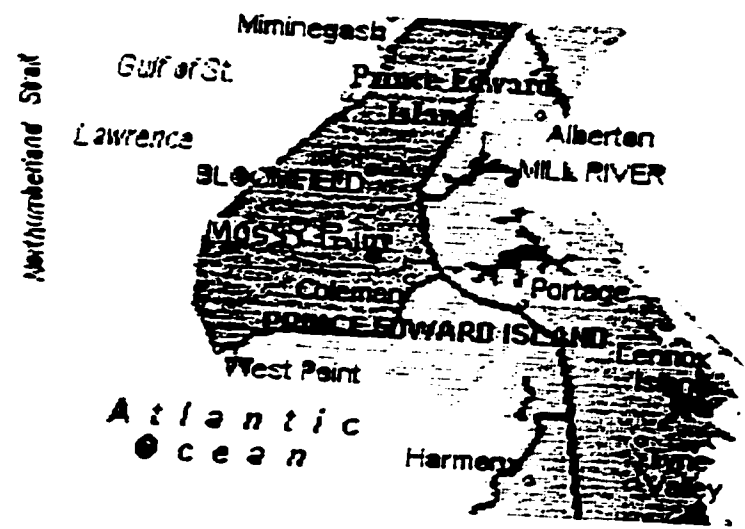


Figure 1.1: Map description of the two areas where soil samples were obtained. The two fulvic acid fractions have the following characteristics:

Elemental Analysis

<u>Element(%)</u>	<u>Mossy Point Fulvic Acid</u>	<u>Laurentian Fulvic Acid</u>
Carbon	49.52	45.1
Nitrogen	0.58	1.1
Hydrogen	4.6	4.1
Oxygen	45.3	49.7

Both have <1% ash, < 1ppm Fe and <3ppmNa

Molecular Weight Range

The number average molecular weight of 951 g mol⁻¹ as determined by vapor phase osmometry for the Mossy Point fulvic acid. The weight average values are significantly larger (1.14).

Functional Group Analysis

¹³C NMR: Characterization of functional groups found in Laurentian Fulvic Acid (1.15-1.20)

<u>Chemical Shift Assignment*</u>	<u>Chemical Shift Regions (ppm)</u>	<u>% C</u>
ketonic	220 - 190	8.8
quinone	190 - 178	15.7
carboxyl	178 - 165	17.2
phenolic/ hydroquinone	165 - 140	3
aromatic	140 - 96	15.6
carbohydrate/aliphatic alcohols	96 - 50	17.8
aliphatics	50 - 0	21.9

* (1.16-1.20)

Fulvic acid molecules are less aromatic in character and smaller than both humic acid and humin. Fulvic acid can be thought of as a flexible, heterogeneous polyelectrolyte mixture whose components may assume varied conformations. The conformation of fulvic acid is sensitive to changes in pH and background electrolyte concentrations. Both humic and fulvic acids are thought to be able to form micelle like structures at higher concentrations in natural waters. Their amphiphilic properties may allow them to form bilayer surface coatings on mineral grains in soils. These properties may also significantly increase the holding capacity of water in soils.

Structural complexity, diversity of functional group geometries and intramolecular interactions offer many possibilities for humic conformations. These characteristics allow humic material to function as surfactants, with the ability to bind to both hydrophobic and hydrophilic materials. In combination with colloidal behaviour these features make fulvic acid and humic acid effective agents in transporting both organic and inorganic contaminants in the environment. The tendency of these substances to interact with hydrophobic organic compounds as well as with heavy metals can have a major environmental impact. Binding (complexation) of contaminants to humic substances may alter the pollutants' fate either by sequestering contaminants or enhancing their transport (1.8, 1.9).

Photoprocesses

Light entering the upper layer of natural waters includes the visible and near-ultraviolet regions of the spectrum. In consequence, the vast majority of dissolved small organic molecules and simple inorganic ions are not important light absorbers. Their spectra lie too far in the ultraviolet wavelength range. The most important chromophores are, in fact, colloidal and fall into two main classes. The first class are "dissolved" organic materials that belong predominantly

to that heterogeneous mixture of polydisperse polymers called humic substances. The second class, are transition metal containing hydrous oxide colloids (1.21, 1.22, 1.23, 1.24).

The absorption spectrum of a typical and "well characterized" fulvic acid (Mossy Point) is shown in Figure 1.2 (1.24). It is quite striking that absorbance extends well into the red region and toward the near-infra-red. This presents more of a puzzle than has usually been acknowledged. The functional group content, degradation, and fractionation studies suggest that the lowest energy transitions are expected to be those of the phenol and carboxylate functional groups, which absorb in the near-UV region as monomers. Why does this small polymer display such profound red shifts? One factor is the degree of conjugation of the chromophores in the polymers. Another factor involves donor-acceptor, charge transfer complexes which appear commonly in polymer photophysics of organic molecules, in particular mixed quinone/hydroquinone-like systems. In this study we give prominence to the accumulating evidence favoring the latter factor to account for the origin of color. Similarities in photophysical behaviour of fulvic acid and quinoid solution mixtures will be described.

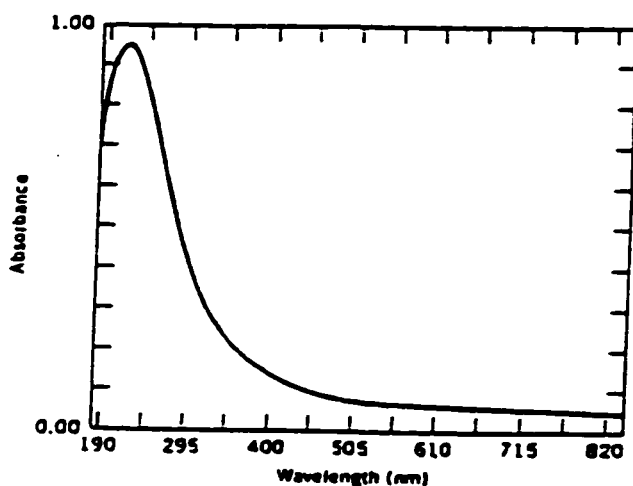


Figure 1.2: Absorption spectrum of Mossy Point fulvic acid (17mgL^{-1} ; pH4). Irradiation work took place between 337 - 355 nm.

Humic substances being the major light absorbers in natural waters will play a significant role in the regulation of natural waters (and the carbon budget) by their own photodegradation and by initiating the photochemical transformations of organic compounds. These reactions have been the subject of increasing study over the last several years. Much work on the photochemistry of natural waters have demonstrated that under solar irradiation, waters containing humic substances generate a variety of reactive intermediates and radicals. Intermediates identified include solvated electrons (picosecond time domain), excited triplet states of the humic substances (microsecond time domain), singlet oxygen (steady state), superoxide (steady state), and hydrogen peroxide (steady state) (1.21-1.33).

The diversity of the photochemistry observed in natural waters cannot be fully understood without a more detailed understanding of the primary photophysical and photochemical pathways by which excited humic chromophores yield reactive states and intermediates. Such detailed analysis must depend on humic materials that are as well defined as possible such as the Mossy Point and Laurentian fulvic acid.

This study is directed toward a description of the overall photophysics and primary photochemistry of the Mossy Point fulvic acid and the Laurentian fulvic acid. The diversity of the photochemistry observed in natural waters first produces a need to determine the primary photoevents and photoproducts formed by excited states of chromophores of the humics. Time-resolved picosecond spectroscopy, time-resolved pulsed photoacoustic spectroscopy, fluorescence quenching studies, as well as a variety of photolysis experiments have been the main tools used in order to elucidate the primary photophysical and photochemical pathways of the fulvic substances (1.34). The work

presented here began in the time domain of 20 psec and pursues the consequences of excitation out of the time domain of 16 days. This study also involved the development of a photochemical -photophysical 'mimic' of fulvic acid, as well as, molecular modeling work in order to complement the results derived from picosecond spectroscopy, magnetic circular dichroism spectroscopy, time resolved pulsed photoacoustic spectroscopy, and photochemical degradation studies.

A discussion of some theoretical aspects of organic photophysics and photochemistry will be given in Chapter 3. The results of primary photoproduct quantum yields for the three major primary photoproducts formed for fulvic acid (solvated electron, associated cation radical and excited state triplets) will be described in Chapters 4 and 5. Investigation of the primary quantum yields for the solvated electron and associated cation radical involves picosecond laser spectroscopy of the Laurentian and Mossy Point fulvic acid (Chapter 4). In Chapter 5 the results of the apparent triplet state quantum yields are presented. These apparent quantum yields were estimated by using Magnetic Circular Dichroism (MCD) spectroscopy to obtain the average triplet energy and then time resolved pulsed photoacoustic spectroscopy to obtain the energy storage associated with the triplet.

After determination of primary photoproduct quantum yields, degradation studies were carried out with the use of solid state NMR and analysis of differential ultra-violet/visible spectra. These results are presented in Chapter 6. These results include an intensive study of the photochemical activity of a variety of fulvic acid solutions for various irradiation times under different conditions of pH, background electrolyte, and concentration. The results of this work are correlated with the picosecond, MCD and time

resolved pulsed photoacoustic data. This chapter also describes the development and behavior of a photochemical / photophysical mimic of fulvic acid.

Finally, molecular modeling work (Spartan), PM3 semi-empirical calculations were used to investigate 'geometries' for a variety of complexes that may occur in fulvic acid, based on the photochemical / photophysical data, elemental analysis and ^{13}C NMR functional group data.

References

- 1.1 Jenny, Hans *Factors of Soil Formation*; Dover Pub. Inc., New York, 1994; pp 1-40.
- 1.2 Stevenson, F.J. *Humus Chemistry, Genesis, Composition, Reactions (2nd Ed.)*; John Wiley & Sons, Toronto, 1992; Chapter 1.
- 1.3 Sposito, G. *The Chemistry of Soils*; Oxford University Press, New York, 1989.
- 1.4 Fortescue, A.C. *Environmental Geochemistry*; Springer-Verlag, New York, 1980.
- 1.5 Elprince, A.M. *Chemistry of Soil Solutions*; Van Nostrand Reinhold, New York, 1989.
- 1.6 Bollag, J.M.; Stotzky, G. Soil Biochemistry; Vol.6, Marcel-Dekker, NY 1990.
- 1.7 Schwarzenback, R., Gschwerd, P.M., Imbodin, D.M. *Environmental Organic Chemistry*; John Wiley & Sons, Toronto, 1993.
- 1.8 Aiken, G.R.; McKinight, D.M.; Wershaw, R.L. *Humic Substances in Soil, Sediment and Water*; John Wiley & Sons, Toronto, 1985.

- 1.9 Buffle, J. *Complexation Reactions in Aquatic Systems. An Analytical Approach*; Ellis Harwood Ltd., Chester, U.K., 1988.
- 1.10 Suffet, I.H.; MacCarthy, P. *Aquatic Humic Substances, Influence on Fate and Treatment of Pollutants*; Advances in Chemistry, Series 219, ACS, Washington, DC, 1989.
- 1.11 Roach, K.B. Msc. Thesis, Concordia University, Montreal, 1983.
- 1.12 Power, J.F. PhD Thesis, Concordia University, Montreal, 1986.
- 1.13 Hansen, E.H.; Schnitzer, M.; *Anal.Chim.Acta*, 1969, 46, 247.
- 1.14 Underdown, A.W.; Langford, C.H.; Gamble, D.S., *Anal.Chem.*, 1981, 53, 2139-2140.
- 1.15 Cook, R.L.; PhD Thesis; University of Calgary, 1997.
- 1.16 Thorn, K.; Arterburn, J., Mikita, M., *Environ.Sci.Tech.*, Vol.30, 1992, No.1, 107-116.
- 1.17 Breitmaier, E. *Structure & Elucidation by NMR in Organic Chemistry*; John Wiley & Sons, New York, 1993.
- 1.18 Williams, D.H.; Fleming, I. *Spectroscopic Methods in Organic Chemistry, 7th Edn.*; McGraw Hill (UK) 1989.
- 1.19 Levy, G.C. *Carbon 13 NMR Spectroscopy, 2nd Edn.*; Wiley Interscience, NY, 1980.
- 1.20 Kalinowski, H.O. *¹³C NMR Spectroscopy - High Resolution Methods and Applications in Organic Chemistry and Biochemistry, 3rd Edn.*; Wiley, 1990.
- 1.21 Helz, G.R.; Zepp, R.G.; Crosby, D.G. *Aquatic & Surface Photochemistry*; Lewis Publishers, London, 1994.

- 1.22 Choudhry, G.G.; *Toxicol. Environ. Chem.*, **1981**, *4*, 261-295.
- 1.23 Cooper, W.J.; Petasne, R.G.; Zika, R.G.; Fischer, A.M.; *ACS Symp. Ser. 219*, **1989**, 333- 362.
- 1.24 Bruccoleri, A.; Lepore, G.; Langford, C.H. *Environmental Oxidants*; Chapter 7, The Physical Chemistry of Photochemical Oxidant Generation in Natural Water Systems; 1994, 187-219.
- 1.25 Choudhry, G.G. *Humic Substances- Photophysical and Free Radical Aspects and Interactions With Environmental Chemicals*; Gordon and Breach Science Publishers, NY, 1984.
- 1.26 Frimmel, F.H.; *Environ. Int.*, **1994**, *20*, 373-385.
- 1.27 Minero, C.; *Chemosphere*, **1992**, *24*, 1597-1606.
- 1.28 Klopffer, W.; *Sci. Total Environ.*, **1992**, *123/124*, 145-159.
- 1.29 Aguer, J.P.; *J. Photochem. Photobiol. A: Chem.*, **1996**, *103*, 163-168.
- 1.30 Frimmel, F., et al.; *Environ. Sci. Technol.*, **1987**, *21*, 541-545.
- 1.31 Haag, W.R.; Hoigne, J.; *Environ. Sci. Technol.*, **1986**, *20*, 341-348.
- 1.32 Lean, D.R.S.; *Prepr. Pap., 203rd Am. Chem. Soc. Natl. Meet., Vol. 32*, No. 1, pp. 80-83, **1992**.
- 1.33 Zafiriou, O.C.; *Prepr. Pap., 203rd Am. Chem. Soc. Natl. Meet., Vol. 32*, No. 1, pp. 76-79, **1992**.
- 1.34 Bruccoleri, A.; Pant, B.C.; Sharma, D.K.; Langford, C.H.; *Environ. Sci. Technol.*, **1993**, *27*, 889-894.

Chapter 2: Experimental

Materials and Methods of Preparation

The fulvic acids used in the present study were extracted from the two soils by the same procedure. In each case, two kilograms of air dried soil was extracted with 20 L of 0.5 M NaOH overnight with occasional shaking. Suspended solids were then removed by settling and centrifuging at 5000 rpm for ten minutes. The extracts were passed through two columns in succession containing Dowex 50W-X8, 20-50 mesh size cation exchange resin in the protonated form. The two columns were a roughing column, 1 m long x 8.5 cm diameter, and a finishing column, 55 cm long x 4.6 cm diameter. The flow rate for both columns was kept at about one drop per second. Atomic absorption tests were performed to determine the concentration of sodium, iron and other metals in the fulvic acid. Acceptable limits are metal concentrations below 1 ppm (solid). When the pH of the effluent from the roughing column rose above 7, the column was regenerated by 0.1 M HCL followed by rinsing with doubly distilled water. The ion exchanged solution was freeze dried in a cabinet type freeze dryer in trays holding 2 L portions. The freeze dried fulvic acid powder was subsequently stored in tightly stoppered flasks in the dark. 'High' molecular weight fractions of fulvic acid were obtained by retaining the portion of Laurentian and Mossy Point fulvic acid solutions that were passed through a YM30 (nominal cutoff 30000 daltons; Sigma Chemical) filter membrane. 'Low' molecular weight fractions refers to the freeze dried filtrate of Laurentian and Mossy Point fulvic

acid solutions that passed through a YM2 (nominal cutoff 1000 daltons; Sigma Chemical) filter membrane.

Fulvic acid stock solutions were prepared at a concentration of 150 mg/L in nano-pure distilled water. The stock solutions were protected from exposure to light and discarded after one week. Fulvic acid solutions that were pH adjusted were allowed to equilibrate for 24 hr in the dark. The pH was adjusted using NaOH or HCl. Both compounds were obtained from Aldrich Chemicals (analytical grade). The standard used in the time-resolved pulsed photoacoustic experiments in order to calibrate the energy of the photoacoustic signal is the compound was tris(5 methyl - 1- 10 - phenanthroline) ferrous perchlorate which was obtained from Smith Chemical Company. Conventional fluorescence quantum yield measurements were standardized using quinine sulphate from Aldrich Chemicals.

The following chemicals were used for the quinone model mixtures and were obtained from Sigma Chemical: 1,4 benzoquinone, 2,5 dihydroxy- benzoquinone, phenol and hydroquinone. All solutions were prepared in the dark in the following manner:

- 1) In all cases the aqueous solutions were prepared to have molar ratios of quinone to hydroquinone and phenol of 1:3:3.
- 2) Solutions were prepared so that maximum absorbance was approximately 1 at 250 nm..
- 3) Solution preparation always involved a first step of mixing (in the dark while stirring) the quinone and hydroquinone first and allowing the solution to stir for approximately 40 minutes before adding the phenol. The solution was then left (with stirring) in the dark for 24 hrs.

The temperature in all cases was maintained at 20 C.

Equipment

Absorption Spectra

Absorption spectra of solutions were measured using a Hewlet Packard 8452A Diode Array Spectrophotometer. It is a single beam, microprocessor controlled, UV-VIS spectrophotometer with collimating optics. This instrument operates from 190 to 820 nm with a spectral resolution of 2 nm. It was controlled by an IBM PC with an HP UV/VIS software package. A 1cm path quartz sample cell was used for all measurements. The reference beam blank was always water.

Fluorescence

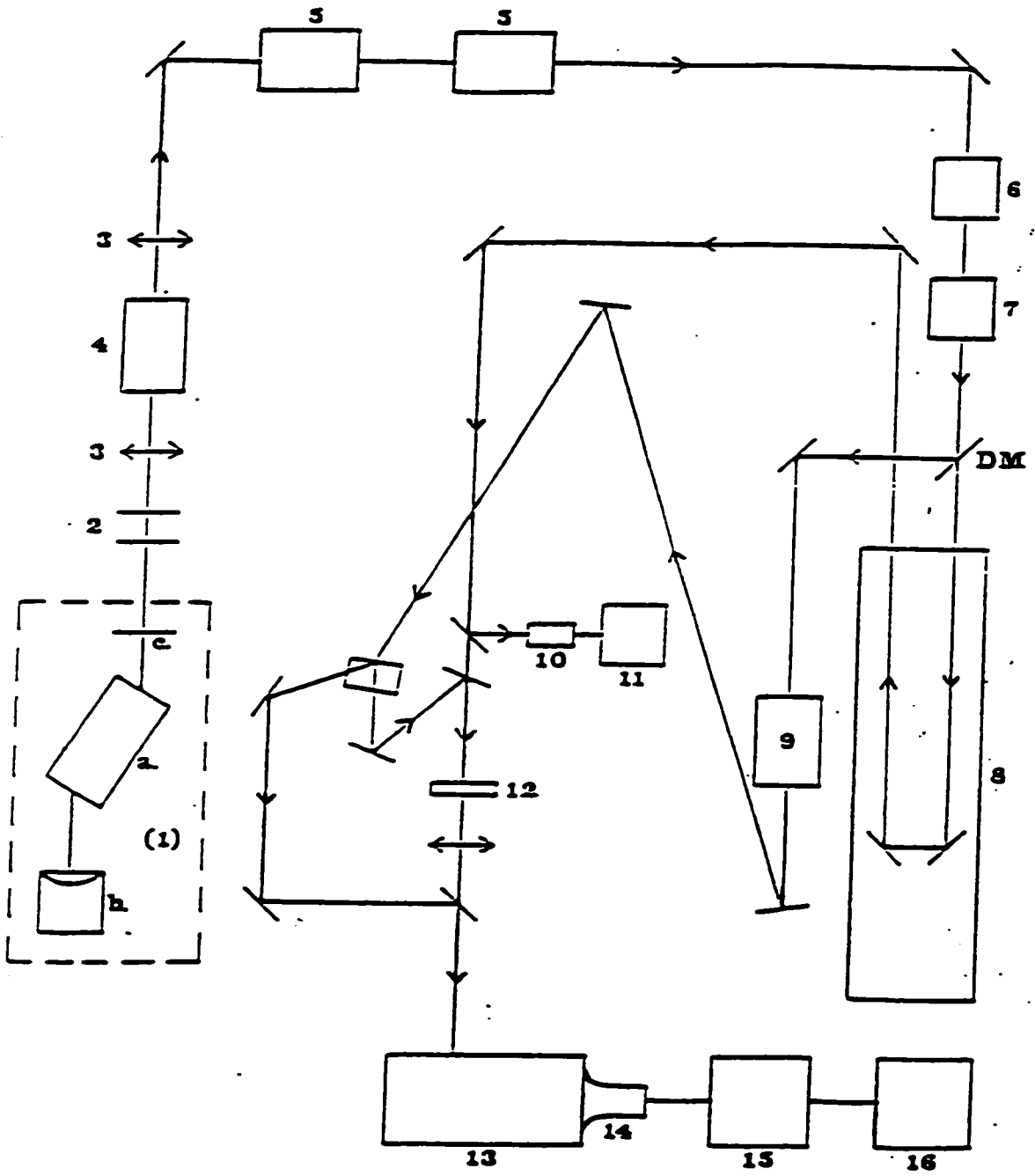
Fluorescence measurements were made with a Perkin-Elmer Model 650-10S scanning spectrophotometer designed for the measurement of fluorescence excitation and emission spectra. The source is a 150 W xenon lamp that is mounted vertically. Spherical lenses focus the source on an entrance slit that is oriented horizontally. The light beam from the xenon lamp is made monochromatic in the excitation monochromator. Fluorescence light from the sample, after passing through the emission monochromator, is detected by the photomultiplier and amplified for transmission to the recorder.

Picosecond Laser Spectroscopy

Transient absorption spectra of Mossy Point and Laurentian fulvic acid samples at different pH values, at a time resolution of 20 ps, were recorded at the Canadian Center for Picosecond Laser Flash Photolysis (CCPLFP) at Concordia University in Montreal. Picosecond laser flash spectroscopy of various fulvic acid solutions at different pH values were carried out in order to determine the quantum yields of solvated electron production and the associated cation radical in the two sets of fulvic acids, Mossy Point and Laurentian. All fulvic acid solutions were prepared fresh as described previously, kept in the dark and allowed to equilibrate for 24 hr before any conventional UV-VIS absorption spectra were determined or any picosecond (20 ps) transient absorption spectra were measured. The picosecond laser system was built by Dr. D.K. Sharma and Professor Nick Serpone at Concordia University and has been described (2.1). The picosecond system is schematically represented in Figure 2.1:

Figure 2.1: Schematic representation of the picosecond flash photolysis experimental setup.

1. Laser: - Head
- Mode-locking cell
- Mirror
 2. Beam expander
 3. Glann-Air Polarizers
 4. Pulse selector
 5. Amplifiers
 6. Second harmonic crystal
 7. Third harmonic crystal
 8. Delay ramp
 9. Continuum cell
 10. Energy detector
 11. Energy meter
 12. Sample cell
 13. Double monochromator
 14. Photodiode array detector
 15. Multichannel analyzer
 16. Computer
- DM Dichroic mirror



The light source is a mode locked Nd:YAG laser (Spectra Physics) having a cavity length of 1.1 m. The passive mode-locking is done with the dye Q-switch I (Kodak, 9470) contained in a specially designed cell (Quantel). The output of the oscillator is a train of 12 pulses at 1064 nm with a pulse width of 30 ps and separated by 6.5 ns. The energy of the pulse is approximately 80 μ J. The beams are expanded before entering the pulse selector to avoid damage to the polarizer. The train of pulses coming from the oscillator are passed through a cross-polarizer to remove any vertical component of the light. The train of pulses then pass through a birefringent crystal which changes the polarization of one pulse. The change in polarization is due to a short voltage pulse of 3.6 kV applied to the crystal following the trigger signal from the earlier pulses. At this point the beam passes another cross-polarizer which is vertically polarized and which lets through only the pulse that had its polarization changed in the crystal. This set of two cross-polarizers and birefringent crystal is called the pulse selector (Quantel, PF 302). The polarized pulse is then passed through 2 amplifiers resulting in an average energy of 80 mJ/pulse. The light then passes through a frequency doubler crystal (potassium dihydrogen phosphate) for second harmonic generation and then a third harmonic crystal which is also made of potassium dihydrogen phosphate. The difference between the two crystals is in the cut of the crystal. The frequency doubler is a class II crystal so it takes the circularly polarized light and gives horizontally polarized light. About one fifth of the 1064 nm light is converted into 532 nm (20 mJ) light. The 1064 nm and 532 nm light are combined in the third harmonic crystal (Class I) to give vertically polarized 355 nm light (3mJ). This was the wavelength used for excitation of all fulvic acid transient absorption spectra. Dichroic mirrors are then used to separate the different wavelengths. The 1064

nm pulse is sent through a D_3PO_4 solution to generate a continuum light pulse. The probe continuum pulse is split into two. One part is focused into the sample cell (reading pulse) and the other part is passed beside the cell and is used as the reference pulse. The second or third harmonic pulses can be used as the pump pulse. Here all results use the third. A ramp delay varies the time of arrival of the pump pulse through the sample cell compared to the probe pulse between 0 ps and 11 ns. The time delay used in all the fulvic acid experiments was 20 ps since earlier work (2.1) had demonstrated that solvated electrons and the corresponding radical appear within 20 ps.

The reference and reading pulses are passed through a double monochromator and sent to a photodiode array detector. A multichannel analyzer reads two arrays of 250 photodiodes. The photodiode readings correspond to specific wavelengths. The results are then passed on to the computer. The two arrays 'I₀' and 'I' (reference and reading pulse respectively) are stored in memory and processed to calculate absorbance at each wavelength. During the first laser shot, the pump beam is blocked so that I₀ and I values correspond to the ground state absorption. Following this, measurement is made of the absorption of the sample following the pump pulse and I₀ and I for the excited state may be obtained. Usually 6 - 15 shots are taken for the ground state absorption and the same number for the excited state absorption at the time delay chosen. Usually rejection of a measurement may arise because the energy of the pump pulse may be too high or low or because a bad continuum pulse is generated in the D_3PO_4 cell.

The computer calculates the absorbance of the sample for each shot ($A = \log I_0/I$) and calculates an average for the sum of the shots done for the ground state and the time

delayed excited state (here 20 ps). The noise on each shot is calculated by the computer software by the equation:

$$N_i = \sum_k \frac{(A_{ik} - A_k)^2}{A_k}$$

where N_i is the noise for the curve I, A_{ik} is the value of absorbance of that shot at the wavelength k, and A_k is the average absorbance value at the same wavelength for all the shots on a specific state. For solutions containing colloidal particles the noise of each curve would be expected to be higher due to light scattering by the particles.

Nevertheless the fulvic solutions used in these experiments did not pose any problems with respect to noise and light scattering. The computer then subtracts the absorbance of the ground state from the absorbance of the excited state. The result is a ΔA (absorbance change) value for every wavelength.

Magnetic Circular Dichroism Spectroscopy

The MCD spectra were recorded by Dr. B. Hollebone at Carleton University, Ottawa (2.2). Fulvic acid solutions were prepared fresh with nano-pure distilled water in Ottawa in the same manner as described earlier. A 24 hour equilibration period was allowed for all solutions. The concentrations of the fulvic acid solutions studied were 20 ppm.

The MCD spectra were recorded on a custom built spectrophotometer (2.3). The light from a 150 W Xenon lamp passes through a double beam monochromator followed by a beamsplitter which sends 20 percent of the radiation to a reference channel. The remaining light goes through a linear polarizer (Quantel) and then a photoelastic modulator crystal (Quantel), the last element in the optic array. The modulator transforms

the radiation into left and right circularly polarized light. The applied electric field creates in the crystal an alternating linear birefringence, whose sign and magnitude depend on the instantaneous value of the modulation voltage. The circularly polarized light then passes through the sample cuvette which is placed in a uniform magnetic field oriented such that the field is parallel to the propagation direction of the beam of circularly polarized light. The transmitted radiation is detected by the photomultiplier. Absorption by the sample gives rise to a small 50 kHz alternating current signal which exits from the preamplifier. The signal is fed to a lock-in amplifier which receives the reference signal from the photoelastic modulator. The lock-in-amplifier discriminates the 50 kHz signal from noise at different frequencies and registers the circular differential absorbance (ΔA). An analog digital converter then plots the information on a personal computer.

Circular dichroism and magnetic circular dichroism are based on the difference in the molar absorptivity of left and right circularly polarized light. The differences in the two techniques stem from their origins. Circular dichroism is caused by inherent structural dissymmetries in the molecule or its environment. Magnetic circular dichroism is the consequence of normal longitudinal Zeeman effect interactions, and as a result can characterize symmetry and angular momentum properties of the ground and excited state. The shape and magnitude of MCD spectra are strongly influenced by degeneracies and near degeneracies in electronic energy levels associated with the degree of rotational symmetry experienced by electrons of the chromophore and, through spin orbit coupling, by degeneracies due to spin. Magnetically induced optical activity is frequency dependant and is proportional to the applied field.

The Faraday effect is only subtly related to natural optical activity. In natural optical activity, the chiral field perturbing the chromophore is within the molecule itself and therefore has a fixed geometrical relation to the chromophore no matter what the orientation of the molecule. In magnetic optical activity, the external magnetic field acts

as the perturbing force on the electronic states of the chromophore and as a result the MCD may not directly represent the molecular geometry of the molecule.

The magnetic field can induce three types of effects in a transition to manifest CD. These effects have been denoted A, B and C terms. Consider first a transition from a ground state to some non-degenerate excited state. If circularly polarized light is used, two transitions, each caused by the absorption of left and right circularly polarized light occur at the same energy, resulting in no net CD. If the excited state of this transition is degenerate the applied magnetic field splits it into equal higher and lower energy levels by the Zeeman effect. These magnetically differentiated transitions absorb left and right circularly polarized light with equal intensity but of opposite sign. If these lineshapes are superimposed the result is an A term, which appears as a symmetrical biphasic signal.

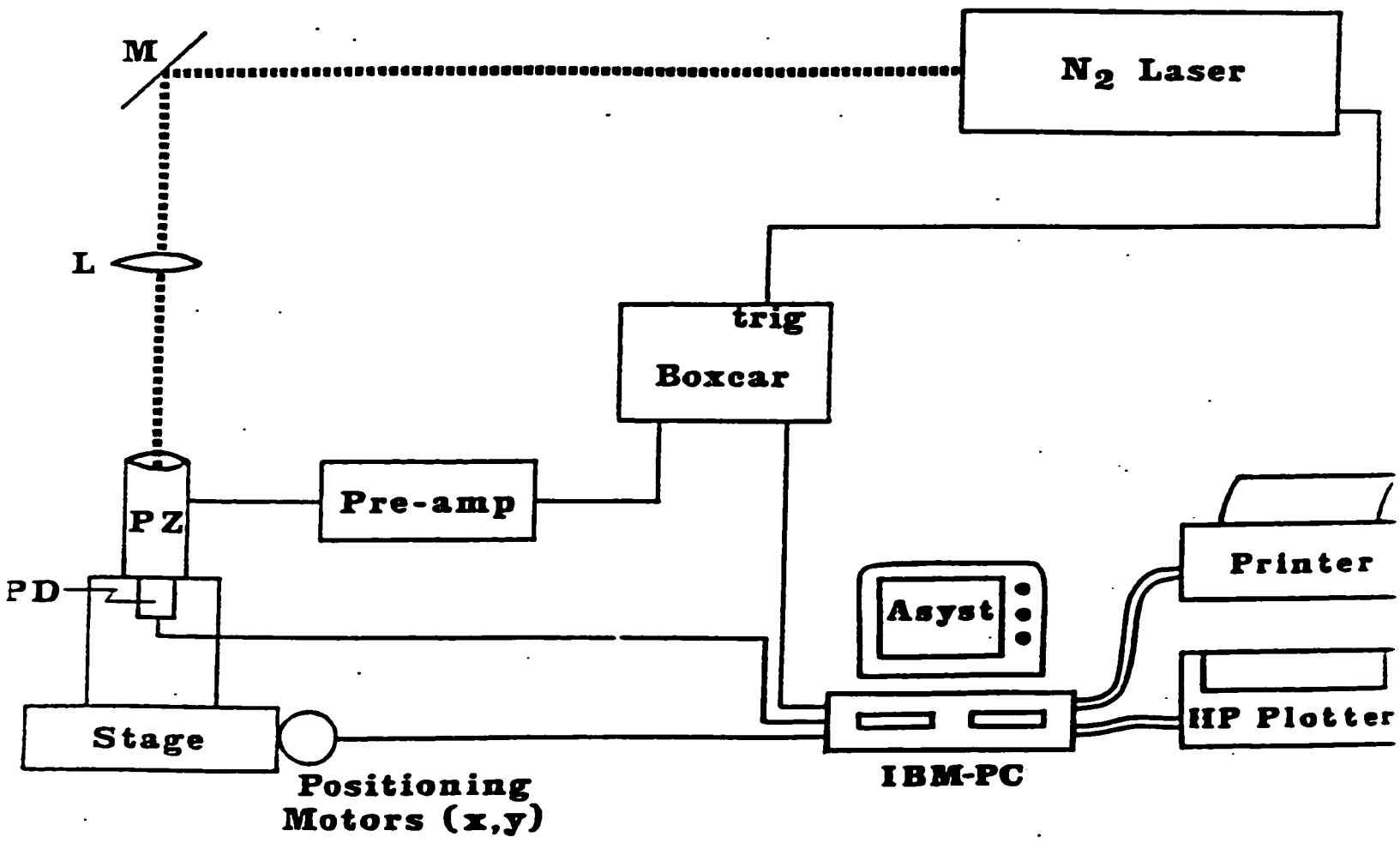
A different lineshape results when a transition takes place from a degenerate ground state to a nondegenerate excited state. As before, each split transition differentially absorbs circularly polarized light resulting in bands of opposite sign. Transitions from the lowest energy level however, have a greater intensity due to a greater Boltzmann population. The resultant MCD spectrum is called a C term. The asymmetry of the C term is inversely proportional to the absolute temperature.

The B term usually has a component of only one sign. It is similar in appearance to an extreme C term but shows no temperature dependence. The B term is ubiquitous in the MCD spectra of organic compounds and arises from the magnetically induced mixing of energy levels that are not degenerate.

Time Resolved Pulsed Photoacoustic Spectroscopy

The photoacoustic data were obtained using a time resolved photoacoustic detection system built by Claude Arbour (2.4) (Figure 2.2). The system consists first of a

nitrogen pulsed laser (PRA-LN 100). The wavelength output consists of a pulse of 30 μJ at 337.1 nm. The pulsewidth was adjusted to 300 ps. The laser can be run at frequencies up to 100 Hz. The laser pulse is focused into the sample cell. The cell consists of a piezoelectric detector tube (PZ5-A, Lead Titanate Zirconate piezoelectric ceramic). The tube has an inner radius of 1.25 cm and a length of 1.00 cm. A quartz window was glued to the bottom of the piezoelectric tube and the sample solutions could be poured directly into the piezoelectric detector. The piezoelectric cell is mounted over a photodiode positioned at the center of the cell. The signal of the photodiode is read by the computer (IBM PC) which controls the movement of two positioning motors to ensure that the laser pulse is centered in the piezoelectric cell. The photoacoustic signal is amplified by a preamplifier (Ithaco Model 1201) and sent to a boxcar signal averager (PAR Model 162-164). In the amplifier, the signal is filtered to remove all frequencies lower than 3 kHz and higher than 100 kHz. The signal is processed in the boxcar signal averager before being sent to the computer. A schematic representation of the photoacoustic detection system is illustrated in Figure 2.2. The laser pulse coming from the nitrogen laser is reflected inside the piezoelectric (PZ) by the mirror (M) after passing through a lens (L). A photodiode (PD) ensures that the laser pulse is directed into the center of the piezoelectric cell. The photoacoustic signal is passed by a preamplifier before being sent to the boxcar signal averager. The computer controls the movement of the positioning motors as well as collecting data.



PHOTOACOUSTIC SYSTEM

Figure 2.2: Photoacoustic system.

Typical photoacoustic experimental conditions are shown below:

Component	Parameters
Laser	Frequency: 10 Hz Energy per pulse: 20 - 60 μ J
Pre-amplifier:	High pass filter: 3 kHz Low pass filter: 100 kHz
Pre-amplifier:	Amplification: 1000 times
Boxcar signal averager:	Integration time: 1 μ s Aperture delay: 20 μ s Percent aperture delay: 15- 65 % Aperture duration: 50 ns

The experimental conditions for the time processing of the photoacoustic signal are set by the experimentalist. The time processing starts with each trigger from the laser and it can be represented by a window which is moved along the signal according to a defined pathway. This pathway follows a voltage ramp sent by the computer to the boxcar signal averager. The position of the window with regard to the trigger is defined according to the equation:

$$W. T. = (\% A.D. + 0.1 V_c) A.D.T.$$

where %A.D. is the initial percent aperture delay, V_c is the voltage sent by the computer and A.D.T. the aperture delay time. The first position of the window will be at %A.D. x A.D.T. since the voltage sent by the computer is 0 V. For a typical experiment, the first position of the window will be at 3 μ s after the trigger. Since the increase is usually 1%, the next position will be at 3.2 μ s. The window will then be moved like this along the signal up to the last value (typically 65%) required by the experimentalist. The computer reads the signal coming out of the boxcar signal averager at each position of the window.

The signal at one position of the window is averaged by the boxcar. The computer starts to read the value of the signal after approximately 50 pulses and stores 100 values to do an average. This process goes on for every position of the window. The overall signal is then a value for every position of the window which creates the acoustic wave seen on the computer.

The signal obtained at the end of the experiment is a wave of frequency equal to the traveling time of the sound in the solution. The first maximum in the wave is the result of the formation of the first acoustic wave in the solution and the other maxima are the result of the echoes. Time resolution is limited by the traveling time of the acoustic wave in the illuminated region of the sample in the piezoelectric cell. This corresponds to a time resolution of approximately 2 microseconds. The sensitivity of the instrument is approximately $7.5 \times 10^{-10} \text{ VJ}^{-1}$.

All steps of the experiment are controlled by a computer through an A/D interface (DT-2801, Data Translation). The data acquisition and analysis was implemented using the ASYST (Macmillan Software) package .

¹³C Nuclear Magnetic Resonance Spectroscopy

Solid state ¹³C NMR spectra were obtained with the help of Mrs. Qiao Wu and Dr. Robert Cook, using a Bruker AMX2-300 spectrometer with a BL4 probe using a ramped cross polarization magic angle spinning technique developed by Robert Cook (2.5). Spectra were obtained at 75.469 MHz at a contact time of 3 ms and a sample

spinning rate of 8 kHz. These parameters follow optimization reported in Cook et al. (2.6).

Photoreactor - Photochemical Studies

The photoreactor used is a Rayonet Reactor (The Southern New England Ultraviolet Company) and operates on a 120 V , 60 cycle current line. The reactor contains 16 lamps (RPR - 350) emitting radiation with wavelength centered at 350 nm.

Computational Chemistry

Molecular modeling, geometrical optimization and energy calculations were performed on an IBM RISC-6000 system at The University of Calgary using the software program Spartan (Version 2.0, Wavefunction Inc.).

References

- 2.1 Power, J.F.; Sharma, D.K.; Langford, C.H.; Bonneau, R.; Jousset-Dubien, J.; *ACS Symp. Ser.*, **1987**, *327*, 157-173.
- 2.2 Bruccoleri, A.; Pant, B.C.; Sharma, D.K.; Langford, C.H.; *Environ. Sci. Technol.*, **1993**, *27*, 889-894.
- 2.3 Hollebhone, B.R.; Langford, C.H.; Malkhasian, A.Y.; *Can. J. Chem.*, **1985**, *V.67*, 7, 1918-1921.
- 2.4 Arbour, C.; PhD Thesis, Concordia University, Montreal, 1987.
- 2.5 Cook, R.L.; PhD Thesis; University of Calgary, 1997.
- 2.6 Cook, R.L.; Langford, C.H.; Yamdagni, R.; Preston, C.M.; *Anal. Chem.*, **1996**, 68, 3979.

Chapter 3 Theoretical Aspects of Organic Photophysics and Photochemistry

3.1 Introduction

This chapter will provide a description of the photophysical and photochemical processes involved in organic compounds similar to those found in the two, well-characterized fulvic acid samples (Mossy Point and Laurentian fulvic acid) which are described in detail in Chapter 1. These molecules, having similar functional groups to fulvic acid will undergo similar electronic transitions when irradiated in the near ultra-violet region of the spectrum. Identification of the major electronic absorption transitions of representative organic molecules will be made and these will be related to the spectroscopic properties of fulvic acid. A discussion will follow that will include a description of : intersystem crossing, fluorescence, phosphorescence and photochemical reaction of such compounds.

3.2 Photophysics - Introduction of Terms

Photophysical processes may be defined as transitions which interconvert electronically⁴ excited states among each other or excited states to the ground state or the reverse. The important photophysical processes are classified as 'radiative' and 'radiationless' processes. Commonly encountered radiative processes have the following characteristics:

1. 'Zero-Order- Allowed' singlet to singlet absorption, which is electronic excitation from a ground singlet state to an excited singlet state.
2. 'Zero-Order - Forbidden' singlet to triplet absorption. Here electronic excitation occurs from a ground state singlet to an excited triplet state.
3. 'Allowed' singlet excited state to singlet ground state emission, called fluorescence.

4. 'Forbidden' triplet excited state to singlet ground state emission, called phosphorescence.

Commonly encountered photophysical radiationless processes include:

1. 'Allowed' transitions between states of the same spin, called internal conversion. That is, a radiationless transition occurs between an excited singlet state and a ground singlet state with the evolution of heat.
2. 'Forbidden' transitions between excited states of different spin, called intersystem crossing. Here a radiationless transition occurs between an excited state singlet to an excited state triplet with the evolution of heat.
3. 'Forbidden' radiationless transitions occur between triplet excited states and the ground state singlet with the evolution of heat. This is also called intersystem crossing.

3.3 Electronic excitation of representative organic compounds in the near ultra violet

Molecular absorption in the ultraviolet and visible region of the spectrum is dependent on the electronic structure of the molecule.

Electronic transitions that can occur in organic molecules excited by radiation in the near ultra violet and visible region are summarized in Figures 3.1 and 3.2 below (3.1):

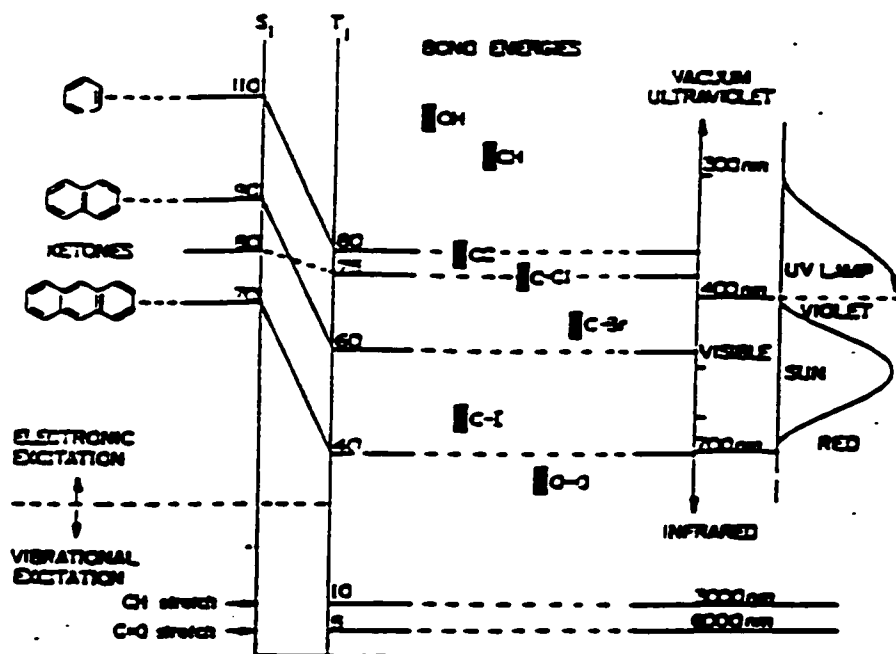


Figure 3.1: Type of excited state energies of electronic states of organic compounds, where S_1 and T_1 are the singlet and triplet excited states, respectively (kcal/mol) (3.1).

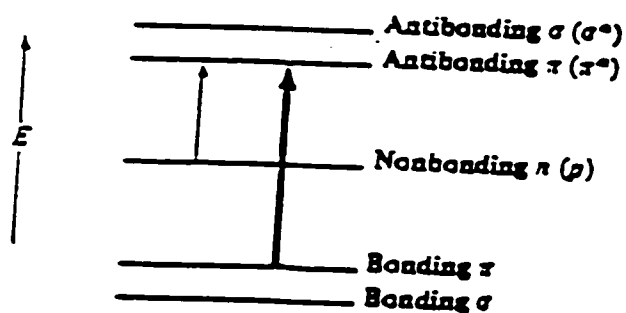


Figure 3.2: Summary of electronic energy levels of unsaturated organic compounds with a heteroatom. Both n, π^* and π, π^* transitions are represented (3.1).

In this figure n,π^* and π,π^* refer to transitions of an n-orbital electron and π -orbital electron to a π -anti-bonding orbital, respectively. Although the energy changes in the figures are not shown to scale, it can be readily seen that an n,π^* transition requires less energy than a π,π^* transition or σ,σ^* transition. Unsaturated organic compounds containing a heteroatom such as oxygen or nitrogen, are present in fulvic acid, may undergo n,π^* and π,π^* transitions when irradiated in the near ultraviolet or visible region of the spectrum. As was described earlier, only radiation in the 337 nm - 355 nm region of the spectrum was used in the photophysical and photochemical study of the fulvic acid solutions. Given the functional group profile (Chapter 1) of these two fulvic acids and the excitation wavelengths used in the study, it is expected that the initial photophysical event will be that of an n,π^* excited state transition. Some π,π^* character will be involved in this transition as will be discussed later (through state mixing).

The electronic absorption spectra of some representative organic compounds (quinones) which undergo n,π^* and π,π^* transitions are shown in Figure 3.3 below (3.3). The most simple spectrum, that of 1,4-benzoquinone, has an intense absorption band (I) near 240-250 nm (π,π^* 'allowed' transition), and two weak bands (II and III) at about 285nm and 434nm respectively. The weak quinonoid n,π^* absorption transitions are 'forbidden' and consequently have low intensity.

The spectra of naphthoquinones, anthraquinones and higher quinones are considerably more complex. The main absorption bands of 1,4-naphthoquinone are at 245, 257 and 335nm (Figure 3.3) and those of anthraquinone at 243, 263, 332 and 405nm (3.3).

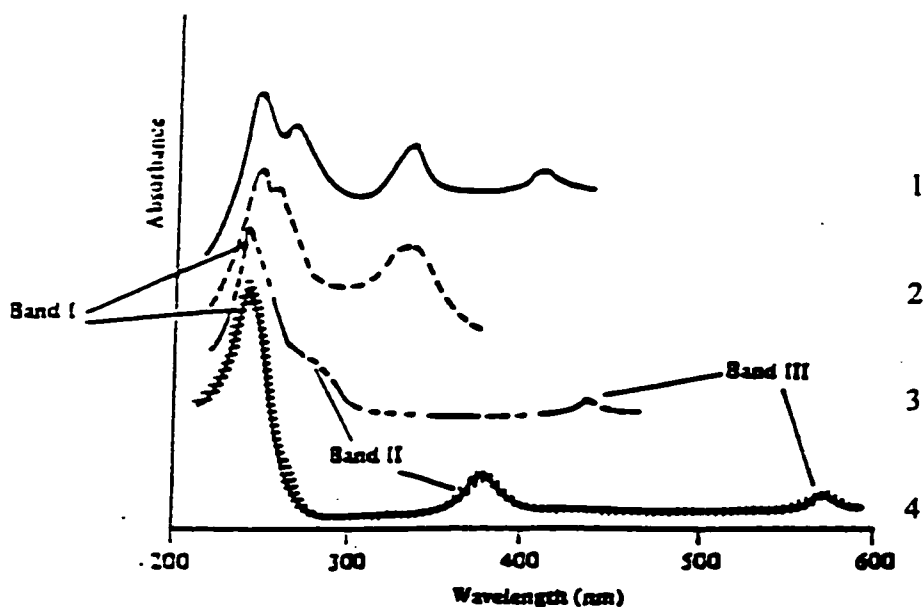


Figure 3.3: The main absorption bands in the electronic spectra of anthraquinone (1), 1,4-naphthoquinone (2), 1,4-benzoquinone (3) and 1,2-benzoquinone (4). The intensities (log scale) of the bands for each compound are only approximate, and no comparison between relative intensities of absorption bands of different compounds is implied (3.3).

Substituent groups influence quinone spectra greatly. Introduction of a substituent into 1,4-benzoquinone produces only small effects on bands (I and III) but band (II) undergoes a significant red shift, in the order -Me (27 nm), -OMe (69 nm), -OH(81 nm). Substituted benzoquinones can therefore absorb in the visible and appear colored.

Absorption spectra of some representative organic structures that occur in humic substances (aromatic aldehydes and ketones) are illustrated in Figure 3.4 below (3.4). All show stronger absorption intensity π,π^* bands at shorter wavelengths and weaker, less intense n,π^* bands at longer wavelengths.

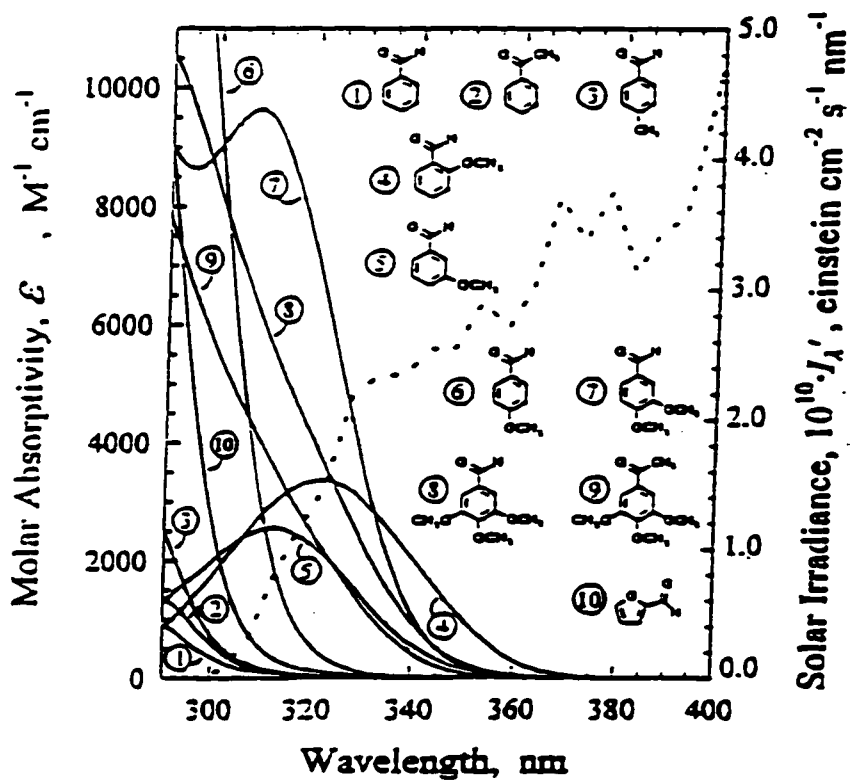


Figure 3.4: Absorption spectra of some aromatic aldehydes and ketones (solid lines). The dotted curve represents solar irradiance for a solar zenith angle of 36 degrees (3.4).

The electronic absorption spectra of many quinoid radicals (semiquinones), formed in the process of irradiation, also absorb in the visible and can form overlapping bands in this region, Figure 3.5- 3.6 (3.5).

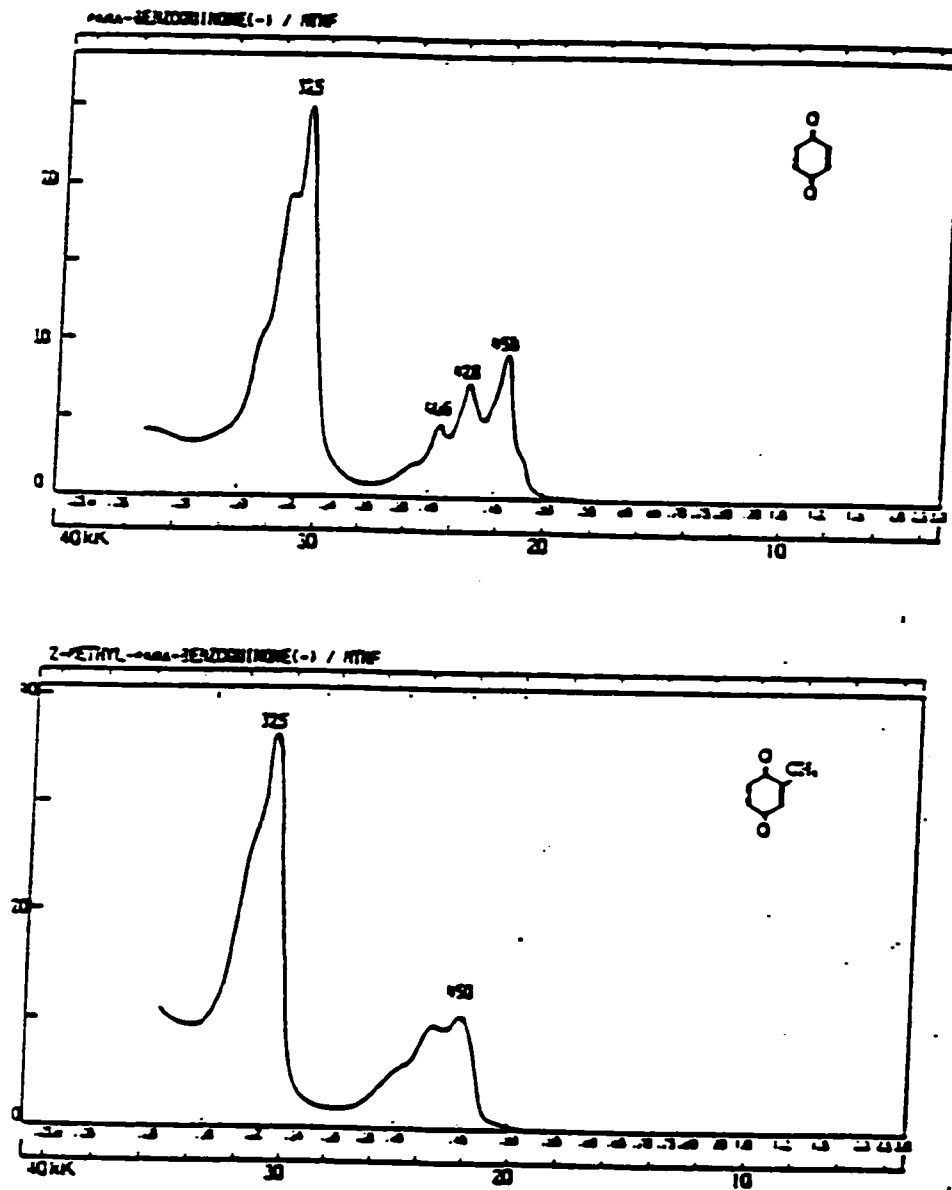


Figure 3.5: The electronic absorption spectra of a variety of quinone radicals (3.5).

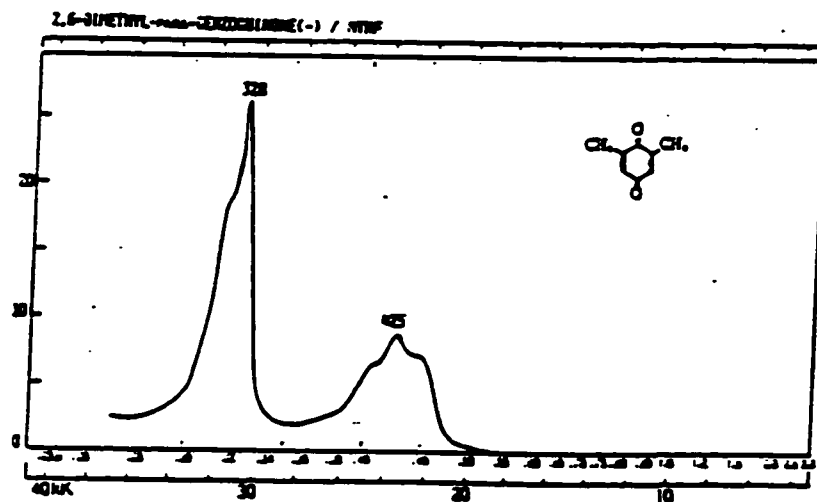
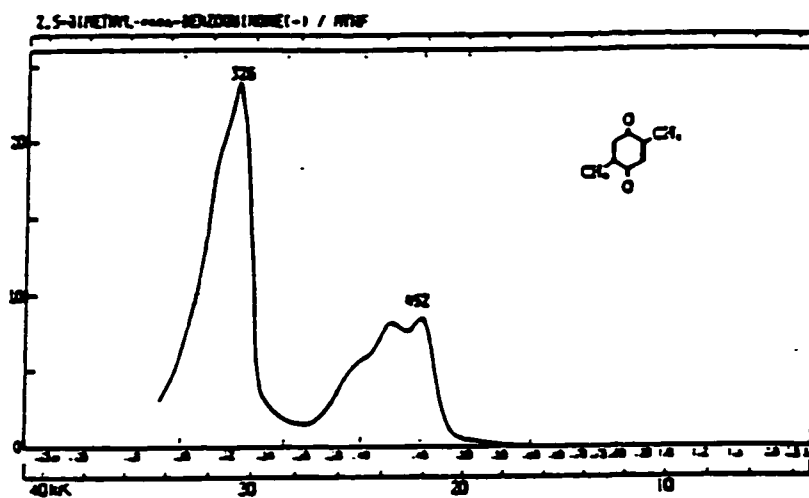


Figure 3.6: Electronic absorption spectra of representative quinoid radicals (semiquinones)(3.5).

It is interesting to note that, in all the electronic absorption spectra of the representative organic compounds (figures above), the stronger, higher intensity π, π^* bands appear at shorter wavelengths than the weaker, less intense n, π^* bands. Spectral overlap of such bands by similar organic 'natural' products account, in part, for the characteristic 'slope-tail' electronic absorption profile of fulvic acid (Chapter 1, Figure 1.2).

Natural products resulting from biodegradation of plant material include a wide variety of products that have substituted phenolics, shikimic acids, quinones and ketonics which have spectral characteristics similar to the compounds illustrated above. The 'humification' process may offer possibilities for the introduction of such compounds into the soil.

3.4 The n, π^* Excited State

Electronic excitation of fulvic acid in the near ultra-violet involve n, π^* transitions which determine both the short time (picosecond) and long time (steady state) photophysical and photochemical characteristics of the irradiated fulvic acid solutions. The photo-behaviour of fulvic acid may be modeled by mechanisms involved in typical n, π^* transitions.

The presence of a π^* electron in either a singlet or triplet n, π^* excited state causes the sp^2 hybridization at the carbonyl carbon to change from sp^2 toward sp^3 . Such a hybridization change is expected to be accompanied by changes in bond lengths, C-O bond mobility, and molecular shape at the n, π^* excited carbonyl of the organic compounds. The C-O bond lengths of singlet and triplet n, π^* excited states are considerably longer (less double-bond character) than the C-O bond length in the singlet ground state. Also, the dipole moments of the singlet and triplet n, π^* excited state of carbonyls are smaller than that of the ground state since there is partial transfer of

charge from the n orbital (localized on O) to the π^* orbital delocalized on C and O. The degree of delocalization will be greater in conjugated excited state carbonyl systems. Differences in molecular shape, electronic structure, geometry and flexibility in the excited state of such n,π^* carbonyl compounds will result in very different chemical properties of the (singlet / triplet) excited state of the carbonyl 'center' compared to the ground state (3.6). These properties will influence and may ultimately determine the photochemical behaviour of fulvic acid and its sensitivity to pH, background electrolyte and concentration.

3.5 Difference in Electronic Energy of Singlet and Triplet n,π^* Carbonyl States

A factor which is important in the determination of the photophysical and photochemical properties is the energy difference between an n,π^* excited singlet and triplet state. For example, small energy differences between these states can translate into large quantum yields for intersystem crossing, either from the singlet excited state to the triplet excited state or from the triplet excited state to the singlet ground state, resulting in different photochemical behaviour.

Theoretically, the difference in electronic energy between singlet and triplet states that are derived from the same electron orbital configuration, results from the 'better' correlation of electron motions in a triplet state. The Pauli principle operates as a type of quantum mechanical 'force' which 'instructs' the two key orbitally unpaired electrons in triplet states how to 'avoid' one another and thereby correlate their motions to minimize electron-electron repulsions.

A brief qualitative description of the magnitude of the electronic energy difference between the singlet and triplet state, ΔE_{ST} , for a typical carbonyl compound is given below (3.6, 3.7):

The state energy may be viewed as the summation of a Zero Order (one electron orbital) energy, plus, electron repulsion energies. For example, the energetics of the ground state and the lowest excited states of a typical carbonyl are given by:

$$E(S_0) = 0 \quad \text{Ground state is zero by definition} \quad 3.1$$

$$E(S_1) = E(n, \pi^*) + K(n, \pi^*) + J(n, \pi^*) \quad \text{Singlet excited state} \quad 3.2$$

$$E(T_1) = E(n, \pi^*) + K(n, \pi^*) - J(n, \pi^*) \quad \text{Triplet excited state} \quad 3.3$$

where J is the matrix element that denotes electron repulsion due to electron exchange and K is the matrix element that measures electron repulsion due to Coulombic interactions. Both J and K are positive (energy increasing) quantities. Note that

$$\Delta E_{ST} = E(S_1) - E(T_1) = 2J(n, \pi^*) > 0 \quad 3.4$$

and since J must be positive we may conclude that $E(S_1) > E(T_1)$.

The Zero Order energy (one electron configuration) of both S_1 and T_1 is $E(n, \pi^*)$, this is the energy required for an orbital jump from an n -orbital to a π^* -orbital (in a one electron orbital approximation) *plus* a correction for Coulombic repulsion of electrons (K). The repulsion does not split S_1 and T_1 but raises the energies of both states. The S_1 and T_1 states are then split in energy by the exchange term, J , which stabilizes the triplet relative to the Zero Order states and destabilizes the singlet relative to the Zero Order states. The value of J represents the electrostatic repulsion between the electrons in an n -orbital and in a π^* orbital and therefore is proportional to the *overlap* of the n -orbital and π^* orbital (Figure 3.7):

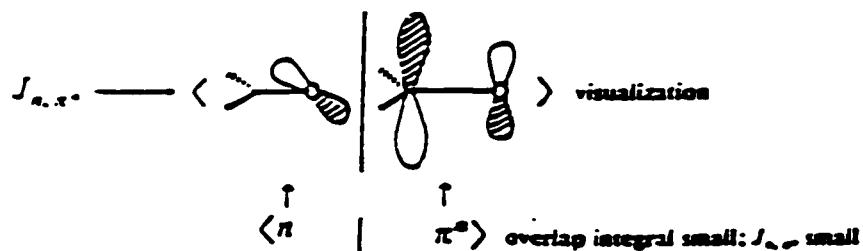


Figure 3.7: Overlap of the n and π^* orbitals at a carbonyl (3.11).

It is important to note that the splitting is small compared to that expected for a π, π^* singlet - triplet splitting because the degree of overlap between the n and π^* orbital is low, that is, these orbitals do not occupy very much of the same region of space with respect to a π, π^* state, (Figure 3.8):

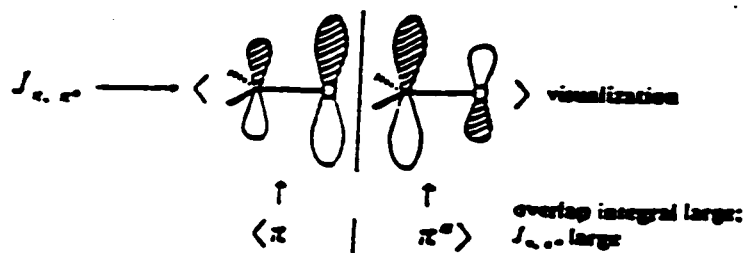


Figure 3.8: Overlap of a π, π^* configuration (3.11).

It may be concluded that J_{π,π^*} will be greater, in general, than J_{n,π^*} . This translates experimentally to singlet-triplet splitting energies of the n,π^* for ketones, conjugated ketones and aromatic ketones to be consistently < 10 kcal/mole, whereas π,π^* singlet-triplet splittings are typically 30-40 kcal/mol. Comparatively small singlet-triplet splitting energies in n,π^* systems usually lead to high expected quantum yields for intersystem crossing. As will be described later, MCD spectra of fulvic acid indicate that the average splitting between singlet and triplet states is approximately ≤ 7 kcal/mol and that the apparent intersystem crossing quantum yields are relatively high (Time Resolved Pulsed Photoacoustic Spectroscopy). This situation is common for n,π^* transitions. A list of carbonyl compounds, singlet-triplet splitting energies and typical intersystem quantum yields is shown in Table 3.1 and Table 3.2 (3.6,3.8).

Table 3.1 Energetics and Dynamics of Carbonyl Compounds (3.6)

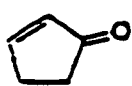
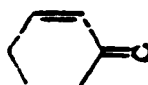

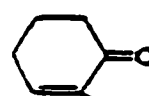
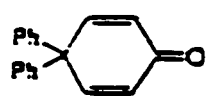
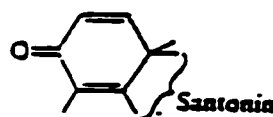

Molecule	E_1^a	E_3^a	k_1^b	k_{12}^b	k_3^b	ϕ_w
Acetone	84	78	10^9	10^9	10^9	1.0
2-Pentanone	84	78	10^9	10^9	10^7	0.9
2-Hexanone	84	78	10^{10}	10^9	10^6	0.5
Cyclobutanone	84	78	10^{11}	10^9	—	0.0
Cyclopentanone	84	78	10^9	10^9	10^6	1.0
Cyclohexanone	84	78	10^9	10^9	10^7	1.0
Acetophenone	80	74	10^{10}	10^{10}	10^3	1.0
Benzophenone	76	69	10^{11}	10^{11}	10^3	1.0
2-Acetophenone	77	59	10^{10}	10^{10}	10^3	0.8
4-Phenylbenzophenone	75	62	10^{10}	10^{10}	10^3	1.0
Fluorenone	65	53	10^9	10^9	10^4	0.9
2-Acetylnaphthalene	75	58	10^9	10^{10}	10^4	0.9
Biacetyl	62	55	10^6	10^6	10^6	1.0
Camphorquinone	57	51	10^6	10^6	10^3	1.0

^a Energies in kcal/mole.

^b Rate constants are in sec^{-1} . k_1 = measured singlet lifetime, k_{12} = measured rate of $S_1 \rightarrow T$ intersystem crossing, k_3 = measured triplet lifetimes. Values are order-of-magnitude only and refer to measurements in "inert" solvents under deaerated conditions.

Table 3.2: The Singlet and Triplet Energies of some Conjugated and related Carbonyls .

(3.8)

Molecule	E_1	E_3
$\text{CH}_2=\text{CH}-\text{CHO}$	77	70
	83	76
	80	75(π, π^*) 74(π, π^*)
	81	75
	-76	76(π, π^*) 68(π, π^*)
	-78	69(π, π^*)
 Santonin	-	70(π, π^*)
$\text{CH}_3(\text{CH}=\text{CH})_2\text{CHO}$	-	44(π, π^*)
$\text{CH}_3(\text{CH}=\text{CH})_3\text{CHO}$	-	36(π, π^*)
$\text{CH}_3(\text{CH}=\text{CH})_4\text{CHO}$	-	32(π, π^*)
	56	50(π, π^*)

3.6 Intersystem Crossing

Quantum yields for intersystem crossing for n,π^* excited states depend upon 'forbidden' spin-orbit coupling mechanisms (3.6, 3.9, 3.10). Spin-orbit coupling provides a magnetic torque (generated by the electron's orbital motion) capable of 'flipping' the electron's spin magnetic moment and can also provide a means of conserving total momentum by coupling the spin-flip with a compensating orbital jump. In other words, the momentum change due to the change in spin momentum can be exactly balanced by a change in orbital momentum. Spin-orbit coupling is most effective if an atom is available which can accommodate an orbital transition, 'jump', (e.g. $p_x \rightarrow p_y$) simultaneously with the spin flip. This is precisely what happens in an n,π^* transition at the oxygen atom on a carbonyl group but does not occur in a π,π^* transition. The spin flip is due to a n,π^* transition, which may be viewed as a jump from a p orbital (e.g. p_x) in the plane of the molecule to a p orbital (e.g. p_y) perpendicular to the plane of the molecule (i.e. the atomic p orbital on oxygen which makes up half of the π^* orbital). The simultaneous $p_x \rightarrow p_y$ orbital jump is thus a one center jump involving a momentum change. As was mentioned above, the orbital momentum change associated with the $p_x \rightarrow p_y$ jump is matched exactly by the spin momentum change associated with the spin flip. It can be immediately seen that the analogue of the $p_x \rightarrow p_y$ jump of ketones does not exist for π,π^* transitions of alkenes such as benzene or ethylene.

Typically therefore, for n,π^* transitions with small singlet-triplet splitting energies, quantum yields for intersystem crossing are usually approximately 1. This is particularly the case for compounds such as benzophenone, arylketones and quinones. Also, remarkably fast intersystem crossing rates ($k_{\text{intersystem}} \gg k_{\text{fluorescence}}$) are typical of certain carbonyl compounds

possessing $S_1(n,\pi^*)$ states with close lying T_1 states such as is the case for benzophenone and quinones (in general).

It is also important to note that ketones possessing $T_1(n,\pi^*)$ states can undergo efficient intersystem crossing back down to the ground state singlet. These factors are consistent with the exceptionally small energy gap between the singlet and triplet states of these carbonyl compounds. This can become an important factor for irradiated, aerated solutions of such organic compounds in terms of diffusion limited quenching of excited state triplets by molecular oxygen. Triplet excited state carbonyl compounds are well known to react with ground state oxygen to give the highly reactive singlet excited state molecular oxygen. However, quantum efficiency for this mechanism will depend in turn on the efficiency for intersystem crossing of the triplet excited state back down to the ground singlet state. These factors will vary, in the case of fulvic acid solutions, with concentration of fulvic acid, pH, background electrolyte and metal loading.

3.7 Fluorescence and Phosphorescence

A general feature of the emission of ketones possessing singlet (n,π^*) states is the relatively small value for the fluorescence quantum yield, (e.g. $\phi_{\text{fluor}} \sim 0$ for benzophenone, and acetone) (3.11). Phosphorescence is also weak (e.g. $\phi_{\text{phos}} < .01$ for benzophenone). Conjugated enones and dienones exhibit only weak emission at best (3.6).

3.8 Radiative Transitions Involving more than One Molecule

In certain cases, two or more molecules may participate in cooperative absorption or emission, i.e., the absorption or emission can only be understood as arising from molecular

complexes. Most commonly, only two molecules are involved in such phenomena. When two molecules act cooperatively to absorb a photon then an absorption complex exists. Mixtures of molecules which possess molecules with a low ionization potential (electron donors) and molecules with a high electron affinity (electron acceptors) can under these conditions also form charge-transfer complexes. Classic examples of such complexes are the carbonyl, quinone-hydroquinone (polyphenolic) charge transfer complexes. For example, quinhydrone is a molecular complex formed between hydroquinone and p-benzoquinone. In solution quinhydrone exists as an equilibrium mixture of free and interacting quinone and hydroquinone. The maximum molar extinction coefficient of quinhydrone is reported to be 890 at 440 nm (3.12), with an association constant of 1.06 at 20^o C in 0.05M aqueous hydrochloric acid solution (these association constants are typically high in error; discussed later). The maximum extinction coefficient of benzoquinone or hydroquinone alone, at 440 nm, is less than 80. Therefore, molecular-absorption complexes of a variety of quinoid-like species could 'increase' observed electronic absorption intensity in the near U.V. and visible region of the spectrum more than would be 'expected' by 'single' species alone undergoing n,π^* transitions.

The self-assembly of amphiphilic species in water, such as fulvic acid, can also result in the formation of 'molecular clusters'. The organization of such reactants (at the molecular level) could lead to higher efficiency of certain photoprocesses such as intersystem crossing or photoionization. Background electrolyte, pH and concentration can influence the formation of a variety of absorption complexes. The photobehaviour of such complexes could be influenced directly by factors such as micelle formation. For example, the interaction of two triplet excited state species in a confined micelle-like reaction space could lead to a higher probability of triplet-triplet annihilation to form two ground state singlet species by radiationless mechanisms.

Under natural water conditions humic substances undergo photochemistry and photophysics of 'micellar assemblies' and /or charge transfer complexes. A variety of 'donor-acceptor' complexes as well as a variety of overlapping π,π^* and n,π^* bands could account for the electronic absorption spectrum 'profile' of fulvic acid.

3.9 State Mixing

The notion that a singlet or triplet excited state is a 'pure' state in the sense of being derived from either a single electronic orbital configuration or from a single spin multiplicity allows for a simple and reliable Zero Order classification of the lowest electronic states of many organic molecules (3.9, 3.13). However, the approximation begins to break down when significant state mixing occurs. State mixing is the first-order or higher order correction to an original Zero Order approximation. Compounds such as benzophenone, quinones, aryl ketones and conjugated ketones have relatively strong n,π^* state and π,π^* state mixing (3.13). As will be discussed, the extent of mixing has far reaching effects on photochemical behaviour, (electron abstraction, hydrogen atom abstraction mechanisms), as well as the spectroscopic properties of a chemical species.

By Zero Order approximation a singlet excited state may be viewed as a 'pure' n,π^* state. In 'reality' the wave function of the singlet excited state has a finite amount of π,π^* character mixed into it. By perturbation theory, for a weak perturbation, a 'mixing' coefficient or the amount of π,π^* character mixed into the singlet n,π^* states is related to (3.9, 3.13):

1. A matrix element for the interaction of the two states that are mixing, $\langle n,\pi^* | H | \pi,\pi^* \rangle$, and
2. The energy difference between the two states, $E_{\pi,\pi^*} - E_{n,\pi^*}$

$$\text{First Order } n, \pi^* \rightarrow \text{Singlet} = n, \pi^* + \frac{\langle n, \pi^* | H | \pi, \pi^* \rangle}{E_{\pi, \pi^*} - E_{n, \pi^*}} | \pi, \pi^* \rangle \quad 3.5$$

The matrix element for mixing may be approximated by considering only the orbitals which are occupied 'differently' in two states, i.e.,

$$\langle n, \pi^* | H | \pi, \pi^* \rangle \text{ can be approximated by } \sim \langle n | H | \pi \rangle \quad 3.6$$

↑ ↑
Occupied in
both states

↑ ↑
Involved in mixing

For purely planar molecules the integral in equation 3.6 equals zero because the n and π orbitals are orthogonal to one another for an idealized planar geometry. However, as the molecule undergoes vibrations which destroy the planar symmetry of the molecule, the n and π orbitals begin to mix, i.e., if H represents electronic interactions which occur during nonplanar vibrations the integral $\langle n | H | \pi \rangle$ does not equal zero. In other words, the n and π orbitals are no longer 'pure', and therefore they are no longer orthogonal. Out of plane vibrations break the planar symmetry of the molecule and so a 'p' shaped orbital that would have the same electron density above and below the symmetry plane (retained in a planar vibration) now has a change of shape in response to the fact that more electron density (due to bonds) are on one side of the plane. We can say that *rehybridization* occurs and imagine that the 'pure p' shaped orbital begins to take on s-character, i.e., out of plane vibration converts the p orbital into a sp^n orbital, where n is a measure of the 'p character' remaining. In the extreme situation $n = 3$, the out of plane vibration causes a continual p (planar) $\leftrightarrow sp^3$ (pyramidal) electronic change. In this case significant vibronic coupling of electronic and nuclear motion occurs due to this vibration. From a classical viewpoint, momentum must be transferred from nuclear motion to electronic motion in order for

vibronic coupling to occur. In the example discussed above, the pure ' p ' orbital did not undergo a momentum change during the in-plane vibration, but the nonplanar vibration allowed a change in nuclear motion to be accompanied by an exchange of momentum between nuclear and electronic motion. An electron in a pure ' p ' orbital has a different momentum than an electron in a sp^3 orbital, so that conservation of momentum is achievable by coupling the planar \approx nonplanar nuclear momentum with the $p \sim sp^3$ orbital momentum change.

From these qualitative considerations we can deduce that the mixing of n,π^* and π,π^* states may depend upon the occurrence of certain vibrations which generate the nonorthogonality of the n and π orbitals. The extent of mixing, in turn, depends on the mixing matrix and the energetic separation. As was mentioned above, aryl ketones, benzophenone and quinones, which are probably present in fulvic acid and are major light absorbers in the 350 nm region, will undergo photochemical reactions with both n,π^* and π,π^* state character due to relatively strong state mixing. In the case of benzophenone, out-of-plane vibrations allow the n orbital to pick up s 'character'. Mixing of the n,π^* and π,π^* states occurs and makes the singlet excited state a hybrid of these two transition types (however, it is still mostly n,π^*). As a result, the $S_0 \rightarrow S_1$ transition has more oscillator strength because of the π,π^* character 'mixed' into S_1 . In a manner of speaking, the S_1 state picks up absorption intensity from its acquired π,π^* character. In the case of acetone, the singlet excited state S_1 is nearly pure n,π^* because of poorer mixing, (energy difference is much larger, equation 3.5), and therefore the absorption intensity is correspondingly lower. Thus state mixing could also account for some of the 'unexpectedly strong' absorption in the 'red-tail' region of the electronic absorption spectrum of fulvic acid if a relatively high concentration of conjugated ketones, enones and quinones exists in the mixture. State mixing

will also have influence on electron abstraction and hydrogen atom abstraction reactions by influencing the 'optimal reaction geometry' of such bimolecular reactions (Section 3.10).

3.10 Photochemistry

Bimolecular photoreactions are typical of n, π^* excited state carbonyl's (3.6, 3.14, 3.15).

These include:

1. Hydrogen atom abstraction to produce a ketyl-hydrocarbon radical pair. The most favorable hydrogen atom donors in fulvic acid would be moieties that are phenolic in nature (i.e., hydroquinones) and aliphatic alcohols, Figure 3.9. Typical n, π^* excited state acceptors would be aromatic ketones or quinone-like species.
2. Abstraction of an electron from an electron donor to produce a radical pair. This reaction could be followed by a fast proton abstraction reaction.

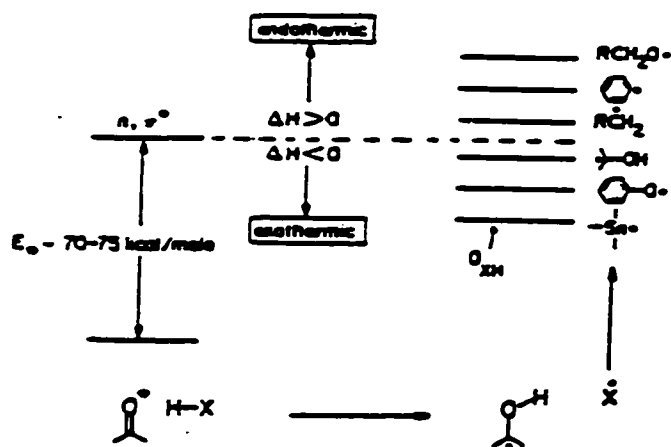


Figure 3.9: Qualitative comparison of the energetics for hydrogen atom abstraction from different H donors HX by the n, π^* states of ketones and aryl ketones (3.6).

In both processes the character of the reaction will be 'radical-like' in nature and will therefore be sensitive to pH, molecular oxygen, and conformational geometries of the reacting species.

The most stabilizing orbital interaction in both cases is expected to result from charge transfer to the half filled n orbital of the n,π^* state of the ketone. The dominant reaction will therefore be one where the preferred reaction coordinate will have the best positive overlap between the one lobe of the n orbital on the oxygen atom of the excited state ketone and the hydrogen atom donor or electron donor. Therefore, whenever an n,π^* state (with little π,π^* mixing) interacts with a molecule possessing a low ionization potential, an orbital symmetry that is more 'in-plane' is favored. The most favored reaction geometry of these reactions will vary according to how much state mixing will occur for the n,π^* excited state transition of the carbonyl species in question.

For example, if an aromatic ketone has strong π,π^* state mixing in its n,π^* transition then the bimolecular electron abstraction reaction will favor more of a 'sandwich, ring-ring overlap' structure interaction between donor and acceptor or 'perpendicular-to-plane' orbital symmetry rather than a 'same-plane' or 'in-plane' approach of the donor and acceptor species. That is, the reaction (electron abstraction or hydrogen atom abstraction) will be more sensitive to steric factors which influence the approach of the substrate above and below the 'faces' of the carbonyl functional group. Examples of compounds exhibiting strong state mixing can be found in Tables 3.1 and 3.2. Also, for aryl-type ketones (i.e., benzophenone, quinones), the n,π^* and π,π^* are closer in energy than for alkyl ketones so that the corresponding singlet and triplet excited state may not be as clearly described in terms of either configuration, that is, the n,π^* and π,π^* configurations. Indeed, for certain substituted benzophenones and all naphthyl ketones and aldehydes, the lowest triplet is generally best classified as π,π^* . This classification implies that: (a) the excited carbonyl oxygen is not as electron-deficient as it is in the n,π^* state, (b) the

excitation energy is partially delocalized into the π -system and may therefore not be available to overcome activation energies for reaction at the carbonyl moiety, and c) primary processes involving the π -system (or groups affixed to it) may occur. Thus (a) may imply that reactivity of the excited state of substituted benzophenones toward hydrogen atom abstraction would be $n,\pi^* > \pi,\pi^*$, based on the premise that hydrogen atom abstraction is an electrophilic process.

“State Switching”, the reversal of an initial state energetic disposition, is a phenomena that can be achieved by variation of ketone structure or solvent polarity. For example, acetophenone possesses a $T1(n,\pi^*)$ and $T2(\pi,\pi^*)$ excited triplet state in nonpolar solvents but a $T1(\pi,\pi^*)$ and a $T2(n,\pi^*)$ state in polar solvents. In general, the energy of an n,π^* state increases with solvent polarity. State switching may occur as a reaction proceeds because of a surface crossing along the reaction coordinate. For example, a molecule initially in a $T1(\pi,\pi^*)$ state may begin to participate in a highly activated ‘in-plane’ hydrogen abstraction reaction, but as the reaction proceeds, a crossing with an n,π^* surface may occur and reduce the barrier for reaction. Such differences in orbital interactions and therefore electron abstraction and hydrogen atom abstraction mechanisms may be important in order to better understand the complex photoactivity apparent in fulvic acid solutions (that appear to follow these bimolecular reaction mechanisms, Chapter 6), as well as, their sensitivity to pH, background electrolyte and concentration.

It is also worth mentioning at this point, that, although the most common reactions of n,π^* excited state carbonyl's are where electrophilic orbital interactions occur with the n orbital of the carbonyl oxygen (important when the n,π^* state interacts with a molecule possessing a low ionization potential), it is also possible that the π^* orbital of the n,π^* state will be important in

terms of orbital interactions if the reaction partner possesses a high electron affinity (i.e., a low energy LUMO). This is the case in some n,π^* quinone-substituted - quinone photoreactions. The heterogeneous fulvic acid mixture offers some possibility for such photo-reactions to occur due to the possibility of numerous available structures and molecular conformations.

The n,π^* states of carbonyls are well known to abstract electrons from electron donors or abstract hydrogen atoms from donors. In each case, bimolecular mechanisms dominate and diradical intermediates are expected. The primary photochemical processes of n,π^* excited states will produce radical species and therefore will initiate radical chemistry. Such intermediates can also react strongly with molecular oxygen in solution and lead to more complex secondary and tertiary reactions that are also strongly dependant upon pH, ionic strength and concentration. The photochemical behaviour of fulvic acid can be described by such a model (Chapter 4, 6).

Excited state ketones often possess the best compromise of the desirable characteristics of a triplet photosensitizer, and, by these properties interact with molecular oxygen. However, self quenching, that is, a non-radiative deexcitation of an excited state molecule by interaction with a ground state molecule of the same type can also occur. The self quenching rate constants for n,π^* excited state ketones are large, Table 3.3 (3.6), and for such molecules self quenching can be a significant pathway for deactivation. Therefore, high intersystem crossing quantum yields do not necessarily translate into high yields of photosensitizer reactivity.

Table 3.3 Self-Quenching Rate Constants of Triplet Ketones (3.6)

Compound	Solvent	k (M ⁻¹ sec ⁻¹)
4-hydroxybenzophenone	benzene	6 x 10 ⁷
4,4'-dimethylaminobenzophenone	benzene	3 x 10 ⁴
benzophenone	acetonitrile	8 x 10 ⁵
	benzene	3 x 10 ⁵
acetophenone	acetonitrile	2 x 10 ⁷
	benzene	8 x 10 ⁵
acetone	acetonitrile	10 ³
methylnaphthylketone	benzene	5 x 10 ⁵
thioxanthone	benzene	2 x 10 ⁹

Reactivities for quenching of n,π^* triplets of ketones by hydrogen atom and electron donors follow a roughly indirect correlation with ionization potential (IP) for substrates possessing IP less than approximately 9 eV. This is the case for polyphenolic type hydrocarbons and quinoid-like species that have ionization potentials below 9eV. Saturated hydrocarbons and alcohols quench predominantly via hydrogen atom abstraction mechanism, whereas polyphenolics and unsaturated hydrocarbons quench via a charge transfer interaction or full-electron transfer (3.6, 3.14, 3.15). Therefore depending on bond energy (D-H) of the hydrogen donor and on its IP, there exists a continuum of mechanisms varying from an extreme of hydrogen transfer (relatively high IP, moderate D-H), to an extreme of electron transfer (relatively low IP, strong D-H). Many possibilities exist in the fulvic acid mixture for variation of substrate structure and reactivity in photochemical hydrogen atom or electron abstraction reactions. The occurrence of photoreduction by an electron transfer rather than a hydrogen abstraction interaction is expected to be evidenced in favorable cases, by direct spectroscopic evidence of cation radicals.

The general concepts developed for understanding hydrogen atom abstraction and electron abstraction reactions of ketones may be extended to the photochemistry of carboxylic acids (and other carbonyl derivatives), as well as to intramolecular reactions. These concepts together with an understanding of electron transfer reactions in micellar assemblies could lead to a more accurate 'model' of fulvic acid's photoactivity.

References

- 3.1 Cowan, D.O., and Drisko, R.L., *Elements of Organic Photochemistry*, New York: John Wiley, 1975.
- 3.2 Becker, R.S., Natarajan, L.V., 1993, *J. Phys. Chem.*, 97, 344-349.
- 3.3 Thomson, R.H., 1976, Isolation and Identification of Quinones, in *Chemistry and Biochemistry of Plant Pigments*, 2nd ed., Vol. 2, Ed. T.W. Goodwin, p. 207., London, Academic Press.
- 3.4 Faust, B., Anastasio, C., Janakiram Rao, C., 1997, *Environ. Sci. Technol.*, 31, 218-232.
- 3.5 Shida, T., 1988, *Electronic Absorption Spectra of Radical Ions* (Physical Sciences Data 34), New York: Elsevier Press.
- 3.6 Turro, N., *Modern Molecular Photochemistry*, Columbia University Press, NY, 1991.
- 3.7 Cohen-Tannoudji, C., Diu, B., Laloe, F., *Quantum Mechanics*, Vol. 1, New York: John Wiley and Sons, 1977.
- 3.8 Birk, J.B., *Photophysics of Aromatic Molecules*, New York: Wiley, 1970.
- 3.9 McGlynn, S.P., Azumi, T., Kinoshita, M., *Molecular Spectroscopy of the Triplet State*, Englewood Cliffs, New Jersey: Prentice Hall, 1969, p. 183.
- 3.10 Henry, B.R., Sisbrand, W., *Organic Molecular Photophysics*, New York: John Wiley & Sons, 1973.
- 3.11 Wilkinson, F., *Organic Molecular Photophysics*, Ed. Birks, J.B., New York: Wiley, 1975, p. 95.

- 3.12 Moser, R., Cassidy, H., 1965, *J. Am.Chem.Soc.*, 87, 15, p.3463-3467.
- 3.13 Dewar, M.J.S., Dougherty, R.C., *The PMO Theory of Organic Chemistry*, New York: Plenum, 1975.
- 3.14 Salem, L., Rowland, C., *Agnew.Chem.Int.Ed.Eng.*, 11, 92 (1971).
- 3.15 Michl, J., *Molec.Photochem.*, 4, 243, 257-287, (1972).

Chapter 4

Primary Photophysical and Photochemical Behaviour of Fulvic Acid

4.1 Introduction

This chapter will describe and discuss laser flash photolysis work performed on Laurentian and Mossy Point fulvic acid solutions in the 'early-time' (20 ps) domain. The results will be compared with reported laser flash photolysis studies in the nanosecond time domain of various other fulvic acid, aromatic ketone, quinone, and phenolic solutions.

4.2 Laser Flash Photolytic Studies of Fulvic Acid

A number of studies of the photochemistry of natural waters have yielded evidence for the participation of a wide variety of transient species (4.1-4.8). Transient species include a solvated electron, organic radicals, excited state triplet species, organic peroxyradicals, singlet oxygen, superoxide, hydrogen peroxide and hydroxyl radicals. The presence in natural water systems of such species suggests dominance of 'free radical' photochemistry and presents a wide variety of possible oxidative and reductive pathways that will be sensitive to the concentration of dissolved organic matter, as well as, pH, background electrolyte and oxygen content (discussed in Chapter 6).

As was discussed in Chapter 3, absorption of UV and/or visible radiation by fulvic acid could involve, n,π^* , π,π^* , a charge transfer transitions, as well as charge transfer to solvent transitions. Fast, flash photolysis studies can help to identify precursors to later transient species and provide mechanistic information concerning electronic transitions involved.

Contemporaneously with work in our laboratories, nanosecond time resolution laser flash photolysis of a variety of natural water samples and solutions of humic substance standards was performed by Fischer and Mill (4.10). The samples were irradiated at 350 nm (near the absorption maximum for excitation of humic substance fluorescence). They resolved two components of transient absorption common to all the samples studied: a component with maximum absorbance at about 475 nm having a lifetime of several microseconds and a transient at 700 nm which was attributed to a solvated electron on the basis of its sensitivity to N_2O and its absorption spectrum. Triplet quenching experiments on the reported '475 nm' transient demonstrated that a signal with triplet character is present at these longer times.

In the detailed work performed by Power (4.6), picosecond and nanosecond laser flash photolysis studies (355 nm) were carried out on the Mossy Point fulvic acid. The work extended from the picosecond to the microsecond time domain and included studies of pH effects, O_2 , N_2O , and metal ion quenching. Three principal transient absorption signals were observed in aqueous solution: a component with a maximum broad absorption at 675 nm and a lifetime of about 1 microsecond (pH 7), a second component with a maximum absorption at approximately 475 nm and a lifetime of 1-10 microseconds and a third component with a broad, featureless transient absorption spectrum and a lifetime in excess of 100 microseconds. The 675 nm signal was attributed to a solvated electron on the basis of lifetime and quenching data and is observed to be fully formed at 20 ps after excitation. The 475 nm signal is believed to be a radical cation on the basis of its concurrent appearance with the electron at 20 ps. The third featureless component emerges nanoseconds after excitation and is believed to correspond to the triplet states of the humic material. It is also interesting to note at this point the similarity in photophysical behaviour from fulvic acid samples retrieved from different areas.

Finally, a fourth fast transient absorption was observed with a lifetime of approximately 50 ns. This transient remained unidentified owing to technical limitations of the equipment.

The observations by Power (4.6) may best be summarized by the kinetic map depicted in Figure 4.1:

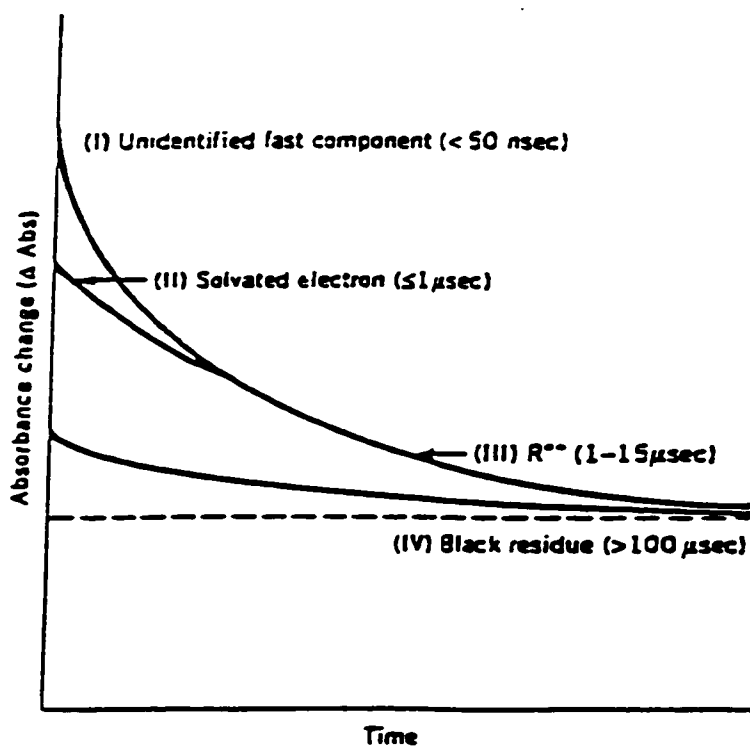


Figure 4.1: Schematic summary of lifetime components observed for the photolysis (355 nm) of Mossy Point fulvic acid (4.6).

4.3 Formation and Decay of the Solvated Electron

The only reported wavelength dependence study of the quantum yield for hydrated electron production from irradiated fulvic acid (Suwanee River) solutions involves steady state measurements as was reported by Blough (4.11). There is a large difference between quantum yields measured in flash photolysis work and steady state yields. The two may not be compared directly. However, the wavelength dependence is interesting to note (even though the same relationship may not hold at early times). The wavelength-quantum yield relation (at steady state) is shown below in Figure 4.2. Higher quantum yield for solvated electron production is found in the 290-300 nm (π,π^* , Chapter 3) region than in the 320-370 nm (n,π^*) region.

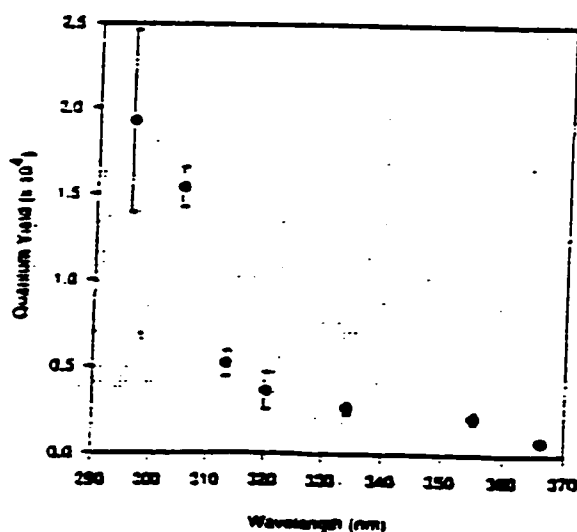


Figure 4.2: Wavelength dependence of quantum yield for solvated electron production from Swannee River fulvic acid (anaerobic) solutions (4.11).

As was first discussed in Chapter 3, the UV-visible profile of fulvic acid is fairly close to those of a variety of aromatic ketones, quinoids and phenolics. Separate flash photolysis work first performed by two different groups (4.12, 4.13) on various aromatic compounds such as quinhydrone, benzoquinone, hydroquinone, cresol, resorcinols, methoxyphenols, benzoic acid, benzyl alcohol, aryl carboxylic acids and various other aromatic compounds yielded in addition to solvated electrons a similar 'free radical' photophysical behaviour as indicated in the laser flash photolysis studies of the fulvic acid solutions. These solutions similarly give higher yields for solvated electron production when wavelengths of irradiation produce (π, π^*) transitions, as well as, when the solvent used is water rather than an organic solvent.

Following the classical observation of Lewis and his school (4.14) of the photoionization of aromatic molecules in rigid solvents, Land (4.15) demonstrated such processes in flash photolysis of aqueous solutions of phenols and suggested that the primary photochemical act involves electron ejection. These solutions were reinvestigated by Stein (4.12) to elucidate the detailed mechanism. The question was whether a (π, π^*) transition or CTTS (charge transfer to solvent) transition was involved in solvated electron production. No evidence was found for even a weak CTTS band. It was concluded that both fluorescence and solvated electron production originated from the π, π^* state.

Similar observations were made by Grossweiner (4.13). Various aromatic phenols and quinones were used in the study and it was concluded that the production of a charge transfer intermediate via the π, π^* excited singlet state releases an electron to the solvent. The essential step is believed to be the escape of the electron from the 'coulomb-valence force' potential well.

Photoinduced electron tunneling reactions are common in chemical and biological charge transfer systems and can result in solvated electron production (4.16).

Photoexcitation of aromatic ketones, quinoids and phenolics that may occur in fulvic acid (4.17, 4.18) must involve predominantly π,π^* character transitions if excited < 310 nm and greater n,π^* character when irradiated above 320 nm. Figure 4.2 suggests that higher yields for solvated electron production in fulvic acid results from π,π^* excited state transitions. This is consistent with theoretical work documented by Turro (4.19), Leigh et al. (20) and Linschitz et al. (21), involving characteristic activity of n,π^* vs. π,π^* states of aromatic ketones, quinoids and phenolics.

Detailed work on excited state photochemistry and photophysics of aromatic ketones, quinones, and phenolics (4.19 - 4.21 and references therein, Chapter 3), as well as the work reported by Stein (4.12) and Grossweiner (4.13), indicate that solutions of these compounds involve photochemistry of 'charge-transfer type' species and that (n,π^*) states undergo preferential intersystem crossing or direct hydrogen atom abstraction from a ground state donor by an excited state acceptor rather than electron transfer followed by a fast proton abstraction. These mechanisms are in competition with solvated electron production.

The π,π^* states for such species undergo preferential electron transfer from the π system (greater overlap in 'preferred' face-to-face aromatic ring 'stacking'). These states do not undergo efficient intersystem crossing (Chapter 3) and do not undergo efficient hydrogen atom abstraction reactions. The end result is that excitation into the π,π^* band of such complexes could result in a higher probability for solvated electron production. Electron tunneling barriers for escape of the electron to the solvent may be lower for the case of a Donor(HOMO)--->

Acceptor *(HOMO) for a π, π^* state than for a n, π^* excited state species. Turro (4.19) notes that singlet π, π^* states will often possess a substantial 'zwitterionic character' as compared to the diradical character of singlet n, π^* states. These differences can result in different 'excited state complex'--solvent interactions which can favor the possibility of 'escape' of the electron to the solvent in the case of a π, π^* excited state complex. Furthermore, work reported by Mattes et al. (4.27) indicates that the formation of a solvated electron and radical may result from the loss of an electron from an excited electron donor-- acceptor complex.

4.4 Formation yield for the Solvated Electron

Estimation of the formation yield for the solvated electron at early times (20 ps) were made by Power (4.6) for the Mossy Point fulvic acid and in the work reported here for the Mossy Point and Laurentian fulvic acid.

Quantum yields were determined directly from time resolved absorption spectra recorded at 20 ps and the molar absorptivity for the solvated electron supplied by the National Bureau of standards (4.25). At 675 nm ($T = 25^\circ \text{C}$), the value is $1.4 \times 10^4 \text{ M}^{-1} \text{cm}^{-1}$. We assume that the solvated electron is the only species contributing to the transient absorbance at this wavelength. The appropriateness of the assumptions were established by the quantitative solvated electron scavenging work by Power (4.25). The pathlength of the cell, volume of irradiation and experimental system are given in Chapter 2. Values obtained in this work for solvated electron formation yield from the Mossy Point and Laurentian fulvic acid are reported in Table 4.1. The Mossy Point values agree satisfactorily with Power (4.25).

Table 4.1 Quantum Yields for Formation of the Solvated Electron for Mossy Point and Laurentian Fulvic Acid (aerated solutions)

Solution	pH	Quantum Yield
Mossy Point	2.0	0.08
Mossy Point	4.0	0.15
Mossy Point	7.0	0.20
Laurentian Fulvic Acid	4.0	0.12
Laurentian Fulvic Acid	7.0	0.16
Laurentian Fulvic Acid	9.0	0.18
High Fraction	4.0	0.15
High Fraction	9.0	0.20
Low Fraction	4.0	0.18
Low Fraction	9.0	0.22

Where high fraction refers to Laurentian fulvic acid solutions that were retained after filtering with a YM 30 (nominal cutoff 30000 Da) filter membrane, and, low fraction refers to Laurentian fulvic acid solutions that were passed by a YM 2 (nominal cutoff 1000 Da) filter membrane.

Quantum yields for the formation of the solvated electron from both the Mossy Point and Laurentian fulvic acid are remarkably similar given that the fulvic acids were obtained from two different environments (boreal forest and coastal regions). These yields are also low compared to apparent triplet quantum yields. In both sets of experiments the fulvic acid solutions were irradiated at 355 nm which might be expected to excite into a primarily n,π^* state that favors large intersystem crossing quantum yields (Chapter 3). These results are consistent with theory concerning n,π^* excited state D--A* complexes involving aromatic ketone--quinone--phenolic species.

It is also interesting to note that results reported by Grossweiner (4.13) indicate that the maximum solvated electron lifetime with benzoquinone is about 14 microseconds, benzoic acid anion 2.4 microseconds, benzyl alcohol 0.9 microseconds, phenyl acetic acid 9 microseconds and naphthoate 1.3 microseconds. By comparison the lifetime for hydroquinone irradiated solutions is > 50 microseconds and for phenol 250 microseconds. Work performed by Power (4.25) yielded a lifetime of approximately 1 microsecond. This could suggest that recombination with the humic component ejecting the electron Donor (HOMO) (ground state, phenols and hydroquinones do not absorb radiation at 355 nm) is not a major pathway but that electron abstraction from an excited state acceptor (A*, i.e., quinone) is favorable. This idea is supported by work by Scott (4.17) and consistent with work by Turro (4.26). Work reported by Grossweiner involved only non-substituted 1,4-benzoquinone species. Substituted quinones (with electron withdrawing groups) or micelle structures surrounding quinoid moieties occur in fulvic acid and could conceivably give values below 14 microsecond solvated electron lifetimes.

It is also important to note at this point that quenching experiments performed by Power (4.25) of the solvated electron with Cu and N₂O yield rate constants that are consistently 2 times lower than literature values (4.32) indicating that fulvic acid affects the solvated electron environment. Complex conformations are possible within fulvic acid solutions. Micelle-like assemblies may form around a photo-active center where a solvated electron may be 'trapped' and isolated.

The possibility of a ground state donor -- excited state acceptor exciplex might account for the unidentified 'fast' 50 ns transient observed by Power. Wilson, R., (4.28) noted a transient with a lifetime of 51 ns in flash photolysis work on a benzoquinone-tetraphenylallene exciplex system.

4.5 Radical Coproducts

The early time spectra indicate a species with a peak at 475 nm. The early formation of this species concurrent with the formation of the solvated electron seems to indicate a radical/cation species associated with the site generating the solvated electron. A variety (Chapter 3) of semiquinone species formed by loss of an electron from hydroquinone relatives (or by electron abstraction by a quinone) absorb in the 400-500 nm region. This is also true of phenoxy radicals and related phenoxymethyl type species. The observations are consistent with aromatic ketone - phenolic donor -- acceptor complexes occurring in the fulvic acid solutions resulting in the formation of semiquinone radicals (4.17). Also irradiated humic substances are known to form 'stable' relatively long lived and strong EPR signals (4.18). This would be consistent with the formation of

semiquinone-like radical species. Combined EPR-photochemical studies prove to be a powerful combination for photophysical work involving humic substances and quinoid solutions.

4.6 The Triplet Transient

Formation and quenching behaviour of the broad-featureless long-lived transient led to its assignment as a variety of overlapping triplet excited state bands (4.25). Results described in Chapter 5 indicate that apparent quantum yields for this species are relatively high. Irradiation of fulvic acid solutions in the 337-355 nm range should preferentially create n,π^* excited state species with a high probability for intersystem crossing to the triplet state. Also, values for triplet states of aromatic ketones and quinones reported by Turro (4.29) are within the lifetime of this transient.

In a series of steady state irradiations of humic solutions, Zepp et al. (4.31) determined the distribution of triplet energies in a series of humic water samples under broadband and sunlight irradiation. The observed distribution was very broad and centered at a reported 250 kJ mol^{-1} value, corresponding to an absorption of 465 nm. This is consistent with the results reported by Power (4.6) and well within the range of values for aromatic ketone and quinone triplets reported by Turro ($\pm 5 \text{ nm}$) (4.30).

In conclusion it appears that time resolved flash photolysis of a variety of fulvic acid solutions are consistent with a ground state donor (hydroquinone, polyphenolic species) -- complex with an excited state acceptor (quinone, aromatic ketone species) as the site of photoactivity.

References

- 4.1. Draper, W., Crosby, D., 1984, *J. Agric. Food Chem.*, 32, 231-237.
- 4.2. Zepp, R., Wolf, N.L., Baughmann, G., Hollis, R.C., 1977, *Nature*, 267, 421-423.
- 4.3. Mill, T., Hendry, D.G., Richardson, H., 1980, *Science*, 207, 886-887.
- 4.4. Carey, J., 1983, *Nature*, 306, 575-576.
- 4.5. Waite, T.D., Morel, F.M., 1984, *Envir. Sci. & Tech.*, 18, 860-868.
- 4.6. Power, J., Langford, C.H., Sharma, D., Bonneau, R., 1987, ACS-Symp. Ser. No. 327, 158-173.
- 4.7. Bruccoleri, A., Langford, C.H., Sharma, D., 1993, *Envir. Sci. & Tech.*, 27, 889-894.
- 4.8. Blough, N., ACS Division of Environmental Chemistry, 216th ACS National Meeting, 38, No. 2, p. 111-113, 1998.
- 4.9. Turro, N., *Modern Molecular Photochemistry*, Chapt. 1, p. 7, John Wiley & Sons, 1991.
- 4.10. Fischer, A.M., Mill, T., Kliger, D.S., Tse, D., *IHSS Symp. Proc.*, Birmingham, UK, 23-28, 1984.
- 4.11. Blough, N., ACS Division of Environmental Chemistry, 216th ACS National Meeting, 38, No. 2, p. 113, 1998.
- 4.12. Stein, G., Solvated Electron, *Adv. In Chem. Ser. 50*, Chapt. 16, p. 230-241.
- 4.13. Grossweiner, L., Hans-Ingo, J., Solvated Electron, *Adv. In Chem. Ser. 50*, Chapt. 20, p. 279-288.
- 4.14. Lewis, G.N., 1942, *J. Am. Chem. Soc.*, 64, 2801.
- 4.15. Land, E.J., 1961, *Trans. Farad. Soc.*, 57, 1855.

- 4.16 Marcus,R.A., Sutin,N., 1985, *Biochimica et Biophysica Acta*, Electron Transfers in Chemistry and Biology, 811, 265-322.
- 4.17 Scott, D., McKnight, D., Harris, E., Kolesar, S., Lovley, D., *Environ. Sci.& Tech.*, 1998, 32, 2984-2989.
- 4.18 Hayes,M., Humic Substances II (In Search of Structure), Chapter 13 and 14, John Wiley & Sons, Toronto, 1989.
- 4.19 Turro,N., *Modern Molecular Photochemistry*, Chapt.7 and 10, John Wiley & Sons,1991.
- 4.20 Leigh,W., 1996, *J.Am.Chem.Soc.*, 118, 12339-12348.4.21 Linschitz,H., Loeff,I., 1993, *J.Am.Chem.Soc.*, 115, 8933-8942.
- 4.22 Guillet, J., *Polymer Photophysics and Photochemistry*, Chapter 7, Cambridge University Press, NY, 1985.
- 4.23 Bruccoleri,A., Langford,C.H., Lepore,G., *Environmental Oxidants*, Chapter 7, p.187-219, 1993.
- 4.24 National Bureau of Standards, Publ.No.69, 1986.
- 4.25 Power, J., PhD Thesis, Concordia University, Montreal, 1986.
- 4.26 Turro,N., *Modern Molecular Photochemistry*, Chapt.10, John Wiley & Sons,1991.
- 4.27 Mattes,S., 1984, *Science*,226, 917-921.
- 4.28 XII IUPAC Symp.on Photochem., 1988, Bologna, 1988.
- 4.29 Turro,N., *Modern Molecular Photochemistry*, Chapt.8, John Wiley & Sons,1991.
- 4.30 Turro,N., *Modern Molecular Photochemistry*, Chapt.9, John Wiley & Sons,1991.
- 4.31 Zepp,R.G., Schlotzhauer, P.F., Sink, R.M., 1985, *Env.Sci.&Tech.*, 19, 74.
- 4.32 Buxton, G., 1988, *J.Phys.Chem.Ref.Data*, V.17, No. 22, pp. 513-886.

Chapter 5

Photophysics in Fulvic Acid Solutions

5.1 Introduction

The goal of this chapter is first to present the major factors involved in radiationless processes common to photoexcited 'model' species that are relevant to fulvic acid. Following this, a presentation and discussion of the results of pulsed photoacoustic energy storage experiments on Mossy Point and Laurentian fulvic acid solutions will be given together with the results of magnetic circular dichroism spectra, which together permit estimates of quantum yields.

5.2 Intersystem Crossing and Photophysical Radiationless Transitions of Excited State Carbonyl Compounds

As discussed in Chapter 3, intersystem crossing is a photophysical radiationless transition which occurs with a change in spin-multiplicity. Given that the experiments performed were all carried out in the near UV region of the spectrum, the major transitions expected will be of the n,π^* type with some π,π^* character (Chapter 3). Intersystem crossing is an efficient photophysical pathway in many n,π^* excited state carbonyl containing moieties (e.g., quinones, aromatic ketones). Experimentally singlet-triplet splittings for n,π^* states of ketones are approximately 10 kcal mol^{-1} , while for molecules with π,π^* singlet-triplet splitting values $> 30\text{-}40 \text{ kcal mol}^{-1}$ are common. Table 5.1 (5.2) lists some experimental values.

Table 5.1 Singlet - Triplet Splittings

Molecule	E_s	E_T	Quantum Yield (Intersystem crossing)
	Kcal/mole		
acetone	85	78	n, π^* 1.0
acetophenone	79	74	n, π^* 1.0
benzophenone	75	69	n, π^* 1.0
anthraquinone	-	62	n, π^* 1.0
camphorquinone	55	50	n, π^* 1.0
1,4-benzoquinone	56	50	n, π^* 1.0
2-acetophenone	77	59	0.8

As will be discussed shortly magnetic circular dichroism spectra of the Mossy Point and Laurentian fulvic acid show splitting energies of approximately 7 kcal/mol. As can be seen from Table 5.1 this is common for n, π^* states of ketones (e.g. quinones and aromatic ketones that may model components of fulvic acid). Similar compounds that have a small singlet-triplet energy splitting and presumably a favorable Frank-Condon factor, typically have intersystem quantum yields of approximately 1. For example, quinoid and aromatic ketones, which undergo n, π^* transitions, have large quantum yields for intersystem crossing as can be seen in Table 5.2 (5.4).

Table 5.2 Quantum Yields for Intersystem Crossing (n,π^* type)

Molecule	Quantum Yield
acetone	1.0
xanthone	1.0
acetophenone	1.0
anthraquinone	1.0
camphorquinone	1.0
2-pentanone	0.9
benzophenone	1.0
4-Phenylbenzophenone	1.0

5.3 Evaluation of Apparent Intersystem Crossing Quantum Yields in Fulvic Acid Solutions

Early time-resolved absorption spectroscopy (Chapter 4) has identified the solvated electron, a corresponding radical (cation), and triplet absorption in a broad excited state absorption band. The main tool complementing the picosecond absorption spectroscopy work is time-resolved photoacoustic spectroscopy (5.5, Chapter 2), from which the apparent triplet quantum yields may be evaluated if an average triplet energy is available (5.6,5.7). The average triplet energy is sought for by magnetic circular dichroism spectroscopy.

5.3.1 Magnetic Circular Dichroism Spectroscopy

Magnetic circular dichroism spectra are useful for identification of spin-forbidden bands because transition intensities depend on the product of electric and magnetic dipole matrix elements and spin-forbidden bands are relatively more intense than in ordinary absorption spectroscopy (5.8-5.10). Moreover, line shape is very useful for assignment. As was discussed in Chapter 2, the three characteristic signal shapes are denoted A, B and C terms. B terms arise from transitions between nondegenerate states. C terms from degenerate ground states, and, A terms are a consequence of a transition to a degenerate excited state. Two of these can arise in the spectra of fulvic acids: A and B terms. A singlet-triplet absorption band is expected to produce an A term. It is from the center of this 'dispersion signal' that the average triplet energy is obtained. Singlet-singlet transitions can produce B terms. The MCD spectrum of the Mossy Point (Armdale) fulvic acid shown in Figure 5.1, exhibits an A term which is assigned to triplet absorption. The center of this triplet region appears at approximately 14000 cm^{-1} (40 kcal mol^{-1}). The main spectral feature is a B term at roughly 16500 cm^{-1} (47 kcal mol^{-1}), which is attributed to a singlet absorption. Similarly, the MCD spectrum for the Laurentian fulvic acid, Figure 5.2, shows an A term which is assigned to triplet absorption. The center of this triplet region appears at approximately 15500 cm^{-1} (about 44 kcal mol^{-1}) and the B term appears at approximately 18000 cm^{-1} (approximately 51 kcal mol^{-1}).

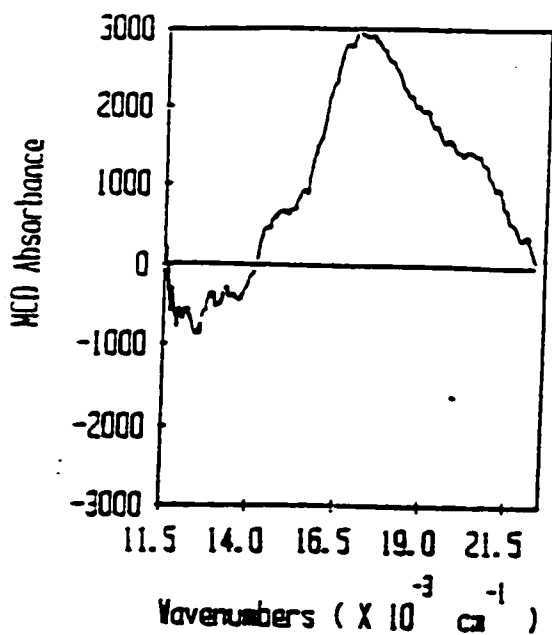


Figure 5.1: Representative MCD spectrum of the Mossy Point fulvic acid solution (pH 8.0, 20 ppm). The center of the A term, which is assigned as a triplet absorption of the fulvic acid appears at approximately 14000 cm^{-1} .

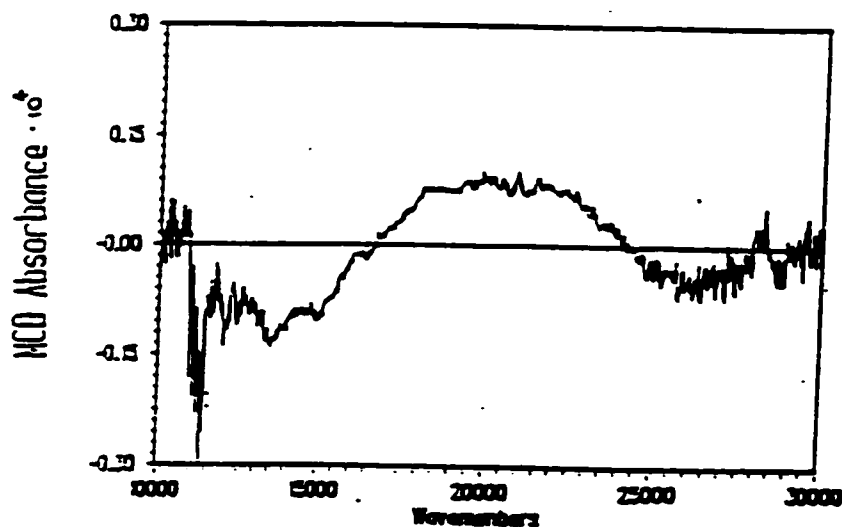


Figure 5.2: Representative MCD spectrum of the Laurentian fulvic acid solution (20 ppm). The center of the A term, which is assigned as a triplet absorption of fulvic acid appears at approximately 15500 cm^{-1} .

As was discussed in Chapter 3 and Section 5.3, the electronic energy difference between singlet and triplet states (ΔE_{ST}), is approximately 10 kcal mol⁻¹ for molecules with n, π^* states (e.g. ketones), while the singlet-triplet splitting values for molecules with π, π^* states is $\geq 30-40$ kcal mol⁻¹. It is apparent from the MCD spectra that the ΔE_{ST} values are approximately 7 kcal mol⁻¹. This value is within splitting energy range common for quinoid and aromatic ketonic species (Table 5.1) and is indicative of a predominantly n, π^* electronic transitional character for fulvic acid when irradiated in the near U.V. High quantum yields for intersystem crossing are also associated with such systems.

Furthermore it is interesting to note that the two values for singlet-triplet energy splitting are close despite the fact that the sites from which soil samples were taken for the fulvic acid extraction are ecologically, geographically and podologically distinct (Chapter 2).

5.3.2 Time Resolved Pulsed Photoacoustic Spectroscopy

Time resolved photoacoustic spectroscopy has emerged as a powerful tool for estimating energetics of photophysical processes. A detailed description of the system and signal production has been given (5.5, Chapter 2). Time resolution is limited primarily by the travelling time of the acoustic wave in the illuminated area. This corresponds to a time resolution of approximately 2 microseconds. Therefore, long-lived excited states that can store energy contribute to reduction of pulsed photoacoustic signals. The results of the apparent triplet quantum yields for the Mossy Point and Laurentian fulvic acid are shown in Tables 5.3 and 5.4 below.

Table 5.3 Apparent Triplet Quantum Yields Calculated for Various Solutions of Mossy Point Fulvic Acid

Solution	pH	quantum yield ^a	ionic strength
fulvic acid	2.0	0.82	< 10 ⁻³
fulvic acid	3.0	0.78	< 10 ⁻³
fulvic acid	5.0	0.65	< 10 ⁻³
fulvic acid	6.0	0.61	< 10 ⁻³
fulvic acid	8.0	0.52	< 10 ⁻³
fulvic acid	9.5	0.35	< 10 ⁻³
fulvic acid + KCl ^b	1.5	0.91	1.0
fulvic acid + KCl ^b	8.5	0.91	1.0

^a Quantum yields were calculated using the triplet energy of $1.7 \times 10^2 \text{ kJ mol}^{-1}$. The standard deviation in the apparent triplet quantum yields is 10%. Fulvic acid solutions were less than or equal to 20 mg L^{-1} . ^c Fulvic acid aqueous solutions were prepared with 1 M KCl.

Table 5.4 Apparent Triplet Quantum Yields Calculated for Various Solutions of Laurentian Fulvic Acid

Solution	pH	quantum yield ^a	ionic strength
fulvic acid	2.0	0.79	< 10 ⁻³
fulvic acid	5.0	0.60	< 10 ⁻³
fulvic acid	9.5	0.28	< 10 ⁻³
high fraction ^a	2.0	0.26	< 10 ⁻³
high fraction	5.0	0.21	< 10 ⁻³
high fraction	9.5	0.15	< 10 ⁻³
low fraction ^b	2.0	0.85	< 10 ⁻³
low fraction	5.0	0.73	< 10 ⁻³
low fraction	9.5	0.31	< 10 ⁻³
high fraction + KCl ^c	2.0	0.32	1.0
high fraction + KCl	5.0	0.27	1.0
high fraction + KCl	9.5	0.18	1.0
low fraction + KCl ^d	2.0	0.88	1.0
low fraction + KCl	5.0	0.88	1.0
low fraction + KCl	9.5	0.86	1.0
fulvic acid + KCl	2.0	0.90	1.0
fulvic acid + KCl	5.0	0.91	1.0
fulvic acid + KCl	9.5	0.90	1.0

^a High refers to Laurentian fulvic acid solutions that were retained on a YM 30 (nominal cutoff 30 000 Da) filter membrane. ^b Low refers to laurentian fulvic acid solutions that were passed through a YM 2 (nominal cutoff 1000 Da) filter membrane. The standard deviation in the quantum yields is 10%. The concentration of KCl in solutions with background electrolyte was 1M.

It is interesting to note that as the pH is increased, the energy stored as triplets for periods longer than 2 μs decreases. That is, some processes of radiationless relaxation to the ground state become important. There are two possibilities. One is that internal conversion of singlets directly to the ground state becomes important. The second is that the radiationless decay of triplets to the ground state becomes more rapid, and an important fraction of the triplets no longer lasts long enough to be identified as energy-storing species on the 2 μs time scale. Since transient absorption spectra suggest a relatively long triplet lifetime, the former process appears to be more important.

It is evident that the major photophysical pathway in acid solution is that of intersystem crossing to form triplet excited states. High values for apparent intersystem crossing quantum yields for fulvic acid solutions would be consistent with n, π^* transitions undergoing intersystem crossing at carbonyl sites for aromatic ketone or quinoid species present in the mixture. It should also be noted that, due to the heterogeneous nature of fulvic acid many opportunities also exist for the formation of donor-acceptor type complexes between quinoid* - phenolic species that may also undergo radiationless $^1(\text{D-A}^*) \rightarrow ^3(\text{D-A}^*)$ transitions. Quinone and phenolic species are well known to form 'molecular-complexes'.

The two fulvic acid samples again show a remarkable similarity in behaviour despite their separate origins. Moreover, molecular weight fractionation of the Laurentian sample indicates that the triplets are associated more with the lower molecular weight components of the mixture. This may be due to the greater ability of smaller species to

form closer contact donor-acceptor molecular-complexes than larger more substituted species.

As was mentioned above, these results support the view that fulvic acid experiences primarily n,π^* transitions in the near U.V. and that the species involved may be 'quinoid or aromatic-ketone-like'. Recall that aromatic ketones and quinones have relatively high quantum yields for intersystem crossing in the near U.V. (Chapter 3, Section 5.4). Interestingly, the quinone, aromatic and hydroquinone regions of the solid state ^{13}C NMR spectrum will be seen to show the most 'change' after irradiation at 350 nm (Chapter 6).

It is also interesting to note that high ionic strength and low pH both induce high apparent triplet quantum yields. The behaviour at high ionic strength mimics the low pH fully protonated sample (even at high pH). It is known that high ionic strength, like low pH, favors compact coiling and aggregation of fulvic acid (5.13) by mitigating the electrostatic repulsions which cause polymer extension. The ionic strength effects argue strongly for a conformation-aggregation explanation of the changing triplet quantum yields. Quinones, hydroquinones, aromatic ketones and aromatic species in general are known to form complexes that are sensitive to conformational effects. Depending on substitution, these aromatic species will interact in a variety of possible geometries.

A fulvic acid contains a range of functional groups that, depending on substitution of neighboring species, can hydrogen bond or have aromatic ring face-to-face overlap interactions enabling donor-acceptor complexation. These features are common traits for 'self-assembly' systems and may play a significant role in determining fulvic

acid's photophysical behaviour. Observations by Wang (5.14) that interactions occur between high and low molecular weight fractions on mixing supports this possibility.

The heterogeneous nature of fulvic acid allows for a variety of possible conformations which can influence photoactive sites or species within the fulvic acid 'matrix'. Surprisingly, however, the heterogeneous complex mixture shows remarkable similarity in 'behaviour' or 'predictability' in terms of photophysical behaviour even for sample sources that are of very different origins. The quinoid characteristics demonstrated in fulvic acid's photophysical behaviour will be seen to carry through into its photochemical behaviour as well (Chapter 6).

References

- 5.1 Tannoudji, Claude; Diu, Bernard, Laloe, Frank, *Quantum Mechanics*, Vol.II, Chapter 4, John-Wiley, N.Y., 1977.
- 5.2 Data gathered from Wilkinson,F., *Organic Molecular Photophysics*, Ed. J.Birks, N.Y. John-Wiley, 1975, p.95 and Birks,J., *Photophysics of Aromatic Molecules*, N.Y., John-Wiley, 1970.
- 5.3 Tannoudji, Claude; Diu, Bernard, Laloe, Frank, *Quantum Mechanics*, Vol.II, Chapter 10, 12, John-Wiley, N.Y., 1977.
- 5.4 Birks, J., *Photophysics of Aromatic Molecules*, N.Y., John-Wiley, 1970.
- 5.5 Arbour, C., PhD Thesis, 1987, Concordia University, Montreal.
- 5.6 Bruccoleri, A., Langford, C.H., Arbour, C., 1990, *Environ.Tech.*, Vol.11,pp.169-172.

- 5.7 Bruccoleri, A., Pant, B., Devendra, S., Langford, C.H., 1993, *Envir.Sci.Tech.*, Vol.27,pp.889-894.
- 5.8 Piepho, S.B., and Schattz, P.N., *Group Theory in Spectroscopy with Applications to Magnetic Circular Dichroism*, John-Wiley, N.Y., 1983, pp. 98-115.
- 5.9 Stephans, P.J., 1970, *J.Chem.Phys.*,52, 3489.
- 5.10 Stephens, P.J., 1976, *Adv.Chem.Phys.*,35, 197.
- 5.11 Bruccoleri, A., Lepore, G., Langford, C.H., 1994, *Environmental Oxidants*, Eds., Jerome Nriagu and Milagros Simmons, Chapt.7, *The Physical Chemistry of Photochemical Oxidant Generation in Natural Water Systems*, pp. 187-220.
- 5.12 Cook, R.L., Ph.D. Thesis, 1997, University of Calgary, Calgary.
- 5.13 Underdown, A.W., Ph.D. Thesis, 1982, Carlton University, Ottawa.
- 5.14 Wang, Z., Pant, B., Langford, C.H., 1990, *Anal.Chim.Acta*, 232, pp.43-49.

Chapter 6

The Photochemistry of Fulvic Acid and Related Compounds

6.1 Introduction and Summary of Primary Quantum Yield Determination

The first portion of this work dealt with the determination of primary photoproduct quantum yields (Chapter 4 and 5). With the quantum yields for the primary photoproducts determined a study of photochemical reaction mechanisms was possible. Photoprocesses are mediated by reaction of the primary photoproducts. As was presented in Chapter 4 and 5, the highest primary quantum yields were determined to be for the fulvic acid triplets. The solvated electron and cation radical quantum yields at 20 ps are much lower than the triplet yields in the microsecond range. Also, the quantum yields for the solvated electron and cation radical were not found to be sensitive to pH or molecular weight fractions used of the fulvic acid. In sharp contrast to the solvated electron and cation radical quantum yields, the triplet quantum yields were determined to be strongly sensitive to pH, background electrolyte and molecular weight fraction of the fulvic acid. The triplet yields are much higher in the low molecular weight fractions than the high molecular weight fractions and the triplet yields for the low molecular weight fractions are more sensitive to background electrolyte than the high fractions. Taking the results of the primary photoproduct quantum yields into account the photochemical study was approached using two techniques.

The first approach involved a study of the photochemical degradation of fulvic acid solutions by ^{13}C NMR. The second approach involved a study of the early photodegradation using differential U.V.-Vis spectra. As was discussed above, the

photoprocesses are mediated by reaction of the primary photoproducts and the triplet pathway is expected to dominate photodegradation reactions. The results of NMR and differential spectra for fulvic acid indicate that a quinone-phenol photochemical mechanism is involved. Quinones have been the center of much speculation in terms of work involving fulvic acid components (6.1-6.2). Investigation of parallel photodegradation behaviour between a quinone, hydroquinone and phenol model mixture and fulvic acid will also be presented and discussed early in the chapter.

Because of the apparent importance of quinonoid moieties in the photoactive centers of fulvic acid the first part of this chapter will involve a brief discussion of the strong charge transfer and free radical photochemical characteristics of quinonoid compounds. These compounds are of particular interest and will be shown to be important in describing fulvic acid photochemistry. Following this, the results of photodegradation work performed on various quinone model solutions will be presented as well as photodegradation of selected Laurentian fulvic acid solutions.

Finally, the photodegradation results of several Laurentian fulvic acid solutions, that were prepared with different pH, background electrolyte and molecular weight fractions will be presented. The photodegradation results show parallel sensitivity to these same 3 factors as did the primary yields of the dominant triplet states presented in Chapter 5. The importance of the excited state triplets in dominating photodegradation mechanisms for fulvic acid and parallel photochemical behaviour of quinones will be discussed.

6.2 Organic Charge-Transfer Complexes and Organic Photochemistry

Quinone and phenolic moieties are known to be present in humic substances (6.2-6.4). These compounds are known to be able to form so-called donor-acceptor complexes that have complex spectroscopic and photochemical characteristics. In the case of the Laurentian fulvic acid, characterization work of functional groups by solid state ^{13}C NMR, indicate that a major band occurs in the quinone (190-178 ppm) and aromatic ketone (220-190 ppm) chemical shift regions of the spectrum (Chapter 1). Therefore, quinone photochemistry and donor-acceptor charge-transfer interactions that quinones undergo could play a significant role in the photochemical and photophysical behaviour of Laurentian fulvic acid. A brief discussion of charge-transfer complexes of quinonoid moieties follows.

In certain cases, two or more molecules may participate in cooperative absorption or emission. The absorption or emission can only be understood as arising from molecular complexes. Most commonly, two molecules are involved in such phenomena. When two molecules act cooperatively to absorb a photon, a charge transfer complex is said to exist.

The important experimental spectroscopic characteristics of charge transfer complexes are (6.5):

1. the observation of a new absorption band which is characteristic of the charge transfer complex but not of either of the components of the complex, and
2. a concentration dependence of the new band.

Mixtures of molecules which possess a low ionization potential (electron donors; e.g., hydroquinone), and a high electron affinity (e.g., quinones, or electron acceptors) often exhibit charge transfer bands which are not separately shown by either component. A typical example is the quinhydrone mixture discussed below. The absorption bands formed are always broad and devoid of vibrational structure. The breadth of the absorption band is explained by the fact that the rather small binding energies of donor-acceptor complexes allows many different structural configurations of the complex to exist in equilibrium with one another. The absorption energy for each configuration will differ slightly and cause an apparent broadening of the band. In solution some charge-transfer complexes are reported to develop 'slowly'. That is, an equilibration time is needed to observe the formation of the charge-transfer band (sometimes hours).

These complexes are formed by weak interactions that include hydrogen bonding and aromatic π - π stacking interactions, as is the case of quinhydrone mixtures. As mentioned above, a 'new' electronic absorption band appears in the equilibrated mixture of such complexes compared to the components alone. For many so-called charge-transfer complexes it may be semantically more correct to speak of 'complexes showing charge-transfer absorption', however, the term 'charge-transfer complexes is often used. It should be emphasized that the description of a particular complex as, for example, a hydrogen-bonded or a charge-transfer complex, is on occasion (e.g.,quinhydrone), one of differing terminology. An important photochemical experimental characteristic of such charge-transfer donor-acceptor complexes (electron, hydrogen atom) is sensitivity to solvent-environment changes due to background electrolyte and/or pH changes.

As was discussed in Chapter 3, the absorption spectrum profile of fulvic acid solutions resembles that of an overlapping electronic absorption band distribution that might be obtained by creating a 'mixture' of aromatic ketones, quinones, phenolics and donor-acceptor charge-transfer complexes these compounds may form. That is, strong absorption occurs in the 200-300 nm region (π, π^*) with a gradual 'tailing off' into 'weak' overlapping electronic absorption bands in the >300-600nm region (n, π^*). This is not to say that the electronic absorption of fulvic acid solutions is solely due to aromatic ketone type of species, but that there is similarity between fulvic acid spectra and the electronic absorption of such compounds that are thought to make up a portion of the fulvic acid heterogeneous mixture. If the above comments on spectra are extended to photochemistry, the most probable organic photoreactions expected for fulvic acid, will arise from singlet (n, π^*), and triplet (n, π^*) excited states. Given that the experiments in this work involved irradiating in the near ultraviolet region of the spectrum, the electronic transitions are mainly of n, π^* character (despite the finite probability of some π, π^* character).

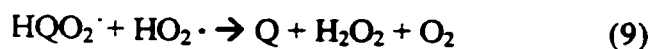
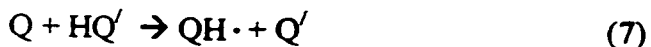
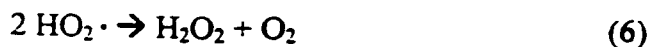
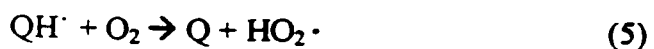
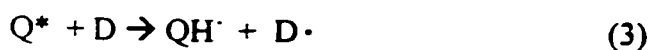
The characteristic primary photochemical processes from n, π^* excited singlet and triplet states is diradical-like to a good approximation. Primary photoreactions from these states are expected to undergo photoreactions characteristic of radicals such as :

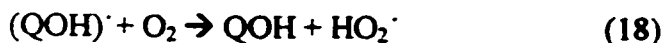
1. hydrogen atom or electron abstractions;
2. radical addition; and
3. cleavage reactions.

Quinone photochemistry has all the characteristics and complexities associated with free radical chemistry, and as will be discussed below, many of these characteristics

can be found within fulvic acid photochemistry (6.6). When irradiation of quinoid species is performed in aerated aqueous solutions several species have been observed to be present: HO_2^\cdot , H_2O_2 , O_2^\cdot , $^1\text{O}_2$, OH^\cdot , organoperoxides as well as a variety of side products expected from free radical chemistry (6.6).

For example, at a quinone concentration of about 10^{-4} M in aerobic aqueous solution in the presence of a hydrogen atom donor (D), a few reaction steps identified are the following (reactions illustrated are not given in any particular order), where Q, Q^\cdot , QH^\cdot , and QH_2 are used to indicate, respectively, the quinone, semiquinone anion radical, the neutral semiquinone and the hydroquinone. QOH is a hydroxy substituted quinone (6.6):





Polymer addition reactions can also occur as well as various oxidation reactions .

These complex free radical reactions may also be expected to occur in irradiated aerobic aqueous fulvic acid solutions.

Among the characteristics of quinones are the relatively stable free-radical intermediates (semiquinones) formed upon one electron reduction. Electron transfer photoreactions, or hydrogen atom abstraction photoreactions, between n,π^* excited state quinones and phenolic (hydroquinone) species lead to semiquinone intermediates. Note that one electron oxidation of a hydroquinone species leads to a semiquinone cation radical intermediate (prior to loss of a proton), or a neutral semiquinone moiety if hydrogen atom abstraction has occurred.

Light induced photoreactions of quinones (usually electron or hydrogen atom abstraction), may also occur between two quinone molecules rather than a quinoid and an electron rich phenolic molecule. A large difference in electron affinities between the two quinones could result in an electron transfer reaction occurring. The substituents on the ring of the quinone will again influence the rate of the reaction and mechanism.

Intramolecular photoreactions interactions have also been documented in quinones with large functionalized side chains.

Whether quinone photochemistry involves intermolecular or intramolecular mechanisms, irradiating aqueous solutions in the near U.V.-visible results in free radical chemistry occurring via semiquinone intermediates. Depending on the species present, polymerization, cycloaddition, electron abstraction, hydrogen atom abstraction, disproportionation, photorearrangement, ring opening fragmentation and complex oxidation reactions may occur (i.e., O_2 - semiquinone peroxyradical interactions, superoxide, etc.).

Similar reactions may be expected for fulvic acid solutions. It is noteworthy that humic substances are known to be rich in free radicals and that production of these radicals are influenced by irradiation, pH, background electrolyte and oxygen (6.7-6.9). Excellent compilations implicating quinoid species to the free radical, photophysical and photochemical characteristics of humic material may be found in (6.2, 6.3; and references therein). Similarities in ESR spectra of humic material and model quinoid compounds are also described (6.2) and implicate semiquinone like species as the free radicals present in humic substances. ESR experiments on the organic radicals within humic substances, including the effects of pH, oxidation, and UV radiation, are consistent with semiquinone moieties (6.10). In a series of papers by Slawinska et al. (6.11-6.13) entitled 'Chemiluminescence in the Photooxidation of Humic Acids', 'Chemiluminescence During Photooxidation of Melanins and Soil Humic Acids Arising from a Singlet Oxygen mechanism' and 'Chemiluminescence and the Formation of Singlet Oxygen in the Oxidation of Certain Polyphenols and Quinones', appearing in Volume 28 (1978) of *Photochemistry and Photobiology*, strong parallels are suggested between the photophysical characteristics of quinoid and humic species (aqueous solutions) when

irradiated with wavelengths of light > 320 nm (under oxygen and nitrogen atmospheres). More recently Scott et al. and Lovley et al. (6.4, 6.14-6.16) suggest that quinone moieties act as electron acceptors in the reduction of humic substances by humic-reducing microorganisms. These suggestions, are supported by work reported by Thom et al. (6.27) confirming the presence of quinones within humic substances using nuclear magnetic resonance (NMR).

It is also important to note that semiquinone radicals (with various side chain functional groups) have a broad electron absorption band that extends from approximately 350 - 450 nm in the U.V.-visible region of the spectrum and can therefore influence that region of the spectrum (Table 6.1) (6.6).

Table 6.1: Absorption Maxima of Selected Semiquinone Radicals (6.6)

<u>Compound semiquinone (aqueous solution)</u>	<u>λ_{max} (nm)</u>
1,4-benzoquinone semiquinone	415
p-hydroxyphenoxyl radical	390
4-t-butyl 1,2- benzoquinone semiquinone	400
4-t-butyl 1,2 dihydroxybenzene	279, 400
o- hydroxyphenoxyl radical	350
m- hydroxyphenoxyl radical	400
2,5-dimethyl 1,4-benzoquinone semiquinone	415
tetramethyl-1,4-benzoquinone semiquinone	430
1,4-naphthoquinone semiquinone	380
2-methyl-naphthoquinone semiquinone	370
Ubiquinone semiquinone	420

6.3 Photodegradation of Laurentian Fulvic Acid and Quinoid Model Mixtures

The results of photodegradation experiments of various Laurentian fulvic acid mixtures and corresponding quinone-hydroquinone-phenol (quinoid) model mixtures are presented below. Mixture preparation and concentrations used have been described earlier (Chapter 2).

The quinoid model mixture was made in order to investigate similarities that may exist between fulvic acid and quinone photochemistry. Early work involving solid state ^{13}C NMR of fulvic acid samples taken before and after irradiation at 350nm indicate that most of the changes occur in the quinone, carboxylic acid and phenolic-aromatic regions of the spectrum (Figure 6.1). These changes were found to be consistent, at least for times under 400 hours of irradiation at 350 nm and concentrations of fulvic acid solutions of 17 mg/L. Recall that the chemical shift region (Chapter 1) for the aromatic - phenol - hydroquinone functional groups is between approximately 96 and 165 ppm. The carboxyl region is 178- 165 ppm, quinone 190-178 ppm and aromatic ketone 220-190 ppm. As is apparent from Figure 6.1, the major functional groups that appear to be most affected by photodegradation are between approximately 96-220 ppm. Most striking is the apparent loss in the aromatic-phenol-hydroquinone and carboxylic acid regions. This is consistent with what would be expected to occur under photooxidation (photodegradation) conditions of phenolic and carboxylic substituted species. The

phenolics in the presence of strong electron acceptors (quinones), or hydrogen atom acceptors (as well as other strong oxidizers such as superoxide, singlet oxygen, etc.) may be oxidized to semiquinone species. These species may also be further oxidized to quinone species as well as other degradation products. The carboxylic acid groups would also be driven off as carbon dioxide during the photooxidative processes. The carboxylic acid region appears to be relatively more sensitive to photodegradation than the quinone region. During photodegradation, the carboxylic acid to quinone ratio in the humic mixture appears to decrease. The formation of 'new' quinones during photodegradation of phenolics may be a possibility.

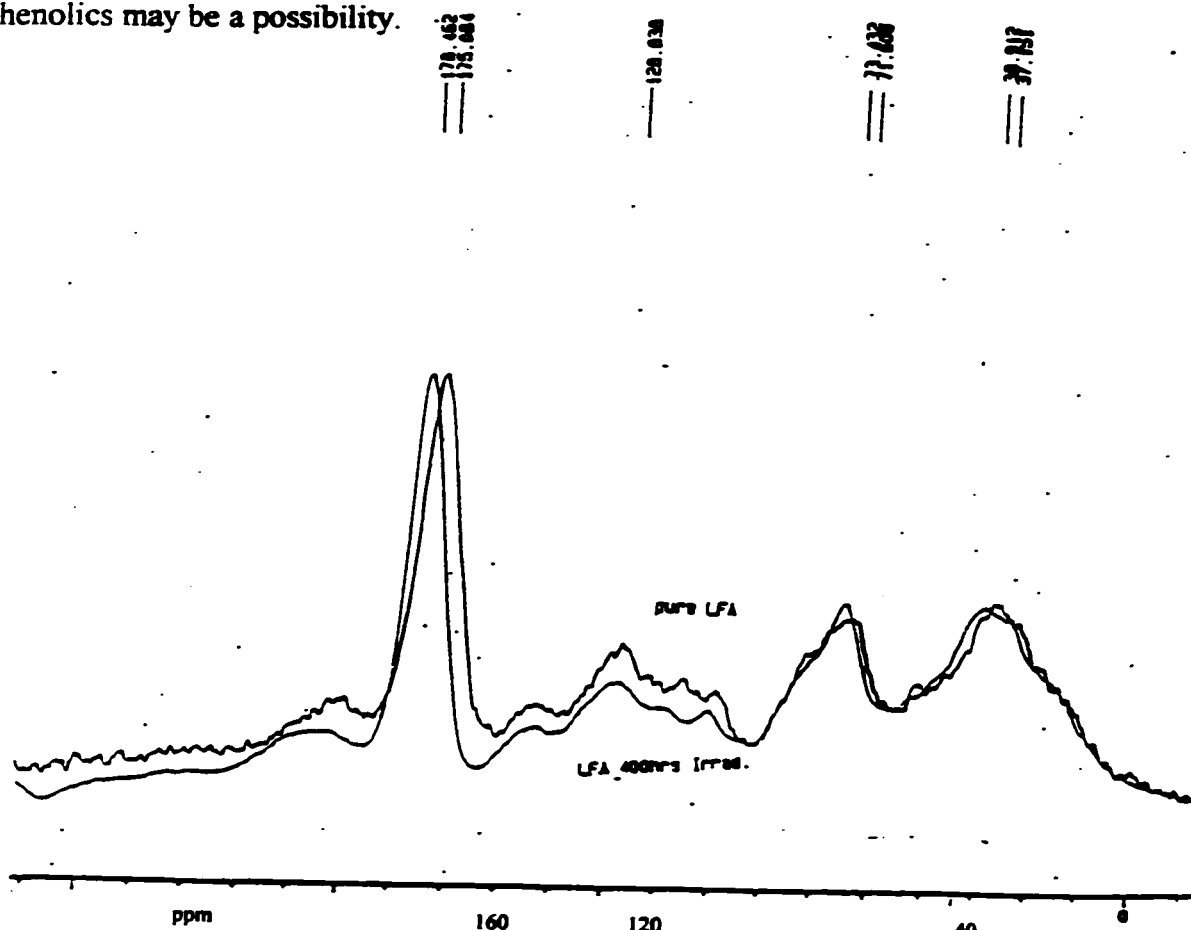


Figure 6.1: Solid state ^{13}C NMR of Laurentian fulvic acid before and after irradiation at 350nm.

The intent of studying the photodegradative behaviour of the relatively simple quinoid model mixture is to determine if parallels exist with the more complex heterogeneous humic mixture. As will be discussed below, sufficiently important similarities exist that strongly support the hypothesis that functionalities in fulvic acid responsible for its photochemical character are homologues of the model components.

6.3.1 Photodegradation of Quinonoid Model Mixtures

Interestingly, a critical step in the procedure to make the quinoid model solution is that the benzoquinone and hydroquinone are prepared in the dark (while stirring) and allowed to equilibrate with stirring for 30-45 min before addition of the phenol. The molar ratios used are approximately 1:3:3 quinone, hydroquinone and phenol. The solution is left in the dark (while stirring) for 24 hours (Chapter 2). Similarly, the ubiquinone (coenzyme Q10) based model was prepared with molar ratios of quinone to hydroquinone and phenol of 1:6:6. Solution preparation always involves a first step (in the dark) in which the ubiquinone and hydroquinone were first sonicated then stirred and allowed to equilibrate for approximately 6 hrs before adding the phenol. The solution was then left (with stirring) in the dark for an additional 24 hrs.

If the quinonoid solutions were exposed to light prematurely or impure components were used, the solutions would not behave as indicated in the figures below. As the solution of quinone (1,4-benzoquinone) and hydroquinone is allowed to equilibrate in the dark a 'new' absorption band appears to form. The band is determined by subtracting the absorption spectrum of the mixture before and after equilibration in the dark and dividing by the initial absorption spectrum ($\Delta A/A_i = (A_{\text{final}} - A_{\text{initial}})/A_{\text{initial}}$) and multiplying by 100, thereby determining a percent absorbance change if

plotted vs. wavelength (Figure 6.2). If the components of the mixture are not allowed to equilibrate for the full length of time and the absorption band does not form, and the photodegradation 'profile' particularly in the >300nm region will not mimic fulvic acid. This phenomena is important and recalls the previous discussion of charge-transfer complex (donor-acceptor complex) formation (band formation) common to quinonoid systems. Although this observation is admittedly circumstantial it is nonetheless important to note. It is also interesting to note that the broad featureless absorption band, Figure 6.2 (quinone model), bears a remarkable similarity to the quinhydrone absorption spectrum reported by Nakamoto (6.18).

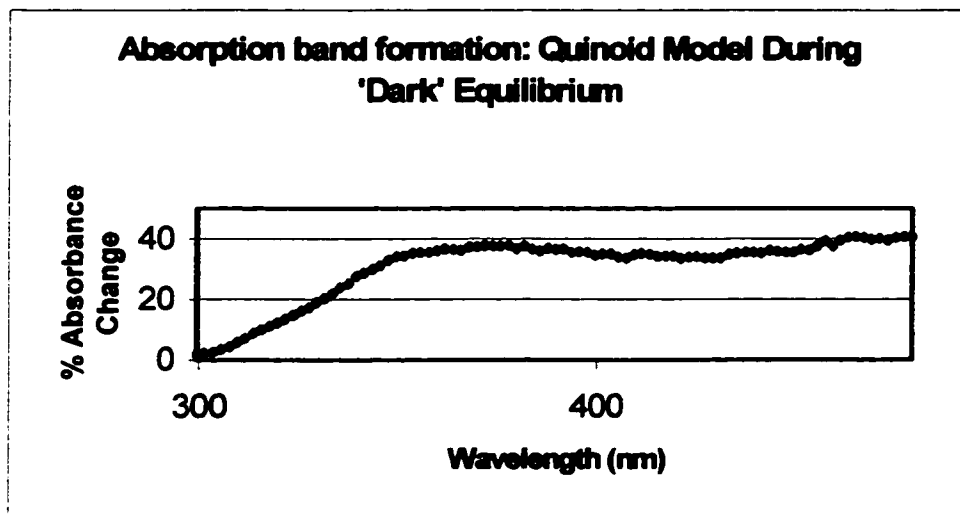


Figure 6.2: Color formation (dark) during 'dark' equilibrium of mixture. The percent absorbance change is calculated by determining the difference between the absorbance spectrum of the quinoid mixture before and after 'dark' equilibrium and dividing by the initial absorbance spectrum of the mixture, and multiplying by 100; $((A_{\text{final}} - A_{\text{initial}}) / A_{\text{initial}}) * 100$. The average of ten trials is illustrated with experimental error of 10%.

The large broad featureless band between 300 and 500 nm is reported by Nakamoto (6.18) which grows in the same region of the absorption spectrum and plateaus out similarly. One maxima near 350 nm is apparent in both spectra. Briegleb et al. (6.19) also identified an apparent broad charge transfer band for a benzoquinone solution in the 350 nm region. Similarly, Matsuda et al. (6.20), report a broad charge transfer band for quinhydrone to occur in the region between 380 and 550 nm (6.20). It is also important to consider that Cassidy and Moser (6.21) and Michaelis and Granick (6.22) found that quinhydrone has an extinction coefficient much larger than quinone or hydroquinone in the > 300nm to 500 nm region of the spectrum.

The figures below of the quinoid models and fulvic acid solutions illustrate relative changes in absorbance verses wavelength determined in the following manner; in this case a positive value for relative absorbance change ($[\text{initial}-\text{final}] / \text{initial}$) indicates 'loss' of absorbance at that wavelength, while a 'negative' value indicates an 'increase' in absorbance at that wavelength. The results are then multiplied by 100 to show % absorbance change.

Figure 6.3 is the UV-Vis spectrum of the quinoid mixture (1,4 Benzoquinone-Hydroquinone-Phenol). Figures 6.4 - 6.6 illustrate photodegradation of various Laurentian fulvic acid solutions with comparison to quinonoid-model mixtures. The fulvic acid solutions used were prepared at various pH and background electrolyte concentrations in order to determine any parallels between the photodegradation results and the apparent triplet quantum yields reported in Chapter 5. The quinonoid model was only prepared at pH 5.8 for these experiments because of 'dark' reactions that occur in alkaline solution.

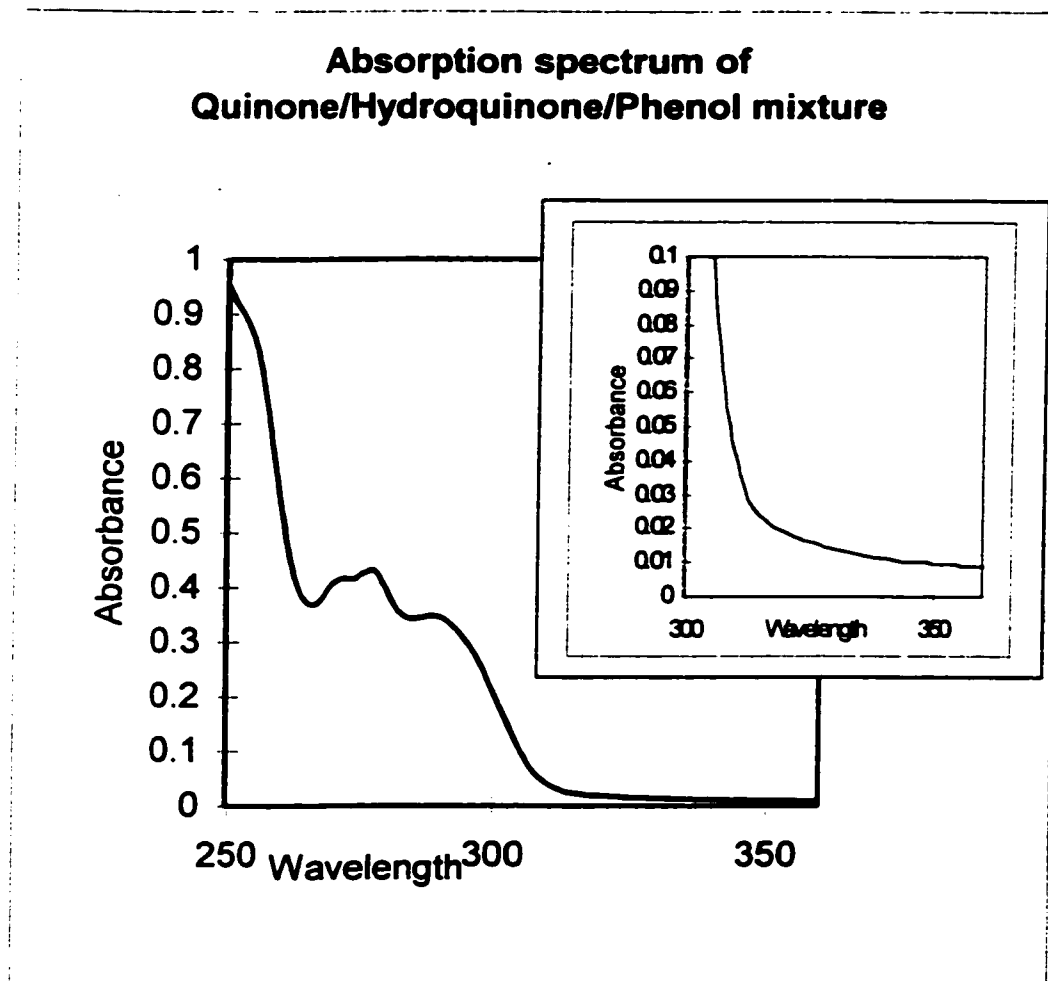


Figure 6.3: UV-Visible absorption spectrum of the quinoid model mixture: 1,4 Benzoquinone-Hydroquinone-Phenol in aqueous solution with a molar ratio of 1:3:3.

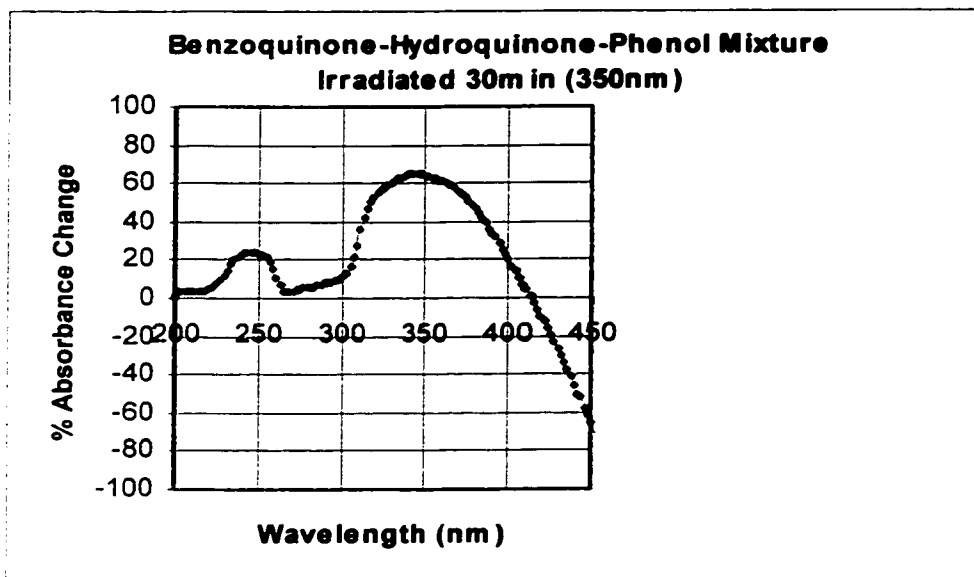


Figure 6.4: Percent change in absorbance vs. wavelength for the quinoid model (1,4benzoquinone-hydroquinone-phenol) after irradiation for 30 min at 350nm. An average of 15 trials is illustrated (standard deviation of 10%).

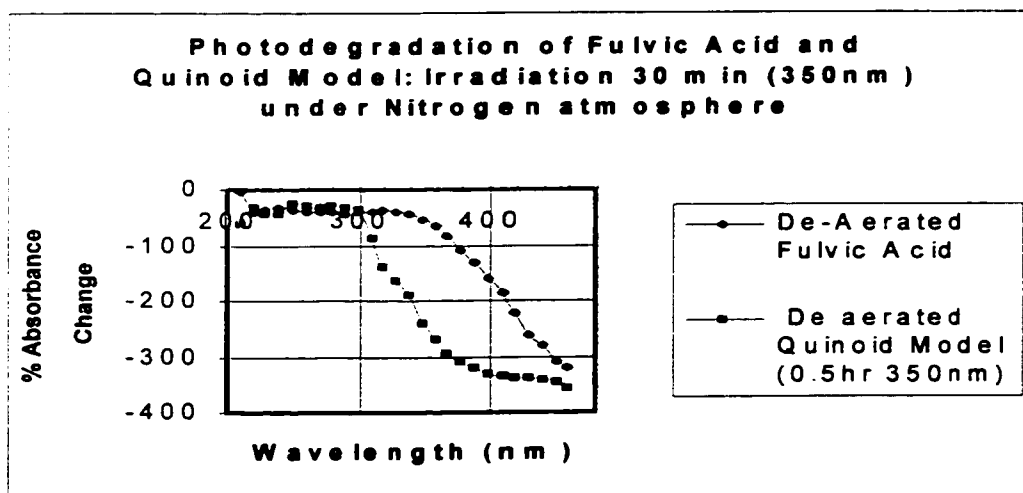


Figure 6.5: Percent change in absorbance vs. wavelength for fulvic acid (17mg/L) and the quinoid model (1,4 benzoquinone-hydroquinone-phenol) with irradiation for 30 min under a nitrogen atmosphere. An average of ten solutions was used for both the fulvic acid and quinoid model solutions (standard deviation 10%).

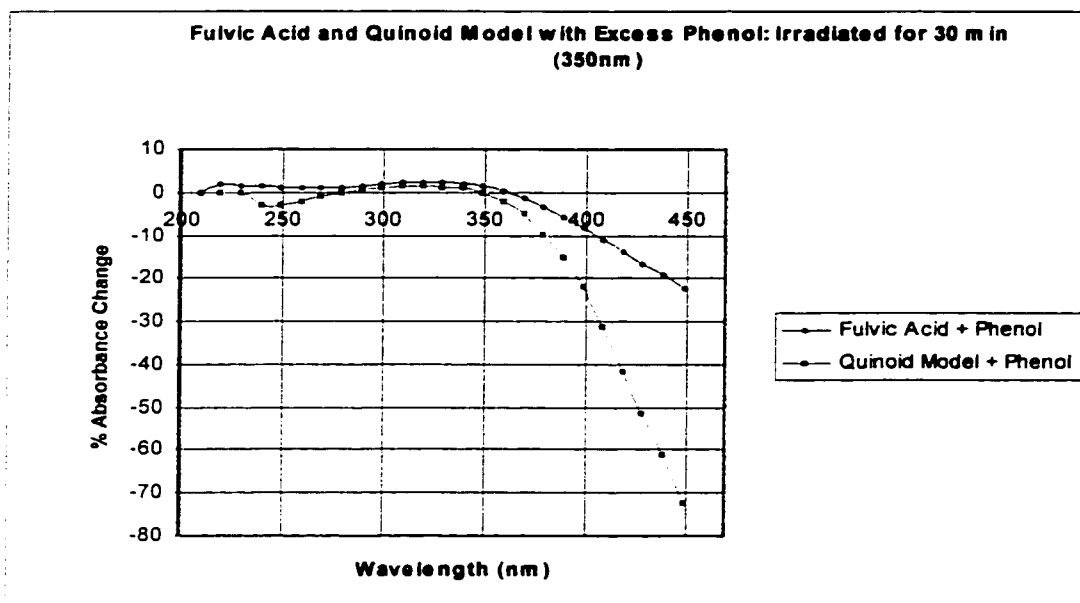


Figure 6.6: Percent change in absorbance vs. wavelength for fulvic acid (17mg/L with 1mg/L added phenol) and quinoid model (with 1mg/L added phenol). Irradiation was carried out for 30 min at 350nm. An average of 10 solutions were used for both (10% standard deviation).

Consider Figure 6.4, the two regions of maximum change occur near 250nm and in the 350nm region of the spectrum. The first region is associated with various quinones (substituted and non-substituted) which have a characteristic band in the 235-250nm region of the spectrum (Chapter 3). The hydroquinone and phenol both have very low absorption relative to quinone in the 250 nm region. As was discussed previously, the region between 300nm-450nm is associated with charge transfer complexes (e.g., quinhydrone complexes) and semiquinone free radical intermediates (including cross-linked polymers). It is important to note that not allowing equilibration (dark) of the quinone and hydroquinone prior to the addition of phenol and irradiating prematurely creates a photodegradation profile unlike that of the fulvic acid only in the region >300nm. Solutions that are not properly equilibrated do not form a charge transfer band so that photodegradation reactions do not disrupt the quinhydrone complexes and 'lose'

color in that region of the spectrum. Instead, color formation occurs in that region via cross-linking polymerization reactions with free radical species.

The photodegradation results of the original model mixture formed by the relatively simple mixture (compared to fulvic acid), unsubstituted 1,4-benzoquinone, hydroquinone and phenol, illustrated in Figure 6.4, shares a remarkable similarity to that of the heterogeneous fulvic polymer mixture (Figures 6.10.-6.12 below). This is consistent with the results of NMR relaxation studies in that the quinoid moieties in fulvic acid are relatively unsubstituted quinones and phenols (6.24). The photodegradation of this simple model suggests that quinones and phenolic moieties appear to dominate the photophysics and photochemistry of fulvic acid.

The model solutions are made up at a pH of approximately 5.8. At that pH, semiquinone radicals are not as stable as in alkaline solution and undergo reaction with oxygen to follow degradative pathways. Since semiquinones and any other polymers formed also absorb in the 300-450 nm region, photodegradation at high pH or under de-aerated conditions will tend to create a color increase rather than loss in that area of the spectrum through cross-linking mechanisms due to increased lifetimes and interaction possibilities of the radicals formed.

In other words, when no oxygen is present the 300-450 nm region is expected to show an 'increase' in absorbance as is seen in Figure 6.5. The 'loss' in this region, for aerated solutions, can be attributed to oxidative processes. Semiquinones are well known to react quickly and efficiently with oxygen to form organo-peroxyradical species. Such species are also known to be highly reactive with phenols. Degradative reaction pathways usually involve ring opening, fragmentation reactions. Oxidative degradation pathways

leading to such smaller products through ring opening mechanisms are more efficient for the more substituted ring species or for species in acidic conditions (6.6). Figure 6.5 illustrates parallel behaviour between the quinonoid model mixture and photodegradation of fulvic acid. Both are dominated by cross-linking polymer mechanisms when no oxygen is present. Oxygen removes reducing radicals such as the solvated electron and forms superoxide and other oxidizing radicals. Oxidizing radicals attack hydroquinone species faster than the quinone species leading to reactive peroxyradical species. With no oxygen present the solvated electron may be preferentially picked up by the quinone. Semiquinones formed could cross link and polymerize. Competition between degradation and polymerization reactions is a characteristic of quinonoid photochemistry (6.6). As was mentioned before, NMR relaxation studies revealed that quinone and phenolic moieties are not heavily substituted, therefore, if intermediates formed have the opportunity to cross-link, they will. This suggests the strong influence of oxygen, in particular singlet oxygen, in degradative mechanisms for fulvic acid.

Figure 6.6 also shows interesting parallel behaviour between the quinone mixture and the Laurentian fulvic acid. Similar effects occur when excess phenol is added to the fulvic acid and to the quinone model mixture in almost the same proportion across the UV-VIS absorption spectrum (200–450nm). Phenol semiquinone/quinone interactions are known to exist (6.6). Phenol may disrupt a quinhydrone complex and decrease color formation in that region and/or the excess phenol may possibly shift the electron transfer equilibrium. The Faust cycle (6.25) suggests that phenoxy radicals may form in similar photo-redox systems. If this is the case phenoxy radicals may undergo cross linking polymerization reactions.

The results of photodegradation experiments of the ubiquinone-hydroquinone-phenol model mixture are presented below in Figures 6.8 and 6.9. Figure 6.7 is the uv-vis. spectrum of the quinoid mixture (Ubiquinone-Hydroquinone-Phenol). Sample preparation was carried as with the benzoquinone mixture except that a molar ratio of 1: 6: 6 of ubiquinone: hydroquinone: phenol was used. The ubiquinone (coenzyme 10 was obtained from Sigma Chemical). Notice that there are two regions of major change in Figs. 6.8 and 6.9, one near 250 nm and the other beyond 350 nm. The first region of maximum change (near 250 nm) is associated with the quinone (Chapter 3), and the second with the charge transfer complex. The hydroquinone and phenol both have very low absorption relative to quinone in the 250 nm region. The region between 300-450 nm is associated with charge transfer complexes (e.g., quinhydrone complexes) and semiquinone free radical intermediates (including cross-linked polymers)

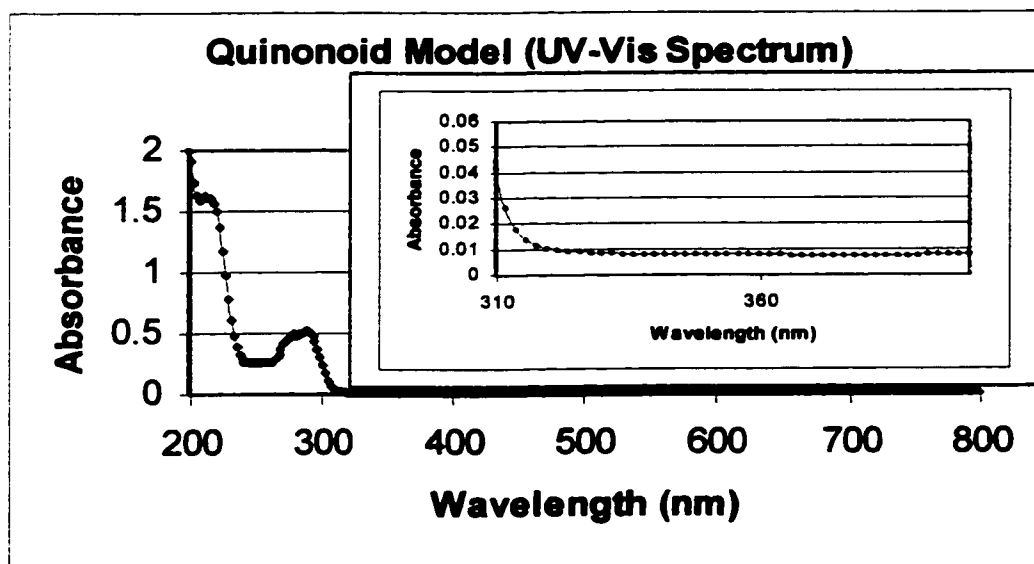


Figure 6.7: UV-Visible absorption spectrum of the quinoid model mixture: Ubiquinone-Hydroquinone-Phenol in aqueous solution. The long wavelength insert is also shown.

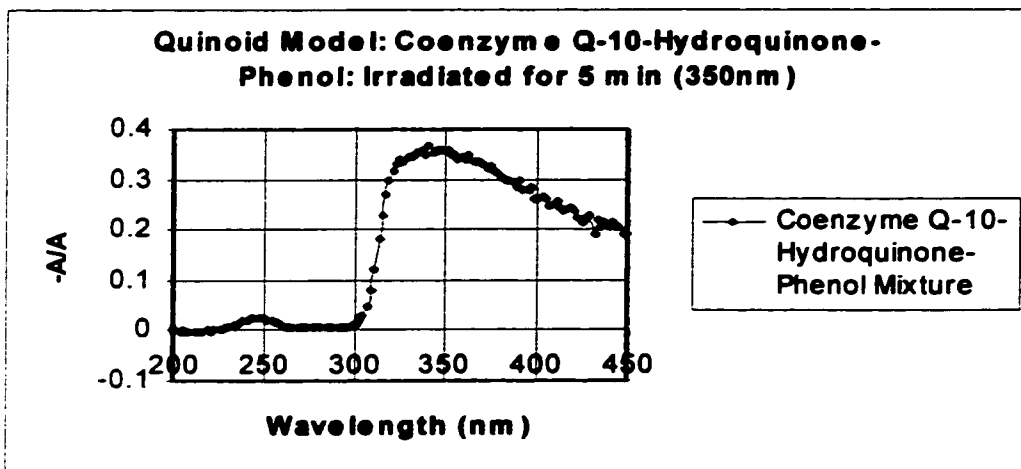


Figure 6.8: Relative change in absorbance vs. wavelength for the quinoid model (Ubiquinone-hydroquinone-phenol) after irradiation for 5 min at 350nm. An average of 10 runs was taken with a standard deviation of 10%.

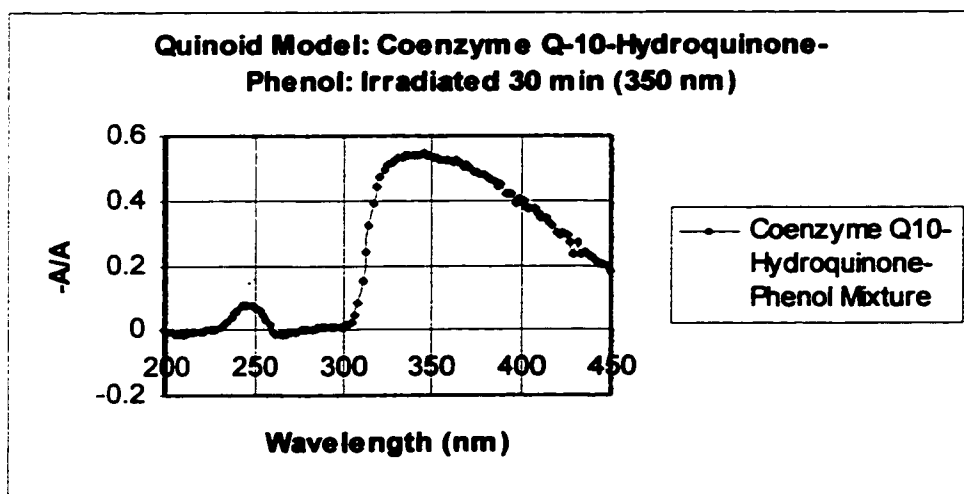


Figure 6.9: Relative absorbance change vs. wavelength for the quinoid mixture (Ubiquinone- hydroquinone- phenol;) irradiated for 30 min at 350 nm. An average of 10 runs was taken with a standard deviation of 10%.

Interestingly, the photodegradation profile of this relatively simple mixture (compared to fulvic acid) also shares a remarkable similarity to that of the heterogeneous polymer mixture (Figures 6.10-6.12 below). This is consistent with the results of the solid state NMR (Figure 6.1) that indicate quinoid moieties in fulvic acid are relatively affected by photodegradation, again suggesting that quinones and phenolic moieties dominate the photophysics and photochemistry of fulvic acid. As mentioned earlier NMR relaxation studies revealed that quinone and phenolic moieties are not heavily substituted therefore if intermediates formed have the opportunity to cross-link, they will (1.26). The fact that fulvic acid solutions preferentially undergo degradative pathways ('loss' in absorbance) and not 'colour' formation over long times in aerated solutions suggests that the quinone and phenolic moieties may be isolated. The quinoid solutions made with the large substituted ubiquinone in the presence of hydroquinone and phenol may be able to 'mimic' the Laurentian fulvic acid solutions at least at times between 5 and 30 minutes because of decreased 'cross-linking' polymerization possibilities and steric effects isolating free radical species in solution. The ubiquinone in this case may be simultaneously mimicking the quinone (photoactive) species in fulvic acid components and larger non-photoactive molecular species present as well. Those larger species in fulvic acid complexes may isolate and protect smaller photoactive quinone moieties by tethering and/or micelle like actions. Qualitative results indicate that the ubiquinone model does not model the fulvic acid well under deaerated conditions as compared to the 1,4-benzoquinone model mixture. Lower 'colour' formation of the ubiquinone mixture may indicate that this quinone represents an upper limit of the quinones present in the

Laurentian fulvic acid (the lower limit being the smaller non-substituted 1,4 benzoquinone).

In either case, photodegradation of fulvic acid solutions seem to be modeled closely by quinonoid solutions when irradiated in the near ultraviolet.

6.3.2 Photodegradation of Laurentian Fulvic Acid

The photodegradation of the Laurentian fulvic acid solutions (Figures 6.10-6.13), under different conditions of pH, background electrolyte, concentration and molecular weight fractions illustrate parallels to the primary apparent triplet quantum yield results reported in Chapter 5.

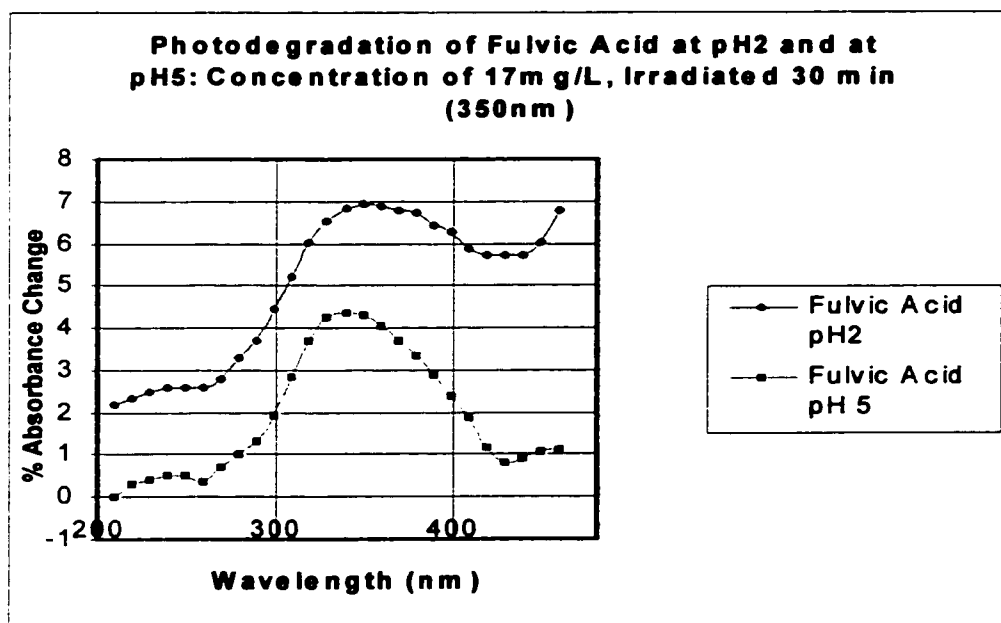


Figure 6.10: Percent change in absorbance vs. wavelength for Laurentian fulvic acid (17mg/L) at pH 2 and pH 5 after irradiation for 30 min at 350nm. Solutions were equilibrated in the dark. An average of 10 trials was used (standard deviation of 10%).

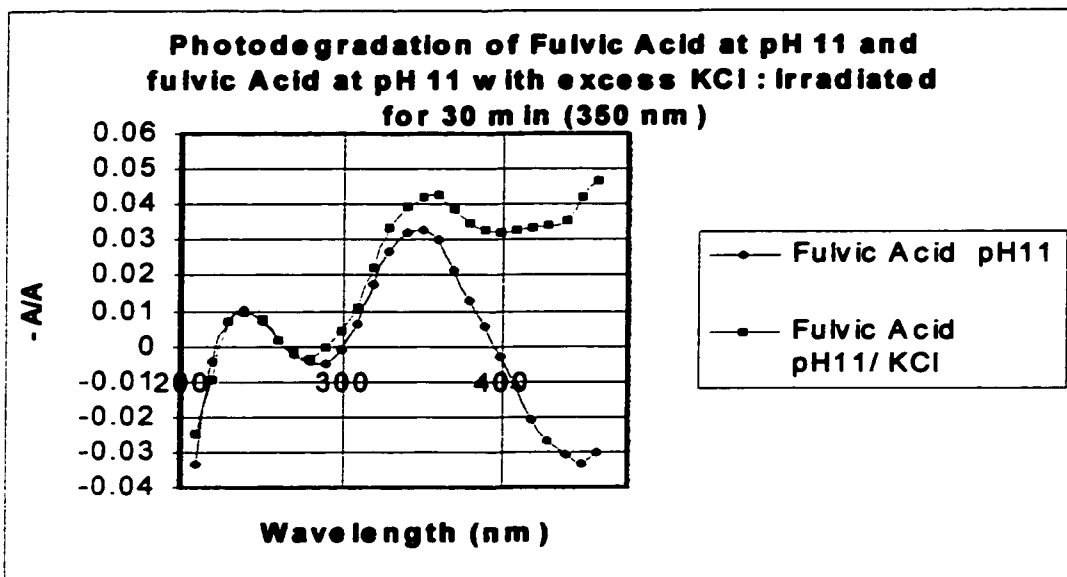


Figure 6.11: Ionic strength effect: Percent absorbance change vs. wavelength for fulvic acid (17mg/L) at pH11 and at pH 11 with 1 M KCl. An average of ten trials was used with a standard deviation of 10%.

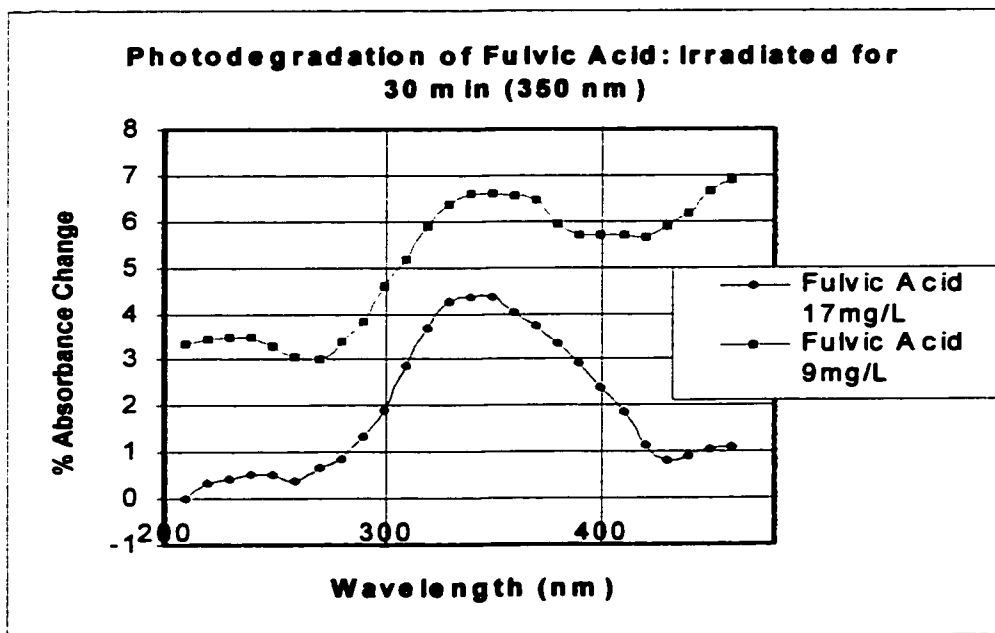


Figure 6.12: Percent absorbance change vs. wavelength for Laurentian fulvic acid at a concentration of 17mg/L and 9mg/L. Samples were irradiated for 30 min at 350nm. An average of ten solutions is illustrated above with a standard deviation of 10%.

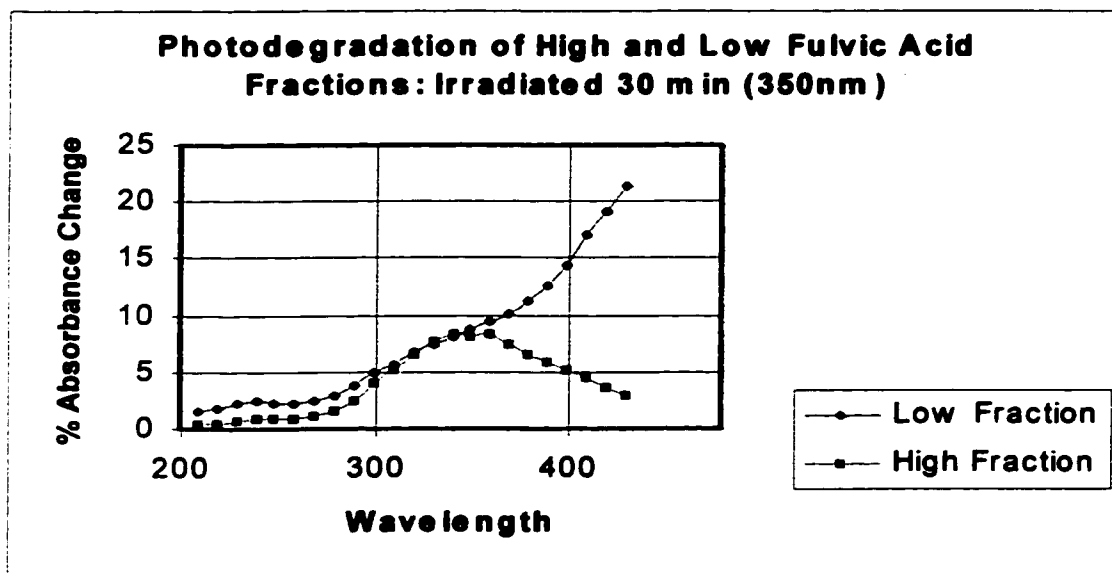


Figure 6.13: Relative change in absorbance vs. wavelength for high molecular weight fraction solutions of Laurentian fulvic acid (fulvic acid solution that were retained after filtering with a YM30(nominal cutoff 30000 Da) filter membrane, and low molecular weight fraction solutions (passed by a YM2 (nominal cutoff 1000 Da) filter membrane. Irradiation was carried out for 30 min (350nm). Average of 10 trials (Std.Dvn. 10%).

As was discussed in Chapter 5, high apparent triplet quantum yields for the fulvic acid solutions may lead to higher yields of singlet oxygen production and therefore more oxidative degradation. Apparent quantum yields presented in Chapter 5, were higher for lower pH values of fulvic acid solutions. Figure 6.10 suggests a parallel between the photodegradation results and the higher triplet quantum yields determined at pH 2. Quinone photochemistry is well known to be sensitive to pH, oxygen content, and background electrolyte (6.6). Interestingly, work reported by Slawinska et al., proposes singlet oxygen photooxidation mechanisms for quinoid species as well as humic substances (6.11-6.13).

Figure 6.11 also would seem to parallel the results of Chapter 5 where high background electrolyte at high pH yielded higher apparent triplet quantum yields for the fulvic acid solutions, compared to high pH solutions without the added background electrolyte. Again, a singlet oxygen degradation pathway is suggested.

Figure 6.12 suggests more efficient photodegradation for the less concentrated fulvic acid solution. Hoigne and Haag (6.23) found that more 'highly coloured' waters produced less singlet oxygen. Concentration affects conformation in humic substances, and, conformational changes may influence excited state triplet lifetimes. These changes could determine singlet oxygen production. NMR relaxation time studies (6.24) suggest that the quinoid and phenolic moieties are not heavily substituted. As will be discussed in Section 6.4, quinhydrone complexes between non-substituted or not heavily substituted species have higher probability for aromatic π - π overlap. For higher concentration solutions 'environmental' interferences with the complex may occur, distorting and disrupting the charge transfer complexes and possibly affecting the excited state lifetimes of the complex.

Figure 6.13 suggests more efficient oxidative degradation in the low molecular weight fractions of fulvic acid than in the higher molecular weight fraction solutions. Recall that the apparent triplet quantum yields were higher for the lower fractions of fulvic acid (Chapter 5) suggesting again that a singlet oxygen mechanism may be involved.

Quinones irradiated in the near ultra-violet are known to undergo efficient n,π^* singlet-triplet intersystem crossing (6.5,6.6, Chapter 3), as apparently do Laurentian fulvic acid solutions (Chapter 5). Results of MCD spectroscopy of Laurentian fulvic acid

solutions also support this hypothesis (Chapter 5). Relatively small energy differences between singlet and triplet excited states are typical of n,π^* excited carbonyl states that have high quantum yields for intersystem crossing (6.5). Magnetic circular dichroism spectroscopy of Laurentian fulvic acid (Chapter 5) indicate that the electronic energy difference between singlet and triplet states (ΔE_{ST}) is approximately 7 kcal/mol. Singlet-triplet splitting values of 10 kcal/mol, or lower, are expected for molecules with n,π^* states (e.g. quinones). Singlet-triplet splitting energies for π,π^* states are typically > 30 kcal/mol (6.5). The value of 7 kcal/mol for Laurentian fulvic acid, is within splitting energy range common for quinoid and aromatic ketonic species (6.5). It is indicative of a predominantly n,π^* electronic transitional character for fulvic acid when irradiated in the near U.V. High quantum yields for intersystem crossing are also associated with such quinone systems as for Laurentian fulvic acid (Chapter 5).

As mentioned above, high apparent triplet quantum yields for the fulvic acid solutions may lead to higher yields of singlet oxygen production and therefore more oxidative degradation. Figures 6.10-6.13 indicate that the photodegradation of fulvic acid solutions is sensitive to changes in pH, oxygen and background electrolyte. Quinone photochemistry is also well known to be sensitive to pH, oxygen content, and background electrolyte (6.6). Similar regions of spectral change (250nm and 340 nm) occur in the photodegradation of fulvic acid (Figures 6.10-6.12) and the quinone model systems. This suggests that quinoid moieties are involved in the photo-oxidation processes of fulvic acid. These results are consistent with the change noted in the quinone-phenol and hydroquinone region of the NMR spectrum presented earlier (Figure 6.1). Work

presented by Schulten et al. (6.17) also shows evidence for loss in the same chemical shift region for aerated degradation experiments of humic material. Interestingly, all three components (quinone, phenol and hydroquinone) are necessary for the quinone models to be able to 'mimic' the uv-vis photodegradation profile of fulvic acid.

Summary of Photochemical Mechanistic Study

Several observations can be made from the photochemical mechanistic study. The first is that NMR results indicate changes in the aromatic, phenolic and quinone regions of the spectrum. Quinones have been the center of much speculation as components of fulvic acid and photodegradation results of quinonoid model solutions indicate parallel behaviour between quinone, hydroquinone, phenol mixtures and fulvic acid only after equilibration time in the sample preparation step allows for the formations of semiquinone derived charge transfer complexes. Photodegradation of fulvic acid and quinonoid model solutions occurs in similar regions of the U.V.-Vis spectrum with maxima occurring at approximately 250 nm and 350 nm. The strong evidence for parallel behaviour is reinforced by the results of the anaerobic irradiation experiments of the fulvic and quinonoid model solutions which indicate similar photo-polymerization behaviour. Parallel photo-polymerization behaviour was also observed through the same U.V.-Vis (200-500 nm) region of the spectrum for both fulvic acid and the quinonoid model solutions that were prepared with excess phenol.

Similarities also exist for fulvic acid and quinones in that both undergo efficient intersystem crossing. From triplet excited states quinones are well known to undergo complex free radical photochemistry in aqueous solutions (6.6). These same

characteristics appear evident for fulvic acid solutions as well. The photodegradation of fulvic acid shows strong trends expected from triplet dominated pathways, including pH, background electrolyte, and molecular weight fraction sensitivity. The much higher primary photoproduct quantum yields for the triplet excited states of fulvic acid dominate photodegradation of fulvic acid (as was expected). Further evidence of the dominance of the triplets can be seen from the concentration dependence of photodegradation of fulvic acid. Singlet oxygen production was shown to be higher in less concentrated humic solutions (6.23).

6.4 Molecular Modeling

Molecular modeling work has been performed on quinone-hydroquinone charge-transfer structures. Figure 6.14 illustrates the effect of substituents on predicted geometry.

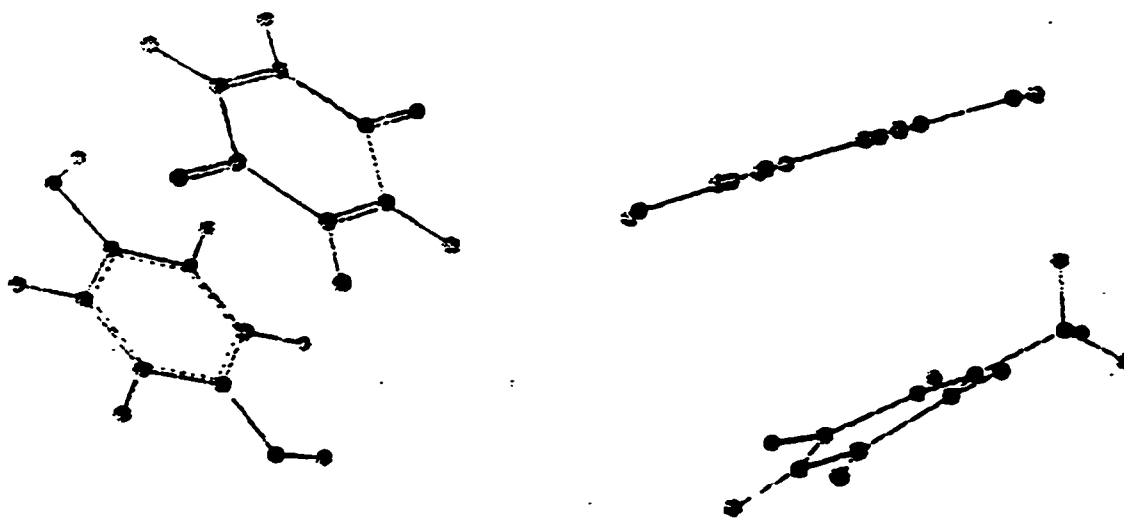


Figure 6.14: Geometrical optimization semi-empirical PM3 calculations (aqueous) performed on 1,4-benzoquinone-hydroquinone (quinhydrone) left, and a methoxy substituted 1,4 benzoquinone-hydroquinone (quinhydrone) in water (right).

There is a remarkable similarity in 'predicted' association geometry between the quinone and hydroquinone compounds that resemble early crystallography data and theoretical work concerning quinhydrone structures and organic charge transfer complexes (Figure 6.14). The nonsubstituted quinhydrone complexes are predicted to favour a relatively more parallel face-to-face ring association geometry than substituted moieties. As substituents are added to the ring structures, or neighboring molecules come into closer contact (especially molecules capable of H-bonding or forming aromatic plane interactions themselves, i.e., phenol or aliphatic alcohols), there seems to be a tendency for twisting of the parallel face-to-face geometry of the quinhydrone complex as its 'outer environment' is modified. Charge transfer interactions in twisted complexes could result in a higher probability for electron escape to the solvent (quantum tunneling or other mechanism) in comparison to parallel complexes.

Molecules with strong intra- and/or intermolecular hydrogen bonding, aromatic stacking and donor-acceptor interactions are interesting examples of moieties that may undergo complex self-assembly interactions (6.28, 6.29).

Synthetic self-assembly work takes advantage of strong H-bonding and aromatic stacking between monomer units in order to add stability to the complexes formed. Without going into detail, these functionalities are useful in synthesis work involving macromolecular structures since they are relatively rigid, act as good spacers and result in good curvature for the complexes.

Interestingly, the 'mechanical' structure of self-assembling systems based on the D-A complex principle are sensitive to the redox properties of the 'environment' and to the level of counterions present in solution. Fulvic acid may share similar 'sensitivities'. A

well known family of self-assembly organizations are the calixarenes and calixarene-like assemblies. These supramolecular structures can be obtained by direct condensation of substituted phenols and cresols and resorcinols in the dark under alkaline conditions. It is tempting to think that similar assemblies may form within certain conditions (pH, oxidation-reduction) in humic solutions (6.28, 6.29).

Data from elemental analysis, NMR and photochemistry can be combined in order to produce a hypothetical model structure. Figure 6.15 illustrates a hypothetical 'monomer' structure of fulvic acid based on the results of elemental analysis, NMR and photochemical data.

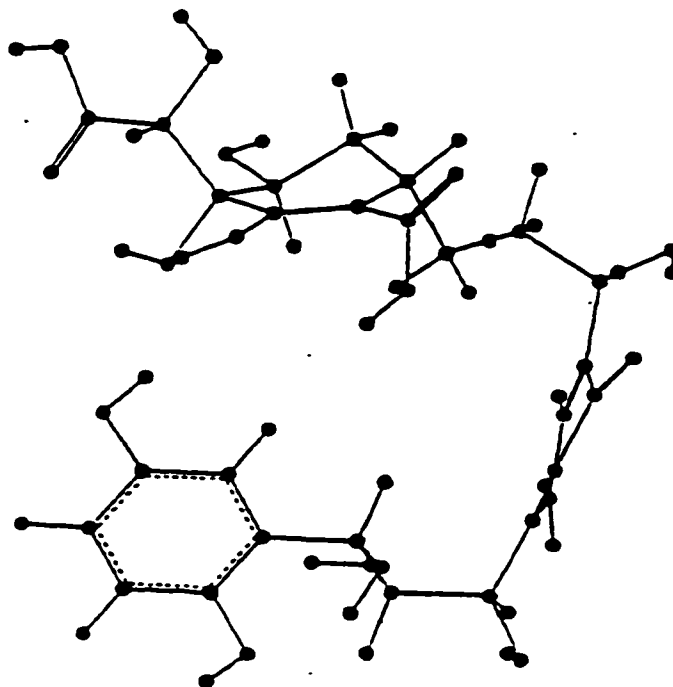


Figure 6.15: Hypothetical 'monomer' structure of Laurentian fulvic acid. Geometrical optimization calculations were performed using semi-empirical PM3 (aqueous) procedures.

It is also interesting to note that in order to 'build' a hypothetical monomer for Laurentian fulvic acid using elemental analysis data, NMR, photochemical data and a number average molecular weight of approximately 900 g/mol (Chapter 1), that it is difficult to end up with a structure that would not have strong H-bonding and/or ring-stacking interactions with another monomer unit. Interestingly, the 'monomer' structure illustrated above (Figure 6.15) has the so-called 'half tennis-ball' structure common in self-assembly units (6.29).

6.5 Conclusion & Future Work

For the first time all primary photoproduct quantum yields have been determined. The major primary photoproduct quantum yield was determined to be due to the triplets which show strong pH, background electrolyte and molecular weight sensitivity. Photodegradation also shows parallel trends.

The strong dependence of triplet quantum yields and photoactivity on pH and background electrolyte recalls the strong relation that exists between the molecular conformation of fulvic acid and the same two factors. Indeed the spectroscopic characteristics of fulvic acid have been shown to be dependent on molecular conformation. The data obtained in this study supports a polymer donor-acceptor charge transfer complex model, similar to a quinone-hydroquinone charge transfer complex, as key to fulvic acid's photobehaviour.

Much future work is needed to exploit this simple 'artificial' model to the fullest. Although at a relatively undeveloped stage, the simple chemical mixture has provided insight into the quinoid charge-transfer character of the 'photoactive' regions of fulvic

acid. The fact that fulvic acid may be 'mimicked' by such a simple combination of relatively small molecules raises many interesting possibilities. A variety of 'simple' quinoid chemical combinations can be made, as well as mixtures involving components representing larger non-photoactive alkane, carbohydrate and / or micellar assembly moieties. Such model mixtures could be used in order to study interactions and effects such compounds and/or micelle assemblies may have on photoactivity. A combination of carefully planned solid state ^{13}C NMR experiments at different stages of photodegradation for various models (different concentrations and functional groups) together with multistage EPR work may help to truly quantify certain functional group regions in the solid state ^{13}C NMR spectrum of fulvic acid. The simple quinoid model studied up to this point reveals that it is possible to track changes kinetically under different conditions of pH, background electrolyte and oxygen content without much difficulty.

Interestingly, quinoid photochemistry (under acidic conditions) and 'dark' alkaline quinone chemistry predict the formation of similar so-called 'humic-polymers'. EPR (Figure 6.16) and fluorescence work of a solution of such alkaline quinone 'humic-polymers' reveals striking similarities with fulvic acid solutions (6.26). The EPR of the quinonoid model and the fulvic acid are similar both in terms of the center of the signal and band number. Although still at an early stage of work these results seem to indicate the existence of a relatively small semiquinone radical. It is also interesting to note that there is parallel fluorescence emission behaviour between the quinonoid mixture and fulvic acid and that the fluorescence emission band is still 'broad' even at 10 K. This is highly suggestive of a non-covalently interacting bimolecular complex (charge transfer

complex). The EPR spectra were carried out on the Bruker (1700) EPR at the University of Calgary. The fluorescence line narrowing work was performed by Dr. C.H. Langford and Dr. F. Arise at the Free University of Amsterdam (6.26).

More extensive work may also be performed in order to study the role that quinoids may play in metal and pesticide binding with humic material through a combination of fluorescence quenching experiments and ESR work. Such studies may also involve the effects of ultraviolet radiation on binding processes.

Finally, the results of chemical modeling work together with parallel ESR and NMR studies may also be of use molecular modeling research of humic materials. Experimental evidence for charge transfer complexes, donor-acceptor complexes, and possibilities for self-assembly must be accounted for in any hypothetical 'monomer' work performed. No doubt, discussions of emergence and complexity towards the problem of humic substance structure may arise in future work. The jump from a quantum mechanical level to the 'macroscopic' level must be made with great care. Some of the newer faces of physical organic chemistry, such as studies in molecular recognition and self-assembly, may be of importance in structural elucidation studies of humic material.

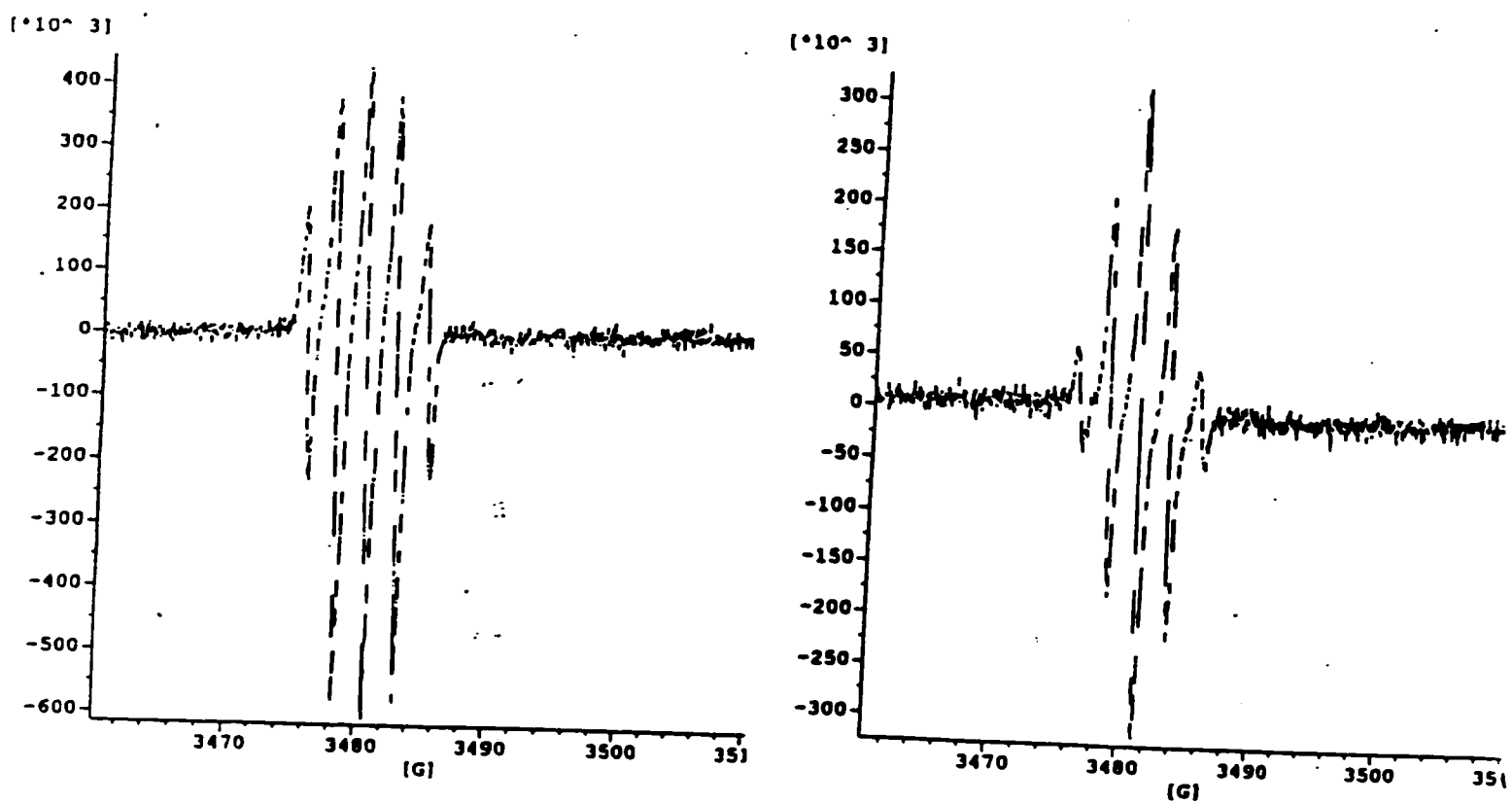


Figure 6.16: EPR spectra of Mossy Point fulvic acid (left) and the Quinonoid (Amsterdam) model (right).

References

- 6.1 Wilkinson, F., *Organic Molecular Photophysics*, Ed. Birks, J.B., NY: Wiley, 1975, p.95.
- 6.2 *Humic Substances II: In Search of Structure*, Eds., Hayes, M.H.B., MacCarthy, P., Malcolm, R.L., Swift, R.S., John-Wiley: NY, 1989.
- 6.3 Choudhry, G.G., *Humic Substances: Structural, Photophysical, Photochemical and Free Radical Aspects and Interactions With Environmental Chemicals*, Gordon & Breach Science Publishers, NY, 1984.
- 6.4 Scott, D., McKnight, D., Harris, E., Kolesar, S., Lovley, D., *Environ.Sci.&Tech.*, **1998**, 32, 2984-2989.
- 6.5 Turro, N., *Modern Molecular Photochemistry*, Columbia University Press, 1991.
- 6.6 Patai, S., *Chemistry of the Quinonoid Compounds*, Vol.1&2, Wiley:NY, 1989.
- 6.7 Rex, R.W., *Nature*, Lond., **1960**, 188, 1185-1186.
- 6.8 Steelink, C., Tollin, G., Free Radicals in soils; *Soil-Biochemistry*, pp.147-169, McLaren, A.D. and Peterson, G.H., Eds., Marcel Dekker, NY, 1967.
- 6.9 Riffaldi, R., Schnitzer, M., *Proc. Soil Sci. Soc. Am.*, **1972**, 36, 301-305.
- 6.10 Senesi, N., Steelink, C., Application of ESR Spectroscopy to the Study of Humic Substances. In *Humic Substances II*, Hayes, M., MacCarthy, P., Malcolm, R., Swift, R., Eds., John-Wiley:NY, 1989, pp.373-408.
- 6.11 Slawniska, D., Slawinski, J., Wlodzimierz, P., *Photochem and Photobiol.*, **1978**, 28, 75-81.
- 6.12 Slawniska, D., Slawinski, J., Wlodzimierz, P., *Photochem and Photobio.*, **1978**, 28, 459-463.

- 6.13 Slawniska, D., *Photochem and Photobio.*, **1978**, *28*, 453-458.
- 6.14 Lovley, D., Coates, J., Blunt-Harris, E., Philips, E., Woodward, J., *Nature*, **1996**, *382*, 445.
- 6.15 Lovley, D., Woodward, J., Blunt-Harris, E., Hayes, L., Philips, E., Coates, J., *Acta Hydrochim. Hydrobiol.*, **1998**, *26*, 152.
- 6.16 Coates, J., Ellis, D., Blunt-Harris, E., Gaw, C., Roden, E., Lovley, D., *App. Environ. Microbiol.*, **1998**, *64*, 1504.
- 6.17 Schulten, H.R., Schmitt-Kopplin, J.P., Hertkorn, N., Kettup, A., *Environm. Sci. & Tech.*, **1998**, Vol. 32, No. 17, pp. 2531-2541.
- 6.18 Nakamoto, K., *J. Am. Chem. Soc.*, **1952**, *74*, 1739-1742.
- 6.19 Briegleb, G., Herre, W., Wolf, D., *Spec. Acta.*, **1969**, Vol. 25A, pp. 39-46.
- 6.20 Matsuda, H., Osaki, K., Nitta, I., *J. Am. Chem. Soc.*, **1958**, Vol. 31, No. 5, pp. 611-620.
- 6.21 Cassidy, H.G., Moser, R.E., *J. Am. Chem. Soc.*, **1965**, *87*, 15, 3463-3467.
- 6.22 Michaelis, L., Granick, S., *J. Am. Chem. Soc.*, **1944**, *66*, 1023-1030.
- 6.23 Hoigne, J., Haag, W.R., *Environ. Sci. Technol.*, **1986**, *20*, 341-348.
- 6.24 Cook, R.L., PhD. Thesis, University of Calgary, Calgary, AB., Canada, 1997.
- 6.25 Faust, B., Anastasio, C., Janakiram, R.C., *Environ. Sci. Technol.*, **1997**, *31*, 218-232.
- 6.26 Langford, C.H., Bruccoleri, A., Yamdagni, R., Arise, F., in preparation.
- 6.27 Thorn, K., Arterburnt, J., Mikita, M., *Environ. Sci. Technol.*, **1992**, No. 1, pp 107-116.
- 6.28 Bohmer, V., *Angew. Chem. Int. Ed. Engl.*, **1995**, *34*, 713-745.

6.29 Rebek, J., *Acc.Chem.Res.*, **1999**, Vol 32, No. 4, 278-286.

Appendix I

The general character of fulvic acid is that of an extremely heterogeneous mixture. The complexity of humic substances prevents the assignment of a precise chemical structure to account for their properties. The most general practices include classification of the various types of humic materials according to isolation and fractionation procedures, or according to their macromolecular properties such as molecular weight and particle size (1-3). The approach of this work has been to study two well characterized fulvic acids, the Mossy Point (Armadale) and Laurentian fulvic acids.

The advantage is that physical and chemical characterization studies have been carried out by various research groups over many years so that the physical and chemical properties of these two fulvic acids are established (3-10). The preparation is in a form which is unambiguous with respect to protonation state and metal ion content (5,6, 9,11). Schnitzer, M., Gamble, D., (1, 9), have determined through titration, derivatization and degradative procedures, the following distribution of functional groups in the Mossy Point sample: 3.3 meq/g phenolics; 7.7 meq/g carboxylate; 3.6 meq/g aliphatic alcohol and 0.6 meq/g quinone. Solid state ^{13}C NMR was used by Cook (12) for the Laurentian fulvic acid functional group characterization.

With characterization information available relating changes in the observed photophysics to the physicochemical properties of the sample becomes possible.

References

1. Gamble, D., Schnitzer, M., Trace Metals and Metal Organic Interactions in Natural Waters, P.S. Singer, Ed., Ann Arbor Science Publishers Inc., Ann Arbor, USA, 1973, p.265.

2. Buffle,J., Deladoey,P., Haerdi,W., 1978, *Anal.Chim.Acta*, 101, 339.
3. Underdown,A.W.,Langford,C.H.,Gamble,D., 1981, *Anal.Chem.*, 53, 2139-2140.
4. Gamble,D.,Langford,C.H.,Underdown,A.W., Lee,S., Aquatic and Terrestrial Humic Materials, R.F. Christman and E.T. Gjessing, Eds., Ann Arbor Science, Ann Arbor, USA, 1983, Chapter 4.
5. Lee,S., Ph.D. Thesis, Carleton University, Ottawa, 1981.
6. Underdown, A.W., Ph.D. Thesis, Carleton University, Ottawa, 1982.
7. Underdown,A.W., Langford,C.H., Gamble,D.,1984, *Can.J.SoilSci.*, 61, 469.
8. Underdown,A.W.,Langford,C.H., Gamble,D., 1985, *Environ.Sci.Tech.*, 19, 132.
9. Hansen,E.H., Schnitzer,M., 1969, *Anal.Chim.Acta.*, 46, 247.
10. Gamble,D., 1972, *Can.J.Chem.*, 50, 2680.
11. Zafiriou,O.C., Zepp,R.G., Zika,R.G., Jousot-Dubien,J., 1984, *Envir.Sci.Tech.*, 18, 358A.
12. Cook,R., Ph.D. Thesis, University of Calgary, Calgary, 1997.